FROM IMPRINTING EFFORTS TO NEW CONCEPTS IN CONTROLLED RELEASE OF PROTEINS

FROM IMPRINTING EFFORTS TO NEW CONCEPTS IN CONTROLLED RELEASE OF PROTEINS

Hoe pogingen tot het maken van eiwitafdrukken in hydrogelen resulteerden in de ontwikkeling van nieuwe ideeën voor gereguleerde afgifte van eiwitten

(met een samenvatting in het Nederlands)

PROEFSCHRIFT

ter verkrijging van de graad van doctor aan de Universiteit Utrecht op gezag van de rector magnificus, prof. dr. G.J. van der Zwaan, ingevolge het besluit van het college voor promoties in het openbaar te verdedigen op woensdag 9 november 2011 des middags te 12.45 uur

door

Ellen Verheyen

geboren op 6 januari 1982
te Herentals, België

Promotor: Prof.dr.ir. W.E. Hennink

Co-promotoren: Dr. C.F. van Nostrum
Dr. B.M. Gadella

When you have extraordinary dreams

When you really believe you can make them come true

Only then does your mind overcome the barrier of the "impossible"

- Walter Bonatti -

TABLE OF CONTENTS

GENERAL INTRODUCTION

HYDROGELS

Hydrogels are hydrophilic three dimensional polymer networks, which are able to absorb large amounts of water, while maintaining their network structure. Because of their high water content as well as their soft consistency, they generally have a good biocompatibility[1, 2]. Moreover, these characteristics give hydrogels tissue mimicking properties and make them highly suitable for a wide range of biomedical and pharmaceutical applications, among which tissue engineering and protein delivery[2-9]. For generating hydrogels, a diverse range of polymers, both of natural (e.g. alginate[10-12], chitosan[13-15], gelatin[16] and dextran[17-20]) and synthetic origin (e.g. poly(ethylene glycol) (PEG)[21-24] and poly(hydroxyethylmethacrylate) (pHEMA))[25-27] have been studied.

The network structure of a hydrogel in aqueous environment is maintained due to the presence of crosslinks, which can be either based on chemical (covalent) bonds or physical (reversible) interactions[2]. Physical crosslinking relies on the formation of non-permanent reversible bonds resulting from e.g. ionic interactions[28-30], hydrogen bonding[31-33], stereocomplex formation[34, 35] or hydrophobic interactions[36-38]. These physical bonds can be easily broken, by e.g. high shear forces[39, 40], or external stimuli such as temperature[18, 40, 41], which allows administration via injection, after which the gel is formed *in situ*. Chemical crosslinking can be achieved by several mechanisms, e.g. radical polymerization[41, 42], Michael addition[43, 44], or click chemistry[45-48]. In general, chemical crosslinking results in hydrogels with a higher mechanical strength than physically crosslinked hydrogels; moreover the chemical crosslinking reaction can be regulated, making it possible to tailor the network density[5, 49]. One has to be aware, however, that chemically crosslinking usually requires the use of toxic reagents and harsh conditions which can affect the structure and activity of the encapsulated therapeutics, and even cause grafting of the therapeutic to the hydrogel network[50-52].

HYDROGELS FOR PROTEIN DELIVERY

Proteins are a very important class of therapeutics, but their widespread application is limited as there are many drawbacks associated with their use, such as chemical, physical and enzymatic instability, short half-life and poor cellular uptake[53]. At present, the main route for administrating therapeutic proteins is parenterally, and mostly repeated injections are required

in order to obtain a therapeutic effect, which is inconvenient for the patient[54]. Moreover, frequent injections give peak plasma concentrations of the protein which are often associated with toxic side-effects[54, 55]. To overcome these hurdles, controlled delivery systems are being developed which are able to improve the therapeutic efficacy and reduce the side-effects. Hydrogels are very attractive systems for the delivery of macromolecular drugs, due to their biocompatibility and the possibility to control the release kinetics by tailoring the network properties. Especially nanoparticulate hydrogels are interesting as they are injectable and can accomplish intracellular delivery[56, 57]. The release of proteins from hydrogels can occur by one or a combination of following three mechanisms: (1) diffusion controlled, (2) swelling controlled and (3) degradation/dissolution controlled[2]. In case of diffusion controlled release, the protein is smaller than the mesh size of the hydrogel network, and consequently it can freely diffuse out of the hydrogel matrix which can result in premature release, for instance already during preparation and storage. By adjusting the gel properties, e.g. by increasing the crosslink density or the solid content of the gel, the release kinetics can be retarded[17, 45, 58-62]. This approach, however, is limited since a too dense gel network can lead to permanent protein entrapment[60, 63] or the protein release can be too slow once the (intracellular) target is reached. To delay the release one can also use hydrogels from which the release is controlled by swelling and/or degradation[19, 44, 64-66]. In these hydrogels, the mesh size of the polymer network is initially smaller than the protein, thus the protein is at first immobilized in the network. Upon swelling or degradation, the mesh size increases and when it exceeds the size of the protein, diffusion and release of the protein can take place. More recently, bioresponsive nanogels, which sense and respond to environmental changes, have received increasing attention because they can deliver their content upon an internal or external trigger, e.g. at the (diseased) site of the body where specific conditions exist. Examples of environmental factors influencing the hydrogel swelling are pH[67-69], temperature[38, 70], and especially interesting for intracellular delivery are redox-potential sensitive drug delivery systems[71, 72]. The latter systems rely on the large difference in redox-potential between intracellular and extracellular compartments where different glutathione concentrations exist (0.5-10 mM[73] and 2-20 μm[74], respectively). Thus, redox-sensitive carriers are designed to be relatively stable in the circulation and extracellular compartments. However, once internalized, the disulfide bonds maintaining the structure of the carrier system will be rapidly cleaved in presence of high concentration of glutathione, resulting in the intracellular release of the entrapped drug molecules[71, 72].

MOLECULAR IMPRINTING WITHIN HYDROGELS

Molecular imprinting is a technique that involves the formation of polymer networks that contain cavities or memory sites and can specifically recognize a given template molecule in presence of structurally similar molecules. The general procedure to prepare these so called molecularly imprinted polymers (MIP) is depicted in Figure 1. The first step involves the mixing of the molecule of interest (template) with one or more functional monomers and an excess of crosslinkers in an appropriate solvent. The functional monomers form a pre-polymerization complex with the template using non-covalent interactions[75, 76], however also covalent interactions[77, 78] or a combination of both[79] are possible (A). Once polymerized, the spatial arrangement of the functional monomers is "frozen" around the template (B). The template can then be removed from the polymer network, leaving behind an imprinted site which is complementary in size, shape and functionality (C). The MIP is now capable to recognize and rebind the template molecule.
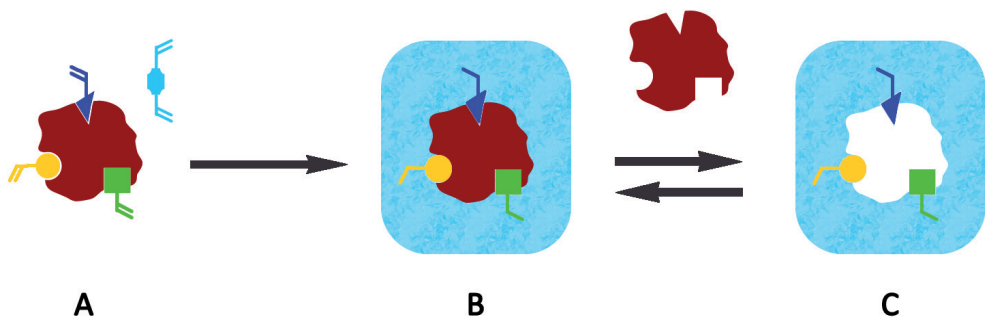

Figure 1. Schematic representation of the principle of molecular imprinting. (A) The template (shown in red), (functional) monomers (shown in yellow, green and blue) and crosslinker (light blue) form a pre-polymerization complex. (B) Polymerization of monomers and crosslinker fixes the complex. (C) Removal of the template leaves rebinding cavities.

Approaches in molecular imprinting

Generally taken, there are two methods of molecular imprinting, the covalent and non-covalent approach, which differ only in the way the pre-polymerization complex is formed and how the template is removed from the crosslinked polymer network. Covalent imprinting was first introduced by the group of Wulff in the 1970's[80-83]. In their approach, the template is bound to the monomer through reversible covalent bonds (e.g. ester bonds, disulfide bonds,

Schiff bases). The template-monomer complex is prepared in one or more steps prior to the polymerization. Once the network is polymerized, the reversible bonds are selectively cleaved, and subsequent rebinding is based on the reformation of the original covalent bond. Using this method, stable and uniform binding sites can be created, but the main disadvantage is the slow kinetics for rebinding, as this is based on the reformation of the initial covalent bond[83]. In 1981, non-covalent imprinting was introduced by Mosbach and Arshady[84]. In their approach the template-monomer complex is formed through non-covalent interactions such as hydrogen bonds, Van der Waals forces, dipole-dipole or hydrophobic interactions. After polymerization the template is removed via simple solvent extraction and the subsequent rebinding is also based on the same non-covalent interaction. Non-covalent imprinting is the most favoured approach due to its simplicity, and therefore also the most studied approach. Moreover, the method is versatile and can be applied to almost any type of template. However, the generated binding sites are very heterogeneous in affinity and selectivity, as the forces which stabilize the template-monomer complex are very weak[85, 86]. In the 90's, the group of Whitcombe introduced a hybrid method, called semi-covalent imprinting, which combines the advantages of both methods[79, 87, 88]. The template-monomer complex is formed through covalent bonds, and after removal of the template by chemical cleavage, the rebinding to the MIP occurs via non-covalent interactions.

The challenge of protein imprinting

Nowadays, molecular imprinting of small, low molecular weight molecules is a well-established technique, which has resulted in a wide range of applications, such as chromatography, chemical sensors, enzyme-like catalysis, drug discovery and drug delivery[89-94]. However, expanding the method towards the imprinting of biomacromolecular molecules and in particular proteins is extremely challenging. Progressive development in the field of protein imprinting is hampered mainly by the proteins' intrinsic properties. Firstly, highly crosslinked polymer networks are required in conventional imprinting to ensure the preservation of the binding cavity after template removal. However, the large molecular size of proteins hinders the protein to leave and reach the binding site. This poor mass transport results in slow rebinding kinetics and can even lead to permanent entrapment of the proteins in the network. To make the binding sites more accessible, one can grind and sieve the bulky polymer to obtain smaller particles, but this leads to poorly defined particles and can lead to damaging of the binding

sites. Therefore, several methods have been developed to directly synthesize imprinted micro- and nanoparticles[95-97]. A more convenient way to overcome the poor mass transfer is to locate the imprint sites close to or at the surface of the polymer (*surface imprinting*)[98-100]. To this end, proteins are immobilized on a supporting surface after which the monomer-crosslinker solution is added and polymerized. The support and template are then detached or dissolved to expose the imprinted surface. The immobilization of the proteins is achieved for instance by covalent attachment[101], metal-ion coordination[102] or adsorption to Langmuir lipid monolayers[103]. An alternative technique is the "epitope approach", as introduced by Rachkov[104, 105]. This method uses a small peptide as template, which represents only a part of the larger protein, and it has been demonstrated that this peptide imprinted polymer can recognize the whole protein.

An even more important limiting factor besides the protein size is the incompatibility of proteins with organic solvents, which are mainly used in the conventional imprint methods. Therefore the choice of solvents for protein imprinting is in general limited to aqueous mixtures. Hydrogen bonding interactions strongly contribute to the affinity of molecularly imprinted polymers (MIPs) for low molecular weight compounds in organic, aprotic solvents, but are seriously hampered in water[106]. Nevertheless, successful imprints have been achieved within hydrogels, where it has been proposed that multiple weak interactions are responsible for the strong binding of the protein to the polymer network in aqueous environment[76, 107]. In this light, polyacrylamide based hydrogels are the most commonly used polymer matrices for protein imprinting, since their introduction by Hjertén and co-workers[107, 108].

MEMBRANE PROTEINS AS TEMPLATE FOR MOLECULAR IMPRINTING

The aim of this thesis was to synthesize protein imprinted nanoparticles (PINAPLES), displaying the imprints of membrane proteins on their surface. The successful creation of membrane protein imprinted nanoparticles would open a wide range of applications, for example selective isolation and purification of membrane proteins from cell lysates which is notoriously difficult. Moreover, the protein imprinted nanoparticles (PINAPLES) can selectively bind to cell surfaces expressing the imprinted protein, which can be used for diagnostic purposes or targeted drug delivery when drugs are incorporated inside the polymer matrix. On the other hand, membrane receptors can also be blocked by binding of PINAPLES, thereby inhibiting their biological function. The advantages of using PINAPLES as targeted drug delivery systems is

found in their high stability (e.g. against pH, temperature), and their low immunogenicity, which are the major drawbacks of the present active drug targeting systems using e.g monoclonal antibodies[94, 109].

For the synthesis of the imprinted nanoparticles, it is important that the membrane protein maintains its native conformation, and thus the protein should be embedded in its natural environment, i.e. a lipid bilayer, with the hydrophilic (extracellular) part of the membrane protein exposed for imprinting. In general there are two approaches for the reconstitution of membrane proteins in artificial bilayers. The first approach involves the reconstitution of proteins in lipid vesicles (proteoliposomes)[110-112], which has been explored for surface imprinting by Joris Schillemans[113]. A second approach, described in this thesis, is the reconstitution into solid-supported lipid bilayers.

Imprints of the membrane protein on the solid support can be made by adding a solution of monomers and crosslinker on top of the bilayer with reconstituted protein (Figure 2A). After polymerization (Figure 2B), the supported bilayer and proteins are removed, resulting in a thin polymer layer, containing the imprint of the extracellular domain of the membrane protein (Figure 2C). Using this approach, membrane protein imprinted hydrogel nanoparticles can be synthesized by applying patterned polymerization techniques such as nanolithography[114] or focused electron beam crosslinking[115, 116].
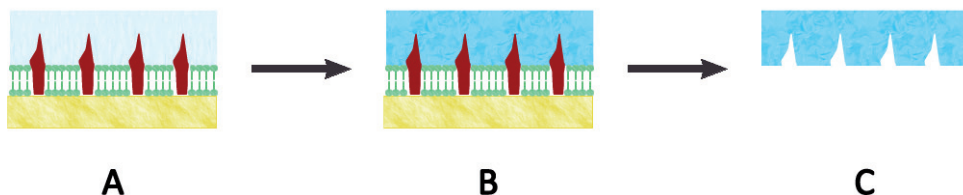

Figure 2. Concept of the preparation of membrane protein imprinted polymers. A membrane protein (red) is immobilized in a planar supported lipid bilayer (green), on top a solution of monomers and crosslinker is added (blue) (A). After polymerization of the monomers a hydrogel is formed around the extracellular part of the membrane protein (B). Thereafter the support, bilayer and proteins are removed, leaving a surface imprinted polymer (C).

A major advantage of surface imprinting is that the template can be easily removed since, as pointed out in this chapter, no diffusion of the protein through a highly crosslinked matrix is required in contrast to bulk-imprinted materials. Another advantage is that characterization of the surface and the imprinted polymer is relatively convenient, for example by using atomic force microscopy (AFM). With AFM, the surface topography of the protein imprints can be

evaluated, before and after rebinding[117]. Moreover, one can use atomic force spectroscopy to directly measure the force of interaction of the protein with the imprinted sites[118].

AIM AND OUTLINE OF THIS THESIS

The aim of this thesis was to develop protein imprinted nanoparticles (PINAPLES) for targeted drug delivery, as described in the previous section. As a spin-off from our attempts to develop these PINAPLES, we established a method for synthesis of protein-macromers, which were also explored for controlled intracellular release of proteins.

Our first step towards surface imprinting of membrane proteins was to reconstitute the membrane protein in its native environment, i.e. a lipid bilayer. In **Chapter 2**, the detergent mediated insertion of hemagglutinin in preformed supported lipid bilayers (SLBs) was explored. The formation of the bilayer and subsequent insertion of hemagglutinin was evaluated with atomic force microscopy. To allow simultaneous comparison of different parameters influencing the reconstitution process, the method was adapted to a 96 well plate format. The detection of the inserted protein was done via a specially developed ELISA based assay.

In a later stage, this well plate format was used for screening different parameters involved in the imprinting of polymers. However, despite many attempts, no successful imprints of the membrane protein could be prepared. Therefore it was decided to first proof the principle of protein imprinting with soluble proteins, such as lysozyme and cytochrome C, by reproducing protocols described in literature for both surface imprinting and classical bulk imprinting. Unfortunately, the few successful attempts we had were not reproducible. Therefore, in **Chapter 3**, the scientific proof of the many published successful data is critically analyzed in relation to our own experimental data. It is clear that protein imprinting still faces some fundamental challenges. Moreover it can be argued that the scientific evidence of molecular imprinting of proteins is not convincing in numerous publications.

In view of the disappointing results obtained so far, it might be inevitable to introduce new concepts for protein imprinting. With this in mind, we propose a novel semi-covalent imprinting approach in **Chapter 4**. An efficient strategy is described to introduce polymerizable methacrylamide moieties to the lysine residues of a model protein, lysozyme, using a novel sacrificial linker. Up to three linker molecules could be introduced with preservation of the protein structure and keeping its lytic activity. The methacrylamide linker contains a disulfide

bond and an esterbond, which creates the possibility to remove the protein from a polymerized hydrogel network after co-polymerization, via hydrolysis or reduction. These protein-macromers were primarily developed for semi-covalent imprinting, but it was anticipated that the methacrylamide modified proteins could also be used for triggered release of proteins from a hydrogel network. This was further assessed in **Chapter 5**, where a second linker molecule, containing only disulfide bonds, was synthesized, thereby aiming for glutathione mediated intracellular release of proteins. The immobilization and subsequent release in different (reducing and non-reducing) conditions was followed in time. Moreover, the protein mobility in the polymer network under the same conditions was studied by fluorescence recovery after photobleaching (FRAP) experiments.

Chapter 6, provides a summary of the work described in this thesis and suggestions for future research in protein imprinting and controlled (intracellular) delivery of proteins.

REFERENCES

1. Park, H.; Park, K. Biocompatibility issues of implantable drug delivery systems, *Pharm Res,* 13 **(1996)**, 1770-1776.
2. Peppas, N. A.; Bures, P.; Leobandung, W.; Ichikawa, H. Hydrogels in pharmaceutical formulations, *Eur J Pharm and Biopharm,* 50 **(2000)**, 27-46.
3. Brandl, F.; Sommer, F.; Goepferich, A. Rational design of hydrogels for tissue engineering: Impact of physical factors on cell behavior, *Biomaterials,* 28 **(2007)**, 134-146.
4. Hoare, T. R.; Kohane, D. S. Hydrogels in drug delivery: Progress and challenges, *Polymer,* 49 **(2008)**, 1993-2007.
5. Hoffman, A. S. Hydrogels for biomedical applications, *Adv Drug Del Rev,* 54 **(2002)**, 3-12.
6. kashyap, N.; Kumar, N.; Ravikumar, M. Hydrogels for pharmceutical and biomedical applications, *Crit Rev Ther Drug Carrier Syst,* 22 **(2005)**, 107-150.
7. Morimoto, N.; Nomura Shin-ichiro, M.; Miyazawa, N.; Akiyoshi, K., Nanogel engineered designs for polymeric drug delivery. In *Polymeric drug delivery II*, American Chemical Society: 2006; Vol. 924, pp 88-101.
8. Stolnik, S.; Shakesheff, K. Formulations for delivery of therapeutic proteins, *Biotechnol Lett,* 31 **(2009)**, 1-11.
9. Van Tomme, S. R.; Storm, G.; Hennink, W. E. In situ gelling hydrogels for pharmaceutical and biomedical applications, *Int J Pharm,* 355 **(2008)**, 1-18.
10. Augst, A. D.; Kong, H. J.; Mooney, D. J. Alginate hydrogels as biomaterials, *Macromol Biosci,* 6 **(2006)**, 623-633.
11. Gombotz, W. R.; Wee, S. Protein release from alginate matrices, *Adv Drug Del Rev,* 31 **(1998)**, 267-285.
12. Pescosolido, L.; Miatto, S.; Di Meo, C.; Cencetti, C.; Coviello, T.; Alhaique, F.; Matricardi, P. Injectable and in situ gelling hydrogels for modified protein release, *Eur Biophys J,* 39 **(2010)**, 903-909.
13. Berger, J.; Reist, M.; Mayer, J. M.; Felt, O.; Gurny, R. Structure and interactions in chitosan hydrogels formed by complexation or aggregation for biomedical applications, *Eur J Pharm Biopharm,* 57 **(2004)**, 35-52.
14. Denkbas, E. B.; Ottenbrite, R. M. Perspectives on: Chitosan drug delivery systems based on their geometries, *Journal of Bioactive and Compatible Polymers,* 21 **(2006)**, 351-368.
15. Hagenaars, N.; Verheul, R. J.; Mooren, I.; de Jong, P. H. J. L. F.; Mastrobattista, E.; Glansbeek, H. L.; Heldens, J. G. M.; van den Bosch, H.; Hennink, W. E.; Jiskoot, W. Relationship between structure and adjuvanticity of N,N,N-trimethyl chitosan (TMC) structural variants in a nasal influenza vaccine, *J Control Release,* 140 **(2009)**, 126-133.
16. Sutter, M.; Siepmann, J.; Hennink, W. E.; Jiskoot, W. Recombinant gelatin hydrogels for the sustained release of proteins, *J Control Release,* 119 **(2007)**, 301-312.
17. Hennink, W. E.; Talsma, H.; Borchert, J. C. H.; De Smedt, S. C.; Demeester, Controlled release of proteins from dextran hydrogels, *J Control Release,* 39 **(1996)**, 47-55.
18. Lévesque, S. G.; Lim, R. M.; Shoichet, M. S. Macroporous interconnected dextran scaffolds of controlled porosity for tissue-engineering applications, *Biomaterials,* 26 **(2005)**, 7436-7446.
19. Van Thienen, T. G.; Raemdonck, K.; Demeester, J.; De Smedt, S. C. Protein release from biodegradable dextran nanogels, *Langmuir,* 23 **(2007)**, 9794-9801.
20. Zhang, R.; Tang, M.; Bowyer, A.; Eisenthal, R.; Hubble, J. A novel pH- and ionic-strength-sensitive carboxy methyl dextran hydrogel, *Biomaterials,* 26 **(2005)**, 4677-4683.
21. Hiemstra, C.; Zhong, Z.; Van Tomme, S. R.; van Steenbergen, M. J.; Jacobs, J. J. L.; Otter, W. D.; Hennink, W. E.; Feijen, J. In vitro and in vivo protein delivery from in situ forming poly(ethylene glycol)-poly(lactide) hydrogels, *J Control Release,* 119 **(2007)**, 320-327.
22. Lu, S.; Anseth, K. S. Release behavior of high molecular weight solutes from poly(ethylene glycol)-based degradable networks, *Macromolecules,* 33 **(2000)**, 2509-2515.

23. Mahoney, M. J.; Anseth, K. S. Three-dimensional growth and function of neural tissue in degradable polyethylene glycol hydrogels, *Biomaterials,* 27 **(2006)**, 2265-2274.

24. van de Wetering, P.; Metters, A. T.; Schoenmakers, R. G.; Hubbell, J. A. Poly(ethylene glycol) hydrogels formed by conjugate addition with controllable swelling, degradation, and release of pharmaceutically active proteins, *J Control Release,* 102 **(2005)**, 619-627.

25. Andac, M.; Plieva, F. M.; Denizli, A.; Galaev, I. Y.; Mattiasson, B. Poly(hydroxyethyl methacrylate)-based macroporous hydrogels with disulfide cross-linker, *Macromol Chem and Phys,* 209 **(2008)**, 577-584.

26. Ferreira, L.; Vidal, M. M.; Gil, M. H. Evaluation of poly(2-hydroxyethyl methacrylate) gels as drug delivery systems at different pH values, *Int J Pharm,* 194 **(2000)**, 169-180.

27. Meyvis, T. K. L.; De Smedt, S. C.; Demeester, J.; Hennink, W. E. Influence of the degradation mechanism of hydrogels on their elastic and swelling properties during degradation, *Macromolecules,* 33 **(2000)**, 4717-4725.

28. Kuo, C. K.; Ma, P. X. Ionically crosslinked alginate hydrogels as scaffolds for tissue engineering: Part 1. Structure, gelation rate and mechanical properties, *Biomaterials,* 22 **(2001)**, 511-521.

29. Lee, K. Y.; Rowley, J. A.; Eiselt, P.; Moy, E. M.; Bouhadir, K. H.; Mooney, D. J. Controlling mechanical and swelling properties of alginate hydrogels independently by cross-linker type and cross-linking density, *Macromolecules,* 33 **(2000)**, 4291-4294.

30. Van Tomme, S. R.; De Geest, B. G.; Braeckmans, K.; De Smedt, S. C.; Siepmann, F.; Siepmann, J.; van Nostrum, C. F.; Hennink, W. E. Mobility of model proteins in hydrogels composed of oppositely charged dextran microspheres studied by protein release and fluorescence recovery after photobleaching, *J Control Release,* 110 **(2005)**, 67-78.

31. Haglund, B. O.; Joshi, R.; Himmelstein, K. J. An in situ gelling system for parenteral delivery, *J Control Release,* 41 **(1996)**, 229-235.

32. Noro, A.; Nagata, Y.; Takano, A.; Matsushita, Y. Diblock-type supramacromolecule via biocomplementary hydrogen bonding, *Biomacromolecules,* 7 **(2006)**, 1696-1699.

33. Wang, Y. T.; Zhou, Y. X.; Sokolov, J.; Rigas, B.; Levon, K.; Rafailovich, M. A potentiometric protein sensor built with surface molecular imprinting method, *Biosens Bioelectron,* 24 **(2008)**, 162-166.

34. de Jong, S. J.; De Smedt, S. C.; Wahls, M. W. C.; Demeester, J.; Kettenes-van den Bosch, J. J.; Hennink, W. E. Novel self-assembled hydrogels by stereocomplex formation in aqueous solution of enantiomeric lactic acid oligomers grafted to dextran, *Macromolecules,* 33 **(2000)**, 3680-3686.

35. Hiemstra, C.; Zhong, Z.; Li, L.; Dijkstra, P. J.; Feijen, J. In-situ formation of biodegradable hydrogels by stereocomplexation of PEG-(PLLA)8 and PEG-(PDLA)8 star block copolymers, *Biomacromolecules,* 7 **(2006)**, 2790-2795.

36. Klouda, L.; Mikos, A. G. Thermoresponsive hydrogels in biomedical applications, *Eur J Pharm Biopharm,* 68 **(2008)**, 34-45.

37. Vermonden, T.; Besseling, N. A. M.; van Steenbergen, M. J.; Hennink, W. E. Rheological studies of thermosensitive triblock copolymer hydrogels, *Langmuir,* 22 **(2006)**, 10180-10184.

38. Jeong, B.; Bae, Y. H.; Lee, D. S.; Kim, S. W. Biodegradable block copolymers as injectable drug-delivery systems, *Nature,* 388 **(1997)**, 860-862.

39. Ni, X.; Cheng, A.; Li, J. Supramolecular hydrogels based on self-assembly between PEO-PPO-PEO triblock copolymers and α-cyclodextrin, *Journal of Biomedical Materials Research Part A,* 88A **(2009)**, 1031-1036.

40. Van Tomme, S. R.; van Steenbergen, M. J.; De Smedt, S. C.; van Nostrum, C. F.; Hennink, W. E. Self-gelling hydrogels based on oppositely charged dextran microspheres, *Biomaterials,* 26 **(2005)**, 2129-2135.

41. Jeong, B.; Bae, Y. H.; Kim, S. W. Thermoreversible gelation of pega-plga-peg triblock copolymer aqueous solutions, *Macromolecules,* 32 **(1999)**, 7064-7069.

42. Chung, J. T.; Vlugt-Wensink, K. D. F.; Hennink, W. E.; Zhang, Z. Effect of polymerization conditions on the network properties of Dex-HEMA microspheres and macro-hydrogels, *Int J Pharm,* 288 **(2005)**, 51-61.

43. Censi, R.; Fieten, P. J.; Di Martino, P.; Hennink, W. E.; Vermonden, T. In-situ forming hydrogels by simultaneous thermal gelling and michael addition reaction between methacrylate bearing thermosensitive triblock copolymers and thiolated hyaluronan, *J Control Release,* 148 **(2010)**, e28-e29.

44. Censi, R.; Vermonden, T.; van Steenbergen, M. J.; Deschout, H.; Braeckmans, K.; De Smedt, S. C.; van Nostrum, C. F.; di Martino, P.; Hennink, W. E. Photopolymerized thermosensitive hydrogels for tailorable diffusion-controlled protein delivery, *J Control Release,* 140 **(2009)**, 230-236.

45. Hiemstra, C.; Zhong, Z.; van Steenbergen, M. J.; Hennink, W. E.; Feijen, J. Release of model proteins and basic fibroblast growth factor from in situ forming degradable dextran hydrogels, *J Control Release,* 122 **(2007)**, 71-78.

46. Malkoch, M.; Vestberg, R.; Gupta, N.; Mespouille, L.; Dubois, P.; Mason, A. F.; Hedrick, J. L.; Liao, Q.; Frank, C. W.; Kingsbury, K.; Hawker, C. J. Synthesis of well-defined hydrogel networks using click chemistry, *Chemical Communications,* **(2006)**, 2774-2776.

47. Ossipov, D. A.; Hilborn, J. n. Poly(vinyl alcohol)-based hydrogels formed by "Click chemistry", *Macromolecules,* 39 **(2006)**, 1709-1718.

48. van Dijk, M.; van Nostrum, C. F.; Hennink, W. E.; Rijkers, D. T. S.; Liskamp, R. M. J. Synthesis and characterization of enzymatically biodegradable peg and peptide-based hydrogels prepared by click chemistry, *Biomacromolecules,* 11 **(2010)**, 1608-1614.

49. Hennink, W. E.; van Nostrum, C. F. Novel crosslinking methods to design hydrogels, *Adv Drug Del Rev,* 54 **(2002)**, 13-36.

50. Cadée, J. A.; de Groot, C. J.; Jiskoot, W.; den Otter, W.; Hennink, W. E. Release of recombinant human interleukin-2 from dextran-based hydrogels, *J Control Release,* 78 **(2002)**, 1-13.

51. Valdebenito, A.; Espinoza, P.; Lissi, E. A.; Encinas, M. V. Bovine serum albumin as chain transfer agent in the acrylamide polymerization. Protein-polymer conjugates, *Polymer,* 51 **(2010)**, 2503-2507.

52. Lin, C.-C.; Metters, A. T. Bifunctional monolithic affinity hydrogels for dual-protein delivery, *Biomacromolecules,* 9 **(2008)**, 789-795.

53. Torchilin, V. P.; Lukyanov, A. N. Peptide and protein drug delivery to and into tumors: Challenges and solutions, *Drug Discovery Today,* 8 **(2003)**, 259-266.

54. Crommelin, D. J. A.; Sindelar, R. D., *Pharmaceutical biotechnology (2nd edition) london: Routledge, 2002*. Blackwell Publishing Ltd: 2004; Vol. 56, p 563-563.

55. Tang, L.; Persky, A. M.; Hochhaus, G.; Meibohm, B. Pharmacokinetic aspects of biotechnology products, *J Pharm Sci,* 93 **(2004)**, 2184-2204.

56. Hamidi, M.; Azadi, A.; Rafiei, P. Hydrogel nanoparticles in drug delivery, *Adv Drug Del Rev,* 60 **(2008)**, 1638-1649.

57. Raemdonck, K.; Demeester, J.; De Smedt, S. Advanced nanogel engineering for drug delivery, *Soft Matter,* 5 **(2009)**, 707-715.

58. Weber, L. M.; Lopez, C. G.; Anseth, K. S. Effects of peg hydrogel crosslinking density on protein diffusion and encapsulated islet survival and function, *J of Biomed Mater Res A,* 90A **(2009)**, 720-729.

59. van Dijk-Wolthuis, W. N. E.; Hoogeboom, J. A. M.; van Steenbergen, M. J.; Tsang, S. K. Y.; Hennink, W. E. Degradation and release behavior of dextran-based hydrogels, *Macromolecules,* 30 **(1997)**, 4639-4645.

60. Meyvis, T.; De Smedt, S.; Stubbe, B.; Hennink, W.; Demeester, J. On the release of proteins from degrading dextran methacrylate hydrogels and the correlation with the rheologic properties of the hydrogels, *Pharm Res,* 18 **(2001)**, 1593-1599.

61.   Carvalho, J. M.; Coimbra, M. A.; Gama, F. M. New dextrin-vinylacrylate hydrogel: Studies on protein diffusion and release, *Carbohydr Polym,* 75 **(2009)**, 322-327.

62.   am Ende, M. T.; Peppas, N. A. Transport of ionizable drugs and proteins in crosslinked poly(acrylic acid) and poly(acrylic acid-co-2-hydroxyethyl methacrylate) hydrogels. Ii. Diffusion and release studies, *J Control Release,* 48 **(1997)**, 47-56.

63.   Stenekes, R. J. H.; De Smedt, S. C.; Demeester, J.; Sun, G.; Zhang, Z.; Hennink, W. E. Pore sizes in hydrated dextran microspheres, *Biomacromolecules,* 1 **(2000)**, 696-703.

64.   Franssen, O.; Vandervennet, L.; Roders, P.; Hennink, W. E. Degradable dextran hydrogels: Controlled release of a model protein from cylinders and microspheres, *J Control Release,* 60 **(1999)**, 211-221.

65.   Nagahama, K.; Ouchi, T.; Ohya, Y. Biodegradable nanogels prepared by self-assembly of poly(l-lactide)-grafted dextran: Entrapment and release of proteins, *Macromol Biosci,* 8 **(2008)**, 1044-1052.

66.   Swaminathan, S.; Cavalli, R.; Trotta, F.; Ferruti, P.; Ranucci, E.; Gerges, I.; Manfredi, A.; Marinotto, D.; Vavia, P. In vitro release modulation and conformational stabilization of a model protein using swellable polyamidoamine nanosponges of β-cyclodextrin, *J Incl Phen Macrocycl Chem,* 68 **(2010)**, 183-191.

67.   Ayame, H.; Morimoto, N.; Akiyoshi, K. Self-assembled cationic nanogels for intracellular protein delivery, *Bioconjug Chem,* 19 **(2008)**, 882-890.

68.   Murthy, N.; Campbell, J.; Fausto, N.; Hoffman, A. S.; Stayton, P. S. Bioinspired pH-responsive polymers for the intracellular delivery of biomolecular drugs, *Bioconjug Chem,* 14 **(2003)**, 412-419.

69.   Shi, L.; Khondee, S.; Linz, T. H.; Berkland, C. Poly(n-vinylformamide) nanogels capable of pH-sensitive protein release, *Macromolecules,* 41 **(2008)**, 6546-6554.

70.   Bromberg, L. E.; Ron, E. S. Temperature-responsive gels and thermogelling polymer matrices for protein and peptide delivery, *Adv Drug Del Rev,* 31 **(1998)**, 197-221.

71.   Meng, F.; Hennink, W. E.; Zhong, Z. Reduction-sensitive polymers and bioconjugates for biomedical applications, *Biomaterials,* 30 **(2009)**, 2180-2198.

72.   Saito, G.; Swanson, J. A.; Lee, K.-D. Drug delivery strategy utilizing conjugation via reversible disulfide linkages: Role and site of cellular reducing activities, *Adv Drug Del Rev,* 55 **(2003)**, 199-215.

73.   Meister, A.; Anderson, M. E. Glutathione, *Annu Rev Biochem,* Vol. 52 **(1983)**, 711-760.

74.   Jones, D. P.; Carlson, J. L.; Samiec, P. S.; Sternberg, P.; Mody, V. C.; Reed, R. L.; Brown, L. A. S. Glutathione measurement in human plasma: Evaluation of sample collection, storage and derivatization conditions for analysis of dansyl derivatives by HPLC, *Clin Chim Acta,* 275 **(1998)**, 175-184.

75.   Mosbach, K. Toward the next generation of molecular imprinting with emphasis on the formation, by direct molding, of compounds with biological activity (biomimetics), *Anal Chim Acta,* 435 **(2001)**, 3-8.

76.   Sellergren, B., The non-covalent approach to molecular imprinting. In *Molecularly imprinted polymers: Man-made mimics of antibodies and their applications in analytical chemistry*, Sellergren, B., Ed. Elsevier: Amsterdam, 2001; pp 113-183.

77.   Gallego-Gallegos, M.; Munoz-Olivas, R.; Camara, C.; Mancheno, M. J.; Sierra, M. A. Synthesis of a ph dependent covalent imprinted polymer able to recognize organotin species, *Analyst,* 131 **(2006)**, 98-105.

78.   Mukawa, T.; Goto, T.; Takeuchi, T. Post-oxidative conversion of thiol residue to sulfonic acid in the binding sites of molecularly imprinted polymers: Disulfide based covalent molecular imprinting for basic compounds, *Analyst,* 127 **(2002)**, 1407-1409.

79.   Whitcombe, M. J.; Rodriguez, M. E.; Villar, P.; Vulfson, E. N. A new method for the introduction of recognition site functionality into polymers prepared by molecular imprinting: Synthesis and characterization of polymeric receptors for cholesterol, *J Am Chem Soc,* 117 **(1995)**, 7105-7111.

80. Wulff, G. The use of polymers with enzyme-analogous structures for the resolution of racemates, *Angew Chem Int Ed Engl,* 11 **(1972)**, 341.

81. Wulff, G.; Grobe-Einsler, R.; Vesper, W.; Sarhan, A. Enzyme-analogue built polymers, 5. On the specificity distribution of chiral cavities prepared in synthetic polymers, *Die Makromolekulare Chemie,* 178 **(1977)**, 2817-2825.

82. Wulff, G.; Vesper, W.; Grobe-Einsler, R.; Sarhan, A. Enzyme-analogue built polymers, 4. On the synthesis of polymers containing chiral cavities and their use for the resolution of racemates, *Die Makromolekulare Chemie,* 178 **(1977)**, 2799-2816.

83. Wulff, G. Cheminform abstract: Molecular imprinting in cross-linked materials with the aid of molecular templates - a way towards artificial antibodies, *ChemInform,* 26 **(1995)**.

84. Arshady, R.; Mosbach, K. Synthesis of substrate-selective polymers by host-guest polymerization, *Die Makromolekulare Chemie,* 182 **(1981)**, 687-692.

85. Mosbach, K.; Haupt, K. Some new developments and challenges in non-covalent molecular imprinting technology, *J Mol Recognit,* 11 **(1998)**, 62-68.

86. Umpleby, R. J.; Baxter, S. C.; Chen, Y.; Shah, R. N.; Shimizu, K. D. Characterization of molecularly imprinted polymers with the Langmuir-Freundlich isotherm, *Anal Chem,* 73 **(2001)**, 4584-4591.

87. Klein, J. U.; Whitcombe, M. J.; Mulholland, F.; Vulfson, E. N. Template-mediated synthesis of a polymeric receptor specific to amino acid sequences, *Angew Chem Int Ed,* 38 **(1999)**, 2057-2060.

88. Whitcombe, M. J.; Vulfson, E. N. Imprinted polymers, *Adv. Mater,* 13 **(2001)**, 467-478.

89. Alexander, C.; Andersson, H. S.; Andersson, L. I.; Ansell, R. J.; Kirsch, N.; Nicholls, I. A.; O'Mahony, J.; Whitcombe, M. J. Molecular imprinting science and technology: A survey of the literature for the years up to and including 2003, *J Mol Recognit,* 19 **(2006)**, 106-80.

90. Blanco-López, M. C.; Lobo-Castañón, M. J.; Miranda-Ordieres, A. J.; Tuñón-Blanco, P. Electrochemical sensors based on molecularly imprinted polymers, *TrAC Trends in Analytical Chemistry,* 23 **(2004)**, 36-48.

91. Chen, L.; Xu, S.; Li, J. Recent advances in molecular imprinting technology: Current status, challenges and highlighted applications, *Chem Soc Rev,* 40 **(2011)**, 2922-2942.

92. Komiyama, M.; Takeuchi, T.; Mukawa, T.; Asanuma, H., Applications of molecularly imprinted polymers. In *Molecular imprinting*, Wiley-VCH Verlag GmbH & Co. KGaA: 2004; pp 75-118.

93. Lanza, F.; Sellergren, B. The application of molecular imprinting technology to solid phase extraction, *Chromatographia,* 53 **(2001)**, 599-611.

94. van Nostrum, C. F. Molecular imprinting: A new tool for drug innovation, *Drug Discov Today: Technol,* 2 **(2005)**, 119-124.

95. Flavin, K.; Resmini, M. Imprinted nanomaterials: A new class of synthetic receptors, *Anal Bioanal Chem,* 393 **(2009)**, 437-444.

96. Guan, G. J.; Liu, B. H.; Wang, Z. Y.; Zhang, Z. P. Imprinting of molecular recognition sites on nanostructures and its applications in chemosensors, *Sensors,* 8 **(2008)**, 8291-8320.

97. Schillemans, J. P.; van Nostrum, C. F. Molecularly imprinted polymer particles: Synthetic receptors for future medicine, *Nanomed,* 1 **(2006)**, 437-447.

98. Bossi, A.; Piletsky, S. A.; Piletska, E. V.; Righetti, P. G.; Turner, A. P. F. Surface-grafted molecularly imprinted polymers for protein recognition, *Anal Chem,* 73 **(2001)**, 5281-5286.

99. Nicholls, I. A.; Rosengren, J. P. Molecular imprinting of surfaces, *Bioseparation,* 10 **(2001)**, 301-305.

100. Yan, C. L.; Lu, Y. Two-dimensional imprinting of protein molecules, *Prog Chem,* 20 **(2008)**, 969-974.

101. Shiomi, T.; Matsui, M.; Mizukami, F.; Sakaguchi, K. A method for the molecular imprinting of hemoglobin on silica surfaces using silanes, *Biomaterials,* 26 **(2005)**, 5564-5571.

102. Kempe, M.; Glad, M.; Mosbach, K. An approach towards surface imprinting using the enzyme ribonuclease A, *J Mol Recognit,* 8 **(1995)**, 35-39.

103. Du, X. Z.; Hlady, V.; Britt, D. Langmuir monolayer approaches to protein recognition through molecular imprinting, *Biosens Bioelectron,* 20 **(2005)**, 2053-2060.

104.   Rachkov, A.; Minoura, N. Recognition of oxytocin and oxytocin-related peptides in aqueous media using a molecularly imprinted polymer synthesized by the epitope approach, *J Chromatogr A,* 889 **(2000)**, 111-118.

105.   Rachkov, A.; Minoura, N. Towards molecularly imprinted polymers selective to peptides and proteins. The epitope approach, *Biochim Biophys Acta - Prot Struc Mol Enzymol,* 1544 **(2001)**, 255-266.

106.   Ramström, O.; Ansell, R. J. Molecular imprinting technology: Challenges and prospects for the future, *Chirality,* 10 **(1998)**, 195-209.

107.   Hjerten, S.; Liao, J. L.; Nakazato, K.; Wang, Y.; Zamaratskaia, G.; Zhang, H. X. Gels mimicking antibodies in their selective recognition of proteins, *Chromatographia,* 44 **(1997)**, 227-234.

108.   Liao, J.; Wang, Y.; Hjertén, S. A novel support with artificially created recognition for the selective removal of proteins and for affinity chromatography, *Chromatographia,* 42 **(1996)**, 259-262.

109.   Holliger, P.; Hudson, P. J. Engineered antibody fragments and the rise of single domains, *Nat Biotechnol,* 23 **(2005)**, 1126-1136.

110.   Jiskoot, W.; Teerlink, T.; Beuvery, E. C.; Crommelin, D. J. A. Preparation of liposomes via detergent removal from mixed micelles by dilution, *Pharmacy World & Science,* 8 **(1986)**, 259-265.

111.   Paternostre, M. T.; Roux, M.; Rigaud, J. L. Mechanisms of membrane protein insertion into liposomes during reconstitution procedures involving the use of detergents. 1. Solubilization of large unilamellar liposomes (prepared by reverse-phase evaporation) by triton X-100, octyl glucoside, and sodium cholate, *Biochemistry,* 27 **(1988)**, 2668-2677.

112.   Rigaud, J.-L.; Pitard, B.; Levy, D. Reconstitution of membrane proteins into liposomes: Application to energy-transducing membrane proteins, *Biochim Biophys Acta (BBA) - Bioenergetics,* 1231 **(1995)**, 223.

113.   Schillemans, J. P. Charged hydrogels for post-loading, release, and molecular imprinting of proteins. Utrecht University, Utrecht, 2010.

114.   Stiles, P. L. Direct deposition of micro- and nanoscale hydrogels using dip pen nanolithography (dpn), *Nat Meth,* 7 **(2010)**.

115.   Hong, Y.; Krsko, P.; Libera, M. Protein surface patterning using nanoscale PEG hydrogels, *Langmuir,* 20 **(2004)**, 11123-11126.

116.   Saaem, I.; Papasotiropoulos, V.; Wang, T.; Soteropoulos, P.; Libera, M. Hydrogel-based protein nanoarrays, *J Nanosci Nanotechnol,* 7 **(2007)**, 2623-2632.

117.   Shi, H.; Tsai, W. B.; Garrison, M. D.; Ferrari, S.; Ratner, B. D. Template-imprinted nanostructured surfaces for protein recognition, *Nature,* 398 **(1999)**, 593-7.

118.   El Kirat, K.; Bartkowski, M.; Haupt, K. Probing the recognition specificity of a protein molecularly imprinted polymer using force spectroscopy, *Biosens Bioelectron,* 24 **(2009)**, 2618-2624.

DETERGENT MEDIATED RECONSTITUTION OF HEMAGGLUTININ IN SUPPORTED LIPID BILAYERS

- ELLEN VERHEYEN - FRITS M. FLESCH - ARJAN BOERKE -

- BART M. GADELLA - WIM E. HENNINK - CORNELUS F. VAN NOSTRUM -

ABSTRACT

For the preparation of surface imprinted polymers of membrane proteins, it is essential that the membrane protein is available in its native conformation, i.e. embedded in a lipid bilayer. Therefore we describe here the optimization of a method for detergent mediated reconstitution of a model membrane protein, hemagglutinin, in preformed lipid bilayers deposited on solid supports (mica and glass). First, the stability of the bilayer in presence of detergents was evaluated by atomic force microscopy and a lipid adsorption assay, to determine the detergent concentration that could be used to promote the protein insertion without solubilizing the lipid bilayer. For simultaneous evaluation of different parameters involved in the reconstitution process, i.e. detergent type and concentration, protein concentration and incubation time, the method was adapted to a 96 well plate format. The reconstituted hemagglutinin was detected via a specially developed detergent free ELISA assay. This approach is very simple, versatile and moreover a very quick manner to optimize the method for reconstitution of an individual membrane protein. The method described in this chapter to reconstitute proteins in lipid bilayers can be used to screen different imprint parameters to finally obtain surface imprinted polymers with the desired binding characteristics for a given membrane protein.

INTRODUCTION

The natural environment of membrane proteins, i.e. the biological membrane, is highly specialized and very complex, as many proteins and other molecules are present, which all interact[1, 2]. For the preparation of membrane protein imprinted polymers, containing surface imprints of the desired protein only, there is a need for "simple" model cell membranes in which the target membrane protein is reconstituted. In this light, solid supported lipid membranes are very interesting as they provide a natural environment for the immobilization of membrane proteins under non-denaturing conditions in a well defined orientation. Imprints of the membrane protein on the solid support can then be made by adding a solution of monomers and crosslinker on top of the bilayer with reconstituted protein (see general introduction). After polymerization, the supported bilayer and proteins are removed, resulting in a thin polymer layer, containing the imprint of the extracellular domain of the membrane protein on its surface. The imprinted surface should now be capable of rebinding the target membrane protein with high selectivity.

In the early 80's, the first artificial cell membrane was introduced by Brian and McConnell[3]. Since their pioneering work, supported lipid-protein bilayers have been intensively and widely investigated as general and versatile model of cell membranes and different methods for functional reconstitution have been developed[4-14]. Brian and McConnell introduced the use of proteoliposomes, i.e. lipid vesicles with incorporated protein, which fuse spontaneously with a solid surface to form supported protein-lipid membranes[3, 10, 12, 15-17]. The major drawback of using proteoliposomes is that the proteins can be randomly oriented in the lipid bilayer of the liposomes (outside-out or outside-in), which makes unidirectional orientation of the protein in the supported lipid bilayer impossible[12, 13, 16]. To circumvent this, a new method has been developed, where the proteins are first immobilized in a controlled way on the surface, after which the lipid bilayer is reconstituted around the proteins[5, 13, 18]. This specific binding can be directed by modifying the surface with nitrilotriacetic moieties (NTA), to which HIS-tagged proteins can selectively bind. However, one has to be aware that by introduction of a HIS-tag, the protein function can be altered[5, 18]. Other possibilities for unidirectional immobilization of proteins are by orienting the protein via electrostatic interactions and by introducing charges (positive or negative) on the surface by specific coating[13]. These methods however are not widely used and fully developed yet.

Another method to prepare lipid bilayers with incorporated membrane proteins that receives increasing attention is detergent mediated protein reconstitution into preformed supported lipid bilayers (SLB)[4, 7-9, 19]. The principle is derived from the method used for reconstitution of membrane proteins in liposomes[20-23] and three consecutive steps can be distinguished. First, a lipid bilayer is formed on a surface by spontaneous fusion of small unilamellar vesicles[24], next a membrane protein solubilized in a detergent solution is added to the preformed bilayer and then after incubation, the excess of protein and detergent is removed by gentle rinsing, resulting in a SLB protruded with membrane proteins. The exact mechanism is not fully clear yet, but it is assumed that the detergent temporally destabilizes the bilayer, thereby loosening its structure and thus facilitating the protein insertion[4, 8]. Sugar-based detergents such as N-octyl-β-glucoside (OG) and dodecyl-β-D-thiomaltoside (DOTM) are frequently used to destabilize lipid bilayers. At present, there is no general protocol available and it is therefore necessary to optimize the protocol for each individual protein, as the characteristics of the obtained membrane is influenced by protein, lipids and the type of detergent, as well as their concentrations[4, 8]. As there are many variables involved, our aim was to set up a method which allows fast and simultaneous comparison of different variables, by using 96 well plates, in order to establish the right conditions (detergent type and concentration in protein-detergent mixture) for reconstituting a specific protein in a short time frame.

First, we visualized the bilayer formation on a microscopic scale with atomic force microscopy (AFM), to determine whether the chosen lipid composition led indeed to the formation of continuous bilayers. As we were using detergent for the reconstitution of membrane proteins, the next step was to assess whether the bilayers were not solubilized in presence of the detergent concentrations that were used in the reconstitution protocol. This was visually evaluated for N-octyl-β-glucoside (OG) by time-laps AFM, and quantitatively assessed for both N-octyl-β-glucoside (OG) and dodecyl-β-D-thiomaltoside (DOTM) by determining the amount of lipid remaining on the glass surface after incubation with the detergents in a well plate assay. Next, the detergent mediated reconstitution of hemagglutinin (HA) was evaluated with AFM. Hemagglutinin, a membrane protein of the influenza virus, was chosen as model protein, as it has a large extracellular domain, which makes it an excellent template for surface imprinting in a later stage. HA consists of two disulfide-linked polypeptide chains, HA1 and HA2, with molecular masses of 58 and 26 kDa, respectively[25-27]. Influenza HA exists as a trimer with a

length of 13.5 nm, from which 7.6 nm extends from the membrane surface, and a radius varying from 1.5 to 4 nm, as determined by X-ray diffraction[25-27].

The method for reconstitution of influenza HA was adopted to be used in a 96 well plate format, and ELISA was used to detect the reconstituted protein. Because detergents (e.g. Tween® 20) that are used in a standard ELISA protocol solubilize the bilayer[28], we developed a new detergent-free ELISA method. After optimizing the reconstitution protocol, the same array format can also be used for screening different parameters involved in protein imprinting to obtain surface imprinted polymers with the desired binding characteristics.

MATERIALS AND METHODS

Materials

All materials were obtained from commercial sources. Linbro 7X® was purchased from MP Biomedicals (Ohio, USA). Egg phosphatidylglycerol (EPG) and dioleoylphosphatidylcholine (DOPC) were obtained from Lipoid GmbH (Ludwigshafen, Germany) and cholesterol (CHOL) was purchased from Sigma-Aldrich (Zwijndrecht, The Netherlands). Glass bottom 96 well plates were obtained from Greiner Bio-one B.V. (Alphen a/d Rijn, The Netherlands). Mica discs (Grade V-4 Muscovite, thickness 0.15 mm, diameter 9.5 mm) were purchased from SPI supplies (West Chester, USA). Polyclonal goat anti-influenza A H1N1 was obtained from AbD Serotec (Dusseldorf, Germany). Rabbit polyclonal anti-goat antibody, labeled with horse radish peroxidase (HRP), was obtained from Abcam (Cambridge, UK).

Hemagglutinin

Influenza virus hemagglutinin (HA, strain A/New Caledonia/20/1999 (H1N1)) was a generous gift from Solvay Pharmaceuticals (Weesp, the Netherlands). The protein stock solution (1.5 µM HA) in phosphate buffered saline, containing sodium deoxycholate to keep the protein solubilized, was stored at 4°C. Besides HA, also a small amount of lipids (total lipid = 10 µM) was present. The HA solution was concentrated using Macrosep® centrifugal concentrators (30 kDa cut-off, Pall Gelman laboratory, New York, USA) to a final protein concentration of ~15 µM and subsequently purified by dialysis (cut-off 20 kDa) against HEPES buffered saline (10 mM HEPES, 150 mM NaCl, pH 7.4, HBS) containing 24 mM N-octyl-β-glucoside (OG) to keep the

hemagglutinin solubilized. It is known that in absence of detergent and lipids, HA will form rosettes (complexes of five to six HA trimers) that will sediment[29]. SDS-gel electrophoresis after purification showed only two bands, corresponding with HA1 (58 kDa) and HA2 (26 kDa).

Preparation and characterization of lipid vesicles

For the preparation of small unilamellar vesicles (SUVs), appropriate amounts of dioleoylphosphatidylcholine (DOPC), egg phosphatidylglycerol (EPG) and cholesterol (CHOL) (molar ratio 4:1:1), were dissolved in chloroform in a round-bottom flask (final concentration 2 mM total lipid). A lipid film was prepared by evaporation of the solvents under reduced pressure using a rotary evaporator and dried further under a stream of nitrogen. Liposomes were formed by hydration of the lipid film (around 10 μmol of lipids with 5 mL HBS). The liposomal dispersion was sequentially extruded through polycarbonate membrane filters (Osmonic, Livermore, CA, USA) with pore sizes varying from 0.2 to 0.03 μm using Lipex high-pressure extrusion equipment (Northern Lipids, Vancouver, Canada). The phospholipid concentration of the liposomal formulation was determined by the colorimetric method of Rouser *et al.*[30]. The mean particle size and size distribution of the liposomes were determined by dynamic light scattering with a Malvern 4700 system (Malvern Ltd., Malvern, UK).

Substrate preparation

Mica discs were used after freshly cleaving, without further surface treatment. Glass bottom 96 well plates were washed with Linbro 7X® glass cleaning solution, followed by extensive rinsing with RO-water. Next, the wells were rinsed three times with methanol and subsequently dried under nitrogen stream for one hour.

Formation of supported lipid bilayers on mica

Supported lipid bilayers (SLBs) were formed on mica using the vesicle fusion method[3], with some modifications. Mica discs (diameter 9.5 mm) were glued onto a Teflon disc (diameter 15 mm) with water-insoluble epoxy (Bison, Goes, The Netherlands). Next, the SUVs were diluted to 20 or 2 μM total lipid in HBS containing 10 mM $CaCl_2$ (Ca^{2+}-HBS) and 100 μL of each dilution was deposited onto freshly cleaved mica discs. The mica discs were transferred into a closed glass container that was subsequently sealed with silicon to prevent evaporation of water. The

SUVs were allowed to adsorb and fuse on the mica surface for one or two hours at 37 or 60°C. Next the samples were cooled to room temperature and subsequently rinsed five times with 1 mL Ca^{2+}-HBS to remove unbound SUVs. The supported bilayers were stored in Ca^{2+}-HBS. Prior to imaging, the Teflon discs were glued to steel discs and mounted onto the AFM stage. To keep the bilayer hydrated during imaging, 100 µL of Ca^{2+}-HBS was added on top of the bilayers.

Atomic Force Microscopy (AFM)

Surface characteristics of supported lipid bilayers

After the formation of the SLBs, surface images were acquired with a Nanoscope IV multimode instrument (Veeco, Santa Barbara, CA), equipped with a 12 µm piezoscanner (E-scanner). Contact mode imaging and nanoshaving were performed with 350 µm standard contact mode tips with a nominal force constant of 0.03 N/m (CSG01, NT-MDT, Micromash, Moscow, Russia). Contact mode imaging was carried out in Ca^{2+}-HBS. To avoid artifacts induced by the tip during scanning, the applied forces were kept below 100 pN[31]. In order to measure the bilayer thickness, a part of the bilayer was removed by nanoshaving. With this technique a high local force (300 nN) is applied to the sample resulting in displacement of surface-adsorbed lipids[32]. Therefore a small area of 0.75 x 0.75 µm was scanned 10 times with high force, and subsequently an image of 2 x 2 µm was scanned with a very low force (< 100 pN). The AFM images were processed using the Nanoscope IIIa software. A first-order flattening was applied to the images[33, 34].

Reversible solubilization of SLBs by N-octyl-β-D-glucoside

The stability of SLBs in presence of 4 mM N-octyl-β-D-glucoside (OG) was investigated with a Nanoscope IIIa (Digital Instruments, Santa Barbara, USA). A 12 µm piezoscanner (E-scanner) was employed and NP-SST20 (silicon nitrite) cantilevers (Veeco, Santa Barbara, USA) were used to image the surface in tapping mode in buffer. The scan rate was 9 Hz and the amplitude 0.38-0.42 V for all recordings. As reference, the initial bilayer was imaged in 100 µL Ca^{2+}-HBS (image size 1 x 1 µm). Next, 20 µL of an OG solution with a concentration at the CMC (24 mM) was added to the bilayer and consecutive topographic scans of the same area were recorded during 30 minutes. The AFM images were processed using the Nanoscope IIIa software. A first-order flattening was applied to the images[33, 34].

Detergent mediated reconstitution of hemagglutinin in SLBs

Hemagglutinin (HA) was reconstituted in preformed SLBs by detergent mediated post-insertion[6, 8], using N-octyl-β-D-glucoside (OG) as detergent. In detail, after formation of the SLBs on the mica surface as described above, 100 μL of a protein-detergent solution (0.1 μM HA, 3 mM OG in Ca^{2+}-HBS) was added to the SLB. This volume was sufficient to cover the complete surface. Next, the mica discs were transferred into a closed glass container that was subsequently sealed with silicon to prevent evaporation of water. The samples were incubated for one hour at 37°C under gentle agitation to allow protein incorporation into the SLB. The samples were allowed to cool to room temperature and subsequently rinsed five times with 1 mL Ca^{2+}-HBS to remove the detergent and the excess of protein. The presence of hemagglutinin in the supported lipid bilayers was investigated by AFM in tapping mode, as described above. To prevent drying of the bilayer during imaging, 100 μL of Ca^{2+}-HBS was added on top of the bilayers. Processing of the AFM images was done using the Nanoscope IIIa software. A first-order flattening was applied to the images as described in the previous section.

Development of screening method in 96 well plates

Bilayer formation in 96 well plates

Cleaned glass bottom 96 well plates were coated with a lipid bilayer by the vesicle fusion method (vide supra). In detail, 80 μL of a SUV suspension in Ca^{2+}-HBS (35 μM total phospholipid) was added to each well and incubated for two hours at 60°C. Next, the wells were gently washed by rinsing five times with Ca^{2+}-HBS and stored in the same buffer at room temperature until use. To determine the amount of lipids adsorbed onto the well surface, the bilayer was removed from the wells by adding three times 100 μL of methanol. The methanol fractions were collected and the phospholipid concentration in these fractions was determined by the procedure of Rouser[30].

Effect of detergents on bilayer stability

The solubilizing effect of detergents on SLBs was assessed by incubating SLBs with different detergents; N-octyl-β-D-glucoside (OG) and dodecyl-β-D-thiomaltoside (DOTM). The detergent concentrations are expressed as % of the corresponding critical micellar concentration (CMC), i.e. 24 mM and 0.05 mM for OG[35] and DOTM[36], respectively. The detergent solutions were

diluted with Ca^{2+}-HBS to 12%, 100% and 200% of their CMC and 80 µL of each dilution was added to preformed lipid bilayers in a 96 well plate, and incubated for one hour at 37°C. Next, the wells were rinsed five times with Ca^{2+}-HBS to remove the unbound lipids. The lipids remaining on the glass surface were solubilized and collected by rinsing the wells three times with 100 µL methanol. The phospholipid content in the methanol fractions was determined by the procedure of Rouser[30]. The amount of lipid remaining after incubating bilayers with buffer only were used as a reference (Remaining lipid= 100%).

Reconstitution of hemagglutinin in preformed SLBs

Hemagglutinin (HA) was reconstituted in preformed SLBs by detergent mediated post-insertion[6, 8] using N-octyl-β-D-glucoside (OG) and dodecyl-β-D-thiomaltoside (DOTM) as detergents. In detail, 80 µL of a hemagglutinin solution of different concentrations (0-0.08 µM in Ca^{2+}-HBS), with or without additional detergent (OG or DOTM) in varying concentrations (0-100% with respect to the CMC) was added to preformed bilayers in a 96 well plate. As the stock solution of HA contains 24 mM OG, the final detergent concentration was not exactly 0% - 100% with respect to CMC but, depending on the dilution of HA, slightly higher (max. 0.5% higher than stated). The well plate was incubated for 45 minutes or 12 hrs at 37°C under gentle stirring. Next, the wells were rinsed with Ca^{2+}-HBS to remove not inserted hemagglutinin. The relative amount of inserted or adsorbed protein was determined by a specially developed ELISA assay (*vide infra*).

ELISA on lipid-protein bilayers

To detect the hemagglutinin reconstituted in preformed bilayers, a detergent-free ELISA protocol based on a standard direct ELISA protocol[28] was developed. In detail, after reconstitution of HA (*vide supra*), nonspecific binding places were blocked with bovine serum albumin (200 µL 1% BSA in Ca^{2+}-HBS). The blocking proceeded overnight at 4°C. Next, the blocking solution was removed by decanting and the surfaces were washed three times with 200 µL Ca^{2+}-HBS, followed by decanting. The primary antibody (anti-influenza A H1N1, 1 mg/mL in PBS) was 1/3000 diluted in Ca^{2+}-HBS containing 0.1% BSA (ELISA buffer), and 100 µL of this buffer was added to each well followed by one hour incubation at 37°C. To remove unbound primary antibody, the wells were rinsed 10 times with ELISA buffer. Next, 100 µL of

the secondary antibody (anti-goat HRP, 1 mg/mL) solution, 1/8000 diluted in ELISA buffer, was added to the wells and incubated for one hour at 37°C. Subsequently, the wells were washed 10 times with 200 μL ELISA buffer to remove the excess of secondary antibody. Detection of the bound secondary antibodies, and thus the reconstituted proteins, was done by adding the 3,3',5,5'-tetramethylbenzidine, a soluble colorimetric substrate for horseradish peroxidase (HRP). The enzymatic conversion of the substrate was stopped after 10 minutes by adding 10 μL of 2 M H_2SO_4 and the absorbance at 450 nm was measured with a Bio-Rad Novapath microplate reader (Biorad Laboratories, Veenendaal, The Netherlands).

RESULTS

Deposition of lipid bilayers on mica

Suported lipid bilayers were deposited on mica by spontaneous fusion of vesicles as described by Tamm and McConnell[24] and studied with AFM. Small unilamellar vesicles (SUVs) composed of DOPC, EPG and cholesterol (4:1:1), obtained by extrusion, had an average diameter of 62 nm (polydisersity index = 0.09). This size is within the range (50-100 nm) which has been determined to be critical for vesicle rupture and subsequent fusion on the surface[37]. Adhesion of the negatively charged SUVs (EPG has a negatively charged head group at physiological pH) to negatively charged mica and subsequent rupture was promoted by adding Ca^{2+}-ions which reduce the repulsive electrostatic forces between the SUVs and mica surface[24, 37-39]. The optimal conditions for bilayer formation were determined by varying (1) the total phospholipid concentration (TL, 2 and 20 μM), (2) the incubation time (one and two hours), and (3) the incubation temperature (37 and 60°C). AFM analysis showed that an incubation time of one hour was not sufficient to obtain complete coverage of the mica surface, whereas incubation for two hours at 60°C, and not 37°C, resulted in full coverage of the surface (data not shown). Figure 1 shows the surface images of supported lipid bilayers, obtained by incubating an SUV suspension (2 and 20 μM TL) with mica for two hours at 60°C. Given that the surface area taken by 1 lipid molecule is ~0.6 nm^2, theoretically 0.14 nmol lipid is needed to cover the mica disc completely (71 mm^2)[40]. When using a small excess of lipids (100 μL of 2 μM TL, i.e. ~0.20 pmol TL per mica disc), incomplete coverage of the mica surface was observed (Figure 1A). Interconnected microsized bilayer patches with several defects (holes) were deposited on

the surface. The height of the bilayer was measured ten times and determined to be 4.2 ± 0.4 nm, which is in line with previously reported heights of supported lipid bilayers[15, 37, 39]. Complete coverage of the mica substrate with a bilayer was achieved by incubating mica with an SUV suspension which was 10-fold higher in lipid concentration than theoretically needed for complete coverage of the surface (20 μM i.e. ~2 nmol per mica disc) (Figure 1B).
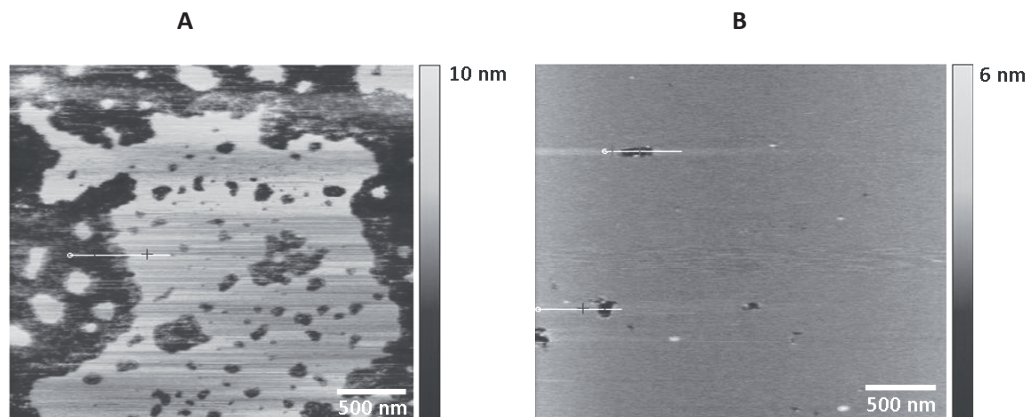
A   **B**

Figure 1. Topographical images of lipid bilayers deposited on mica surfaces by spontaneous fusion of SUVs. Bilayers were formed by adding 100 μL of a SUV suspension to freshly cleaved mica and incubating 2 h at 60°C. (A) Mica incubated with 2 μM SUV suspension resulted in big bilayer patches scattered over the mica surface (4.2 ± 0.4 nm difference in height). (B) After incubating with 20 μM SUV suspension, a nearly perfect supported lipid bilayer that fully covered the whole mica surface is formed. The vertical false-color scale represents the heights in the image, from 0 nm (dark colored area) to 6 nm (1B) or 10 nm (1A) (light colored area).

Depending on the type of lipids, as well as the buffer (high salt, presence of Ca^{2+}), the lipid vesicles will interact differently with the surface, and different surface coverages (single lipid bilayers or a single layer of intact vesicles) can be obtained[15, 37, 39, 41-43]. The SLB formation takes place in three subsequent steps. First, the vesicles approach the surface and adsorb to the surface, then the vesicles will fuse with each other, until the growing vesicles rupture and finally the lipid bilayer is formed by spreading of the ruptured versicles over the surface[37, 39, 42]. This has been visualized by AFM[37, 39], QCM[39] and fluorescence microscopy[41]. The combination of lipids used in this study and the presence of divalent ions (Ca^{2+}), will most likely lead to the formation of a single bilayer. To confirm that a single lipid bilayer was indeed deposited on the mica surface, and not multiple bilayer structures, a part of the SLB was displaced from the mica surface by nanoshaving[32], achieved by applying a high local pressure with the AFM tip on the surface. The pressure induces high shear forces during scanning, thereby displacing the lipids from the mica surface, resulting in a lipid-free area[32]. Figure 2 shows the surface image of a

bilayer after nanoshaving. A relatively small area (0.75 x 0.75 µm) was scanned consecutively while applying a high force on the surface. To visualize the effect of the nanoshaving, a larger area (5 x 5 µm), including the shaved area, was scanned with a much lower force. The shaved area was clearly visible as a dark sharp edged square of approximately 0.75 x 0.75 µm. The height difference between the lower (dark colored) part of the square (assumed to be bare mica) and the surrounding bilayer (light colored) was determined to be 5.2 nm, which corresponds to the height of one single bilayer (*vide supra*).
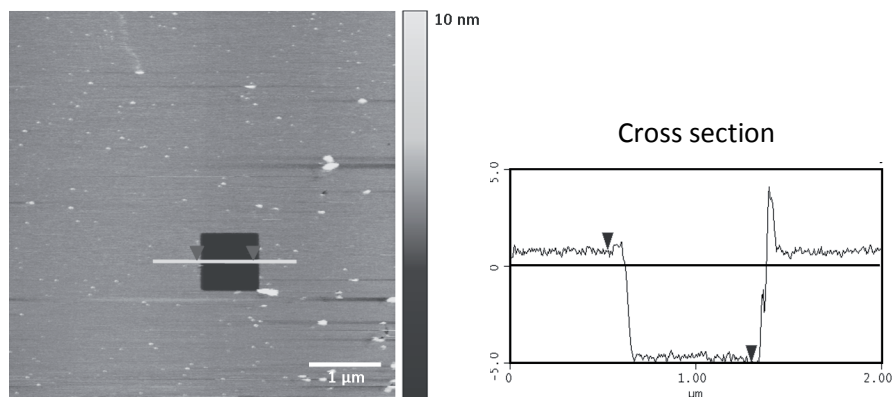

Figure 2. AFM analysis of a supported lipid bilayer after nanoshaving. By applying a high local force on the lipid surface, lipids are displaced from the mica surface, leaving a bilayer free mica surface (dark square). The height difference between the mica surface and the bilayer was determined by cross section analysis (right). The height difference between lipid free mica and the SLB was 5.2 nm. The scale of the vertical false color bar is 0 (dark) to 10 nm (light).

Stability of supported lipid bilayers in presence of detergent

The optimal experimental conditions for detergent mediated reconstitution of membrane proteins in preformed supported lipid bilayers were investigated. Sugar-based detergents such as N-octyl-β-D-glucoside (OG), with a relatively high critical micellar concentration (24 mM), and dodecyl-β-D-thiomaltoside with a low CMC (0.05 mM), have been frequently used for protein reconstitution into liposomal as well as solid supported lipid bilayers[4, 6, 8, 11, 44]. It is assumed that the detergent destabilizes the lipid bilayer, thereby temporally loosening the bilayer packing and thus facilitating the insertion of membrane proteins, but the full mechanism of this reconstitution method is not fully understood yet[4, 9]. It is however important to use a detergent concentration which is high enough to destabilize the bilayer and allowing insertion of the membrane protein of interest, without fully solubilizing it. To identify conditions under which

bilayers were not solubilized during the reconstitution process, first the stability of the SLB in presence of OG and DOTM at different concentrations was studied. Therefore, the method for bilayer formation was adapted to a 96 well plate format. The bilayers were deposited on the glass surfaces of the wells and detergent solutions of varying concentrations (0%, 6%, 12% and 100%, with respect to the CMC) were added to the preformed bilayers and incubated for one hour at 37°C. The amount of lipid that remained adsorbed to the surface after incubation was determined via a lipid adsorption assay (Figure 3). The lipid remaining on the surface after incubating with detergent free buffer was set as 100%.
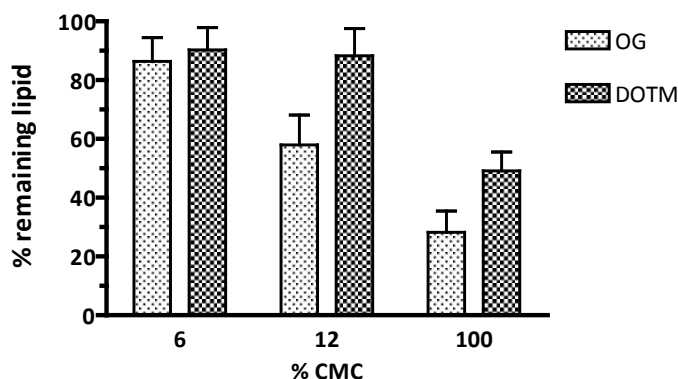

Figure 3. Relative amount of lipids remaining on the well surface after incubation with solutions with increasing concentrations (in % of CMC) of OG and DOTM. Data are expressed as mean ± SD (n=6).

After incubating the bilayers with both OG and DOTM at a concentration of 6% CMC, approximately 90% of the lipid remained adsorbed onto the surface of the well; a similar result was obtained after incubating with 12% DOTM. However, after incubation with OG at 12% CMC, only 58 ± 10% of the lipid remained deposited onto the surface. When adding a solution at 100% CMC, 30 ± 7% and 50 ± 6% of the lipids, for OG and DOTM respectively, remained attached to the well. When incubating the lipid bilayers with OG and DOTM at twice the CMC (200%), less than 10% (detection limit of method) of the initial amount of lipid was retrieved in the methanol wash fractions for both detergents, indicating that more than 90% of the lipids have been removed after incubation with the detergent and subsequent washing (data not shown). These results show that, when using detergent concentrations of 12% and 100% CMC for OG and DOTM respectively, bilayers were solubilized by the detergents and subsequently removed most likely as mixed micelles[21, 45, 46]. Moreover, it was shown that OG has

stronger solubilizing properties than DOTM, as OG already caused partial solubilization of the lipid bilayer at a concentration of 12% CMC, whereas after the addition of DOTM at 12% CMC, most of the lipids remained adsorbed to the glass surface. At this point, it is unclear whether a detergent concentration below or at 6% CMC (or ≤ 12% CMC in case of DOTM), at which the bilayer remains largely intact, is sufficient to temporally loosen the bilayer packing by insertion of detergent molecules in the bilayer, and thus facilitate the protein insertion.

Reversible bilayer solubilization by N-Octyl-β-D-Glucoside imaged by real time AFM

As there is insufficient insight on how the detergent mediates the reconstitution of membrane proteins, we assessed the effect of OG on the bilayer immediately after adding the detergent solution (final concentration 4 mM) to the SLB with AFM. This detergent concentration was chosen as it has been used for the successful reconstitution of membrane proteins in SLBs before[11, 44]. Figure 4A shows a typical topographic image of an SLB composed of DOPC:EPG:CHOL (4:1:1) deposited on mica and recorded in standard buffer (100 µL Ca^{2+}-HBS) before the addition of OG. The defect in the bilayer made it possible to measure the height difference between the surface and the covering layer, which was determined to be 4.2 ± 0.4 nm, indicating the presence of a single lipid bilayer[15, 37, 39]. Next, 20 µL of an OG solution at the CMC (24 mM) in Ca^{2+}-HBS was added to the bilayer, resulting in a final detergent concentration of 4 mM which is far below the CMC. Figure 4B-F, shows the consecutive AFM images of the same area (1 x 1 µm) at different time-points after adding the OG solution to the bilayer. Six minutes after exposing the SLBs to OG (Figure 4B), a localized lipid free area was detected, which grew in size during the next three minutes (Figure 4C). The cross section of the white line in Figure 4C is depicted in Figure 4G and illustrates that the height differences between valley and surrounding bilayer is 4.2 nm, indicating that the remaining surface coverage is still a single lipid bilayer[15, 37, 39]. It is assumed that detergent at concentrations far below their CMC temporally destabilize the bilayer, due to insertion of the detergent molecules, thereby loosening the densely packed bilayer structure[4, 8, 23]. However, here we observed very local solubilization of the lipid bilayer after adding the OG solution (final concentration 4 mM). This local effect could be due to local high OG concentrations, as there was no mixing step after addition of the detergent (20 µL of a OG solution at CMC = 24 mM). Interestingly, twelve minutes after exposing the bilayer to OG (Figure 4D), the lipid free area became smaller, possibly by re-depositing of lipids onto the bare surface[6, 47]. Another explanation is that lipids in supported lipid bilayers are mobile and can

move over the surface, resulting in (partial) healing of the bilayer coating[48, 49]. After 15 minutes, a bigger area was scanned (5 x 5 µm) to determine whether also other parts of the bilayer were solubilized (Figure 4E) and indeed, some other defects are visible. Within 30 minutes after adding the detergent solution, the defect areas were fully healed, yielding again a continuous bilayer (Figure 4F). This implies that adding a solution with a concentration of OG far below CMC to a supported bilayer has a transient solubilizing effect, which can be beneficial for reconstitution of membrane proteins in supported lipid bilayers.
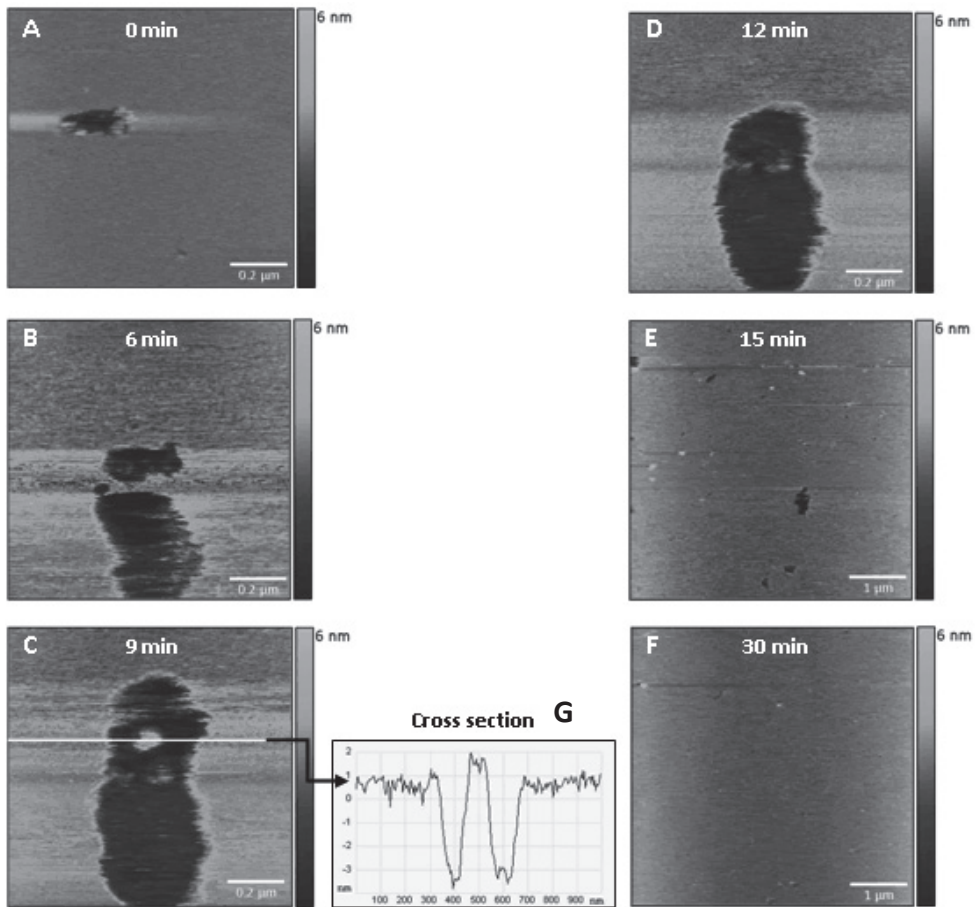

Figure 4. Effect of N-octyl-β-D-glucoside (OG), at a concentration of 4 mM on supported lipid bilayers. Consecutive AFM images of the same area are recorded in time. (A) Lipid bilayer before adding detergent (dark area: defect in bilayer, depth = 4.2 nm). Figures B to F were recorded on consecutive time-points after adding OG. (G) Represents the cross section of the white line in figure C. The scan size was 1 x 1 µm (A-D) and 5 x 5 µm (E, F). The scale of the vertical false color bar is 0 (dark) to 6 nm (light).

However, there are some contradictions with the results obtained with the lipid adsorption assay. With the latter one it was observed that an OG concentration of 3 mM (12% with respect to the CMC) resulted in an irreversible decrease (~40%) of the remaining amount of lipids adsorbed onto the wells. While with AFM, after adding a 20 µl of 24 mM solution of OG resulting in a final concentration of 4 mM (16% CMC), transient solubilization of the bilayer was observed, after which again a continuous bilayer was formed (Figure 4). Even though the detergent concentration was comparable for both AFM experiments and lipid adsorption assay (i.e. 4 mM and 3 mM respectively), it should be mentioned that the amount of detergent added to the same surface area is different. In the lipid adsorption assay, 80 µl of 3 mM OG (0.24 µmol) is added to a well surface of 34 mm^2, i.e. 7.1 nmol/mm^2 OG. Whereas to the mica disc (285 mm^2), 20 µl of 24 mM (0.48 µmol) is added, i.e. 1.7 nmol/mm^2 OG. Assuming that the amount of lipid per surface area unit is the same for both mica and glass surfaces (surface area of a single lipid molecule is ~0.6 nm^2), it can be calculated that the detergent/lipid ratio is ~4 times higher in the wells than on the mica surface. This means that more detergent molecules can penetrate the lipid bilayer, resulting in a stronger destabilization, and finally solubilization of the lipid bilayer.

Detergent mediated protein reconstitution in preformed SLBs

It is important to choose a detergent concentration which is low enough to avoid permanent solubilization and irreversible removal of the bilayer, but on the other hand the detergent concentration should be high enough to destabilize the bilayer and facilitate protein insertion[6, 50]. In this study, hemagglutinin (HA) was used as model membrane protein to evaluate the method of protein reconstitution into supported lipid bilayers. HA was incorporated in a preformed SLB deposited on mica by adding a solution of HA (0.1 µM solubilized in 3 mM N-octyl-β-D-glucoside (OG)) to a solid supported lipid bilayer. The detergent concentration (3 mM) was selected to induce transient destabilization of the SLB as described above, allowing the protein to be inserted in the bilayer. After removal of the detergent by rinsing with Ca^{2+}-HBS, AFM was used in tapping mode to image the membrane-reconstituted HA. The addition of OG-solubilized hemagglutinin to the supported lipid bilayer resulted in a protrusion of the bilayer with many particles, which were uniform in size (on average 2.1 ± 0.2 nm in height and 32.8 ± 4.2 nm in width; Figure 5) and speculated to be hemagglutinin. However, the dimensions as obtained from the AFM images are not consistent with those described in literature, i.e. for

the HA trimer a length of 13.5 nm, from which 7.6 nm extends from the membrane surface, with a radius varying from 1.5 to 4 nm, as determined by X-ray diffraction was reported[25-27]. It is hypothesized that the extracellular domain of the HA molecules is bend towards the bilayer surfaces, instead of fully protruding out into the aqueous phase. Another possibility is that due to interaction of the AFM tip with hemagglutinin, the extracellular domain of the protein is dragged sideward by the moving AFM tip, resulting in an incorrect representation of the inserted protein[51, 52]. These homogeneous particles were not detected after adding detergent only (Figure 4) which suggests that we successfully reconstituted hemagglutinin in supported lipid bilayers.
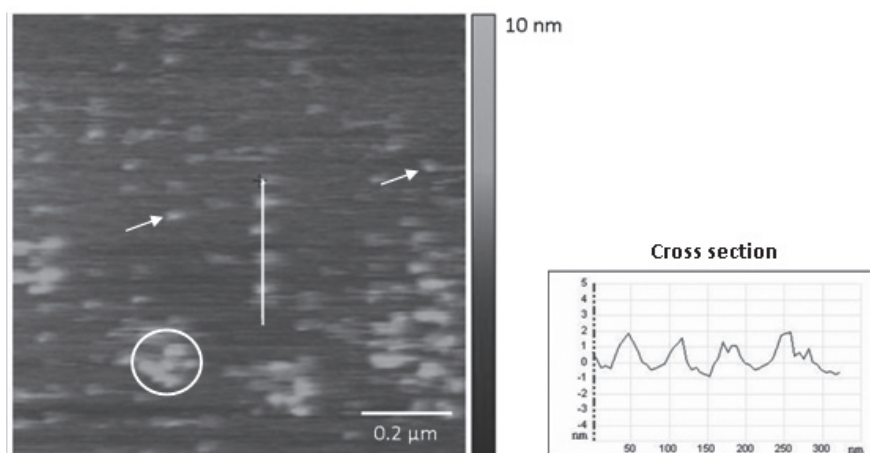

Figure 5. Topographic image of hemagglutinin (HA) inserted in a lipid bilayer via detergent mediated reconstitution. The bilayer was incubated with 0.1 µM HA solubilized in OG (3 mM) for one hour at room temperature. After detergent removal by rinsing with Ca^{2+}-HBS, the surface was imaged with AFM in tapping mode. The light dots (white arrows), are particles with an average height of 2.1 ± 0.2 nm and average width of 32.8 ± 4.2 nm, and were identified as hemagglutinin. Some regions of the bilayer show a dense protein packing (white circle). On the right, a cross section is presented (white line in AFM image). The scan size was 1 x 1 µm and the scale of the vertical false color bar is 0 (dark) to 10 nm (light).

High-throughput screening: Protein reconstitution in 96 well plates

As AFM is a time consuming (and expensive) technique which requires trained and experienced personnel, our goal was to develop a straight forward method that allows quick optimization of the method for protein reconstitution in supported bilayers. Therefore, the reconstitution method was adapted for reconstitution in a 96 well plate format. The parameters to be optimized were detergent type and concentration, incubation time as well as the optimal

protein concentration which results in maximum protein density. To this end, hemagglutinin was diluted in detergent solutions (OG and DOTM) of varying concentrations (0%, 6%, 12% and 100%, with respect to the CMC) and the concentration of the HA solutions was varied from 0.625 nM to 80 nM. As the HA stock solution contains OG at CMC (24 mM) to keep HA in solution, a solution without detergent cannot be realized, but it will always contain traces of OG (max. 0.5% in the solution with the highest HA concentration). The wells were first coated with lipid bilayers, as described in the Materials and Methods section, and subsequently the different HA solutions were added to the wells. The hemagglutinin inserted in the bilayer was detected via a detergent free ELISA assay. The optical density (λ = 450 nm) after substrate conversion by HRP was measured and the absorbance of wells to which no protein was added, was used to determine the background absorbance. The effect of incubation time (2 and 12 hours) on the amount of HA present in the wells was assessed, but no significant difference in absorbance at 450 nm was observed. Therefore, the incubation time was set to two hours. When the wells were incubated with solutions with increasing concentrations of HA, a higher absorption value was measured until a plateau value was reached when ~3 pmol HA was added (Figure 6).
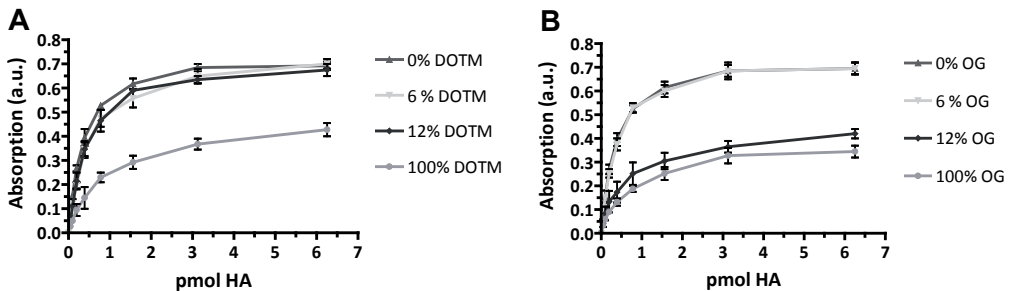

Figure 6. ELISA-absorption curves after incubating uncoated and bilayer coated wells with solutions of different concentrations of HA solubilized in different concentrations DOTM (A) and OG (B). The detergent concentrations are expressed as % in respect to the CMC. Data are presented as mean ± SD (n=3).

After incubating the bilayer with HA solutions in the presence of OG and DOTM at 6% CMC, we observed a similar absorption of the generated dye at 450 nm in the ELISA assay as when no additional detergent was used. This indicates that the concentration of OG present in the stock solution of HA (i.e. 0.12 mM (or 0.5% CMC) in case of the highest HA concentration) was already sufficient for insertion of HA in the bilayer and thus that a solution with higher detergent concentration does not result in a more efficient reconstitution of HA. From this we

may conclude that (partial) transient solubilization, as shown in Figure 4, is not necessary to allow insertion of the hemagglutinin in the lipid bilayers. Also DOTM at 12% CMC did not result in a more efficient reconstitution, indicating that (partial) solubilization, as shown in Figure 4, is not necessary for insertion of the hemagglutinin in the lipid bilayers. Also using DOTM at 12% CMC, did not result in a more efficient reconstitution. On the other hand, when adding solubilized HA in the presence of a solution of DOTM at the CMC (0.05 mM, i.e. 100%), the intensity of the absorption signal was significantly lower, indicating less protein was inserted into the lipid bilayer. Most likely the bilayer has been (partially) solubilized by the detergent, resulting in micelle formation. As a consequence, it can be expected that the hemagglutinin was entrapped in the micellar structures and removed from the well plate together with the lipid during rinsing after the incubation step. For OG, a similar decrease in protein insertion was already observed for a concentration of 12% CMC, indicating that OG has stronger solubilizing properties at concentrations far below the CMC than DOTM. This strong solubilizing effect of OG has been reported in previous studies with liposomes[21, 53] as well as with supported lipid bilayers[4, 8]. With the lipid adsorption assay (*vide supra*), it was also observed that these high detergent concentrations (12% and 100% CMC for OG and DOTM, respectively) resulted in a decrease of the remaining amount of lipids adsorbed onto the well surface, which indicates a correlation between both observations.

CONCLUSIONS

In this study, the use of detergents to facilitate the insertion of a model membrane protein, hemagglutinin, in supported lipid bilayers was investigated. It was demonstrated that the choice of detergent as well as its concentration are important variables in the optimization of the reconstitution protocol. The detergent concentration should be chosen carefully so it destabilizes the bilayer by local and transient solubilization, which can facilitate the protein insertion. On the other hand, complete solubilization has to be avoided by using solutions with sufficient low detergent concentrations or with weaker detergents. To detect the protein reconstituted in supported lipid bilayers, we developed an ELISA protocol avoiding the use of surfactants. This well plate format allows fast and parallel analysis of varying reconstitution methods. Moreover, after optimizing the reconstitution method, the array format can be applied for screening various imprint parameters for the development of surface imprinted

polymers containing imprints of the target membrane protein with the desired binding capacity and selectivity.

Acknowledgements

REFERENCES

1. Gennis, R. B., *Biomembranes: Molecular structure and function*. Springer-Verlag: London, **1989**.
2. Yeagle, P. L., *The structure of biological membranes*. 2 ed.; CRC Press: Boca Raton, **2005**; p 540.
3. Brian, A. A.; McConnell, H. M. Allogeneic stimulation of cytotoxic t cells by supported planar membranes, *Proc Natl Acad Sci U S A,* 81 **(1984)**, 6159-6163.
4. Berquand, A.; Lévy, D.; Gubellini, F.; Le Grimellec, C.; Milhiet, P.-E. Influence of calcium on direct incorporation of membrane proteins into in-plane lipid bilayer, *Ultramicroscopy,* 107 **(2007)**, 928-933.
5. Giess, F.; Friedrich, M. G.; Heberle, J.; Naumann, R. L.; Knoll, W. The protein-tethered lipid bilayer: A novel mimic of the biological membrane, *Biophys J,* 87 **(2004)**, 3213-3220.
6. Karlsson, O. P.; Löfås, S. Flow-mediated on-surface reconstitution of g-protein coupled receptors for applications in surface plasmon resonance biosensors, *Anal Biochem,* 300 **(2002)**, 132-138.
7. Ikematsu, M.; Sugiyama, Y.; Iseki, M.; Muneyuki, E.; Mizukami, A. Direct reconstitution of bacteriorhodopsin into planar phospholipid bilayers -- detergent effect, *Biophys Chem,* 54 **(1995)**, 155-164.
8. Milhiet, P.-E.; Gubellini, F.; Berquand, A.; Dosset, P.; Rigaud, J.-L.; Le Grimellec, C.; Lévy, D. High-resolution AFM of membrane proteins directly incorporated at high density in planar lipid bilayer, *Biophys J,* 91 **(2006)**, 3268-3275.
9. Milhiet, P.-E. G., MC; Baghdadi, O;Ronzon, F;Roux,B;Le Grimellec, C. Spontaneous insertion and partitioning of alkaline phosphatase into model lipid rafts., *EMBO Reports,* 3 **(2002)**, 485.
10. Puu, G. A., E.; Gustafson, I.; Lundstrom, M.; Jass, J. Distribution and stability of membrane proteins in lipid membranes on solid supports, *Biosens Bioelectron,* 15 **(2000)**, 31-41.
11. Rieu, J. R., F; Place, C; Dekkiche, F; Cross, B; Roux, B. Insertion of GPI-anchored alkaline phosphatase into supported membranes: A combined AFM and fluorescence microscopy study, *Acta Biochim Pol,* 51 **(2004)**, 189-197.
12. Salafsky, J. G., J.T.; Boxer, S.G. Architecture and function of membrane proteins in planar supported bilayers: A study with photosynthetic reaction centres, *Biochemistry,* 35 **(1996)**, 14773-14781.
13. Trepout, S.; Mornet, S.; Benabdelhak, H.; Ducruix, A.; Brisson, A. R.; Lambert, O. Membrane protein selectively oriented on solid support and reconstituted into a lipid membrane, *Langmuir,* 23 **(2007)**, 2647-2654.
14. Wagner, M. L.; Tamm, L. K. Tethered polymer-supported planar lipid bilayers for reconstitution of integral membrane proteins: Silane-polyethyleneglycol-lipid as a cushion and covalent linker, *Biophys J,* 79 **(2000)**, 1400-1414.
15. Jass, J. T., T. and Puu, G. From liposomes to supported, planar bilayer structures on hydrophilic and hydrophobic surfaces: An atomic force microscopy study, *Biophys J,* 79 **(2000)**, 3153-3163.
16. Puu, G.; Gustafson, I. Planar lipid bilayers on solid supports from liposomes - factors of importance for kinetics and stability, *Biochim Biophys Acta - Biomembranes,* 1327 **(1997)**, 149-161.
17. Zagnoni, M.; Sandison, M. E.; Marius, P.; Lee, A. G.; Morgan, H. Controlled delivery of proteins into bilayer lipid membranes on chip, *Lab on a Chip,* 7 **(2007)**, 1176-1183.
18. Ataka, K.; Giess, F.; Knoll, W.; Naumann, R.; Haber-Pohlmeier, S.; Richter, B.; Heberle, J. Oriented attachment and membrane reconstitution of his-tagged cytochrome *C* oxidase to a gold electrode: In situ monitoring by surface-enhanced infrared absorption spectroscopy, *J. Am. Chem. Soc.,* 126 **(2004)**, 16199-16206.
19. Davis, R. W.; Flores, A.; Barrick, T. A.; Cox, J. M.; Brozik, S. M.; Lopez, G. P.; Brozik, J. A. Nanoporous microbead supported bilayers: Stability, physical characterization, and incorporation of functional transmembrane proteins, *Langmuir,* 23 **(2007)**, 3864-3872.
20. Jiskoot, W.; Teerlink, T.; Beuvery, E. C.; Crommelin, D. J. A. Preparation of liposomes via detergent removal from mixed micelles by dilution, *Pharm World Sci,* 8 **(1986)**, 259-265.

21. Paternostre, M. T.; Roux, M.; Rigaud, J. L. Mechanisms of membrane protein insertion into liposomes during reconstitution procedures involving the use of detergents. 1. Solubilization of large unilamellar liposomes (prepared by reverse-phase evaporation) by triton X-100, octyl glucoside, and sodium cholate, *Biochemistry,* 27 **(1988)**, 2668-2677.

22. Rigaud, J.-L.; Levy, D.; Nejat, D., Reconstitution of membrane proteins into liposomes. In *Methods in enzymology*, Academic Press: **2003**; Volume 372, p 65.

23. Rigaud, J.-L.; Pitard, B.; Levy, D. Reconstitution of membrane proteins into liposomes: Application to energy-transducing membrane proteins, *Biochim Biophys Acta - Bioenergetics,* 1231 **(1995)**, 223-246.

24. Tamm, L. K.; McConnell, H. M. Supported phospholipid bilayers, *Biophys J,* 47 **(1985)**, 105-113.

25. Skehel, J. J.; Wiley, D. C. Influenza haemagglutinin, *Vaccine,* 20 **(2002)**, S51-S54.

26. Wilson, I. A.; Skehel, J. J.; Wiley, D. C. Structure of the haemagglutinin membrane glycoprotein of influenza virus at 3 Å resolution, *Nature,* 289 **(1981)**, 366-373.

27. Böttcher, C.; Ludwig, K.; Herrmann, A.; van Heel, M.; Stark, H. Structure of influenza haemagglutinin at neutral and at fusogenic pH by electron cryo-microscopy, *FEBS Letters,* 463 **(1999)**, 255-259.

28. AbD serotec Direct ELISA with streptavidin-biotin detection. http://www.abdserotec.com/support/recommended-protocols-658.html

29. Ruigrok, R. W.; Wrigley, N. G.; Calder, L. J.; Cusack, S.; Wharton, S. A.; Brown, E. B.; Skehel, J. J. Electron microscopy of the low pH structure of influenza virus haemagglutinin, *EMBO Journal,* 5 **(1986)**, 41-49.

30. Rouser, G.; Fkeischer, S.; Yamamoto, A. Two dimensional then layer chromatographic separation of polar lipids and determination of phospholipids by phosphorus analysis of spots, *Lipids,* 5 **(1970)**, 494-496.

31. Engel, A.; Schoenenberger, C. A.; Müller, D. J. High resolution imaging of native biological sample surfaces using scanning probe microscopy, *Curr Opin Struct Biol,* 7 **(1997)**, 279-284.

32. Liu, G.-Y.; Xu, S.; Qian, Y. Nanofabrication of self-assembled monolayers using scanning probe lithography, *Acc Chem Res,* 33 **(2000)**, 457-466.

33. Kiely, J. D.; Bonnell, D. A. In *Quantification of topographic structure by scanning probe microscopy*, The fourth international conference on nanometer-scale science and technology, Beijing (China), 1997; AVS: Beijing (China), **1997**; pp 1483-1493.

34. Ricci, D.; Braga, P. C. Recognizing and avoiding artifacts in AFM imaging, *Methods in molecular biology (Clifton, N.J.),* 242 **(2004)**, 25-37.

35. Lorber, B.; Bishop, J. B.; DeLucas, L. J. Purification of octyl β-d-glucopyranoside and re-estimation of its micellar size, *Biochim Biophys Acta - Biomembranes,* 1023 **(1990)**, 254-265.

36. Kühlbrandt, W. Three-dimensional crystallization of membrane proteins, *Q Rev Biophys,* 21 **(1988)**, 429-477.

37. Reviakine, I.; Brisson, A. Formation of supported phospholipid bilayers from unilamellar vesicles investigated by atomic force microscopy, *Langmuir,* 16 **(2000)**, 1806-1815.

38. Cremer, P. S.; Boxer, S. G. Formation and spreading of lipid bilayers on planar glass supports, *J. Phys. Chem. B,* 103 **(1999)**, 2554-2559.

39. Richter, R.; Mukhopadhyay, A.; Brisson, A. Pathways of lipid vesicle deposition on solid surfaces: A combined QCM and AFM study, *Biophys J,* 85 **(2003)**, 3035-3047.

40. De Young, L. R.; Dill, K. A. Solute partitioning into lipid bilayer membranes, *Biochemistry,* 27 **(1988)**, 5281-5289.

41. Johnson, J. M. H., Teakjip; Chu, Steve; Boxer, Steve. Early steps of supported bilayer formation probed by single vesicle fluorescence assays, *Biophys J,* 83 **(2002)**, 3371-3379.

42. Raedler, J.; Strey, H.; Sackmann, E. Phenomenology and kinetics of lipid bilayer spreading on hydrophilic surfaces, *Langmuir,* 11 **(1995)**, 4539-4548.

43. Richter, R. P.; Berat, R.; Brisson, A. R. Formation of solid-supported lipid bilayers: An integrated view, *Langmuir,* 22 **(2006)**, 3497-3505.

44. Alves, I. D.; Salgado, G. F. J.; Salamon, Z.; Brown, M. F.; Tollin, G.; Hruby, V. J. Phosphatidylethanolamine enhances rhodopsin photoactivation and transducin binding in a solid supported lipid bilayer as determined using plasmon-waveguide resonance spectroscopy, *Biophys J,* 88 **(2005)**, 198-210.

45. Almgren, M. Mixed micelles and other structures in the solubilization of bilayer lipid membranes by surfactants, *Biochim Biophys Acta - Biomembranes,* 1508 **(2000)**, 146-163.

46. Lichtenberg, D. Characterization of the solubilization of lipid bilayers by surfactants, *Biochim Biophys Acta - Biomembranes,* 821 **(1985)**, 470-478.

47. Grant, L. M.; Tiberg, F. Normal and lateral forces between lipid covered solids in solution: Correlation with layer packing and structure, *Biophys J,* 82 **(2002)**, 1373-1385.

48. Cremer, P. S.; Groves, J. T.; Kung, L. A.; Boxer, S. G. Writing and erasing barriers to lateral mobility into fluid phospholipid bilayers, *Langmuir,* 15 **(1999)**, 3893-3896.

49. Tawa, K.; Morigaki, K. Substrate-supported phospholipid membranes studied by surface plasmon resonance and surface plasmon fluorescence spectroscopy, *Biophys J,* 89 **(2005)**, 2750-2758.

50. Garner, A. E.; Alastair Smith, D.; Hooper, N. M. Visualization of detergent solubilization of membranes: Implications for the isolation of rafts, *Biophys J,* 94 **(2008)**, 1326-1340.

51. Müller, D. J.; Amrein, M.; Engel, A. Adsorption of biological molecules to a solid support for scanning probe microscopy, *J Struct Biol,* 119 **(1997)**, 172-188.

52. Müller, D. J.; Fotiadis, D.; Scheuring, S.; Müller, S. A.; Engel, A. Electrostatically balanced subnanometer imaging of biological specimens by atomic force microscope, *Biophys J,* 76 **(1999)**, 1101-1111.

53. Levy, D.; Gulik, A.; Seigneuret, M.; Rigaud, J. L. Phospholipid vesicle solubilization and reconstitution by detergents. Symmetrical analysis of the two processes using octaethylene glycol mono-n-dodecyl ether, *Biochemistry,* 29 **(1990)**, 9480-9488.

CHALLENGES FOR THE EFFECTIVE
MOLECULAR IMPRINTING OF PROTEINS

- ELLEN VERHEYEN[#] - JORIS P. SCHILLEMANS[#] - MARTIN VAN WIJK -

- MARIE-ASTRID DEMENIEX - WIM E. HENNINK - CORNELUS F. VAN NOSTRUM -

[#] Equal contribution

ABSTRACT

Molecular imprinting is a technique that is used to create artificial receptors by the formation of a polymer network around a template molecule. This technique has proven to be particularly effective for molecules with low molecular weight (< 1500 dalton), and during the past five years the number of research articles on the imprinting of larger (bio) templates is increasing considerably. However, expanding the methodology towards imprinted materials for selective recognition of proteins, DNA, viruses and bacteria appears to be extremely challenging. This paper presents a critical analysis of data presented by several authors and our own experiments, showing that the molecular imprinting of proteins still faces some fundamental challenges. The main topics of concern are proper monomer selection, washing method/template removal, quantification of the rebinding and reproducibility. Use of charged monomers can lead to strong electrostatic interactions between monomers and template but also to undesired high nonspecific binding. Up till now, it has not been convincingly shown that electrostatic interactions lead to better imprinting results. The combination of a detergent (SDS) and acetic acid, commonly used for template removal, can lead to experimental artifacts, and should ideally be avoided. In many cases template rebinding is unreliably quantified, results are not evaluated critically and lack statistical analysis. Therefore, it can be argued that presently, in numerous publications the scientific evidence of molecular imprinting of proteins is not convincing.

INTRODUCTION

Molecular imprinting is a technique used to create artificial receptors by the formation of a polymer network around a template molecule (Figure 1). In the pre-polymer mixture, several possible interactions, such as hydrophobic interactions, hydrogen bonds, Van der Waals forces and electrostatic interactions determine the spatial arrangement of monomers around the template. This spatial arrangement is then fixed by polymerization of monomers and crosslinker. Removal of the template leaves a chemically and sterically complementary void (imprint) in the polymer network, which is able to rebind the template.
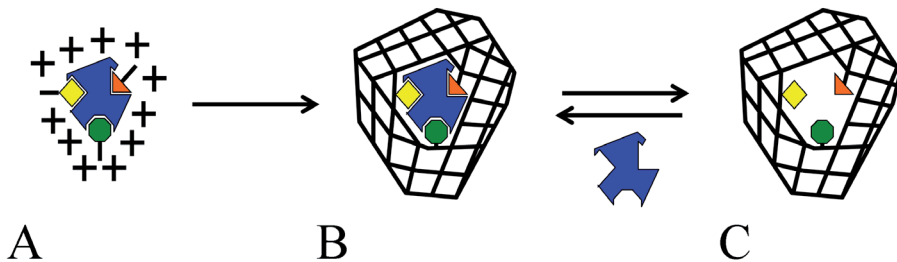

Figure 1. Schematic representation of the principle of molecular imprinting. (A) The template (shown in blue), (functional) monomers (shown in yellow, green and orange) and crosslinker (+) form a pre-polymerization complex. (B) Polymerization of monomers and crosslinker fixes the complex. (C) Removal of the template leaves rebinding cavities.

Although the first paper describing the formation of imprints was published in 1931[1], research on molecular imprinting was scarce until the 1980's. In an excellent and extensive review, Whitcombe *et al*. illustrated the maturation of the field by the dramatic increase in publications seen over the past 20 years (Figure 2A)[2]. From this and many other reviews that describe the progress made over the years, it becomes clear that molecular imprinting is a very promising and rapidly evolving technology, with many possible applications such as analytical separations, enzyme-like catalysis, chemical sensors and drug delivery[2-6].

Molecular imprinting has proven to be particularly successful for low molecular weight compounds[7-10]. Although imprinting of larger, more complex molecules such as proteins, DNA, and even whole cells and viruses has also been reported[11-14], the number of research papers using such templates is relatively small (Figure 2B).
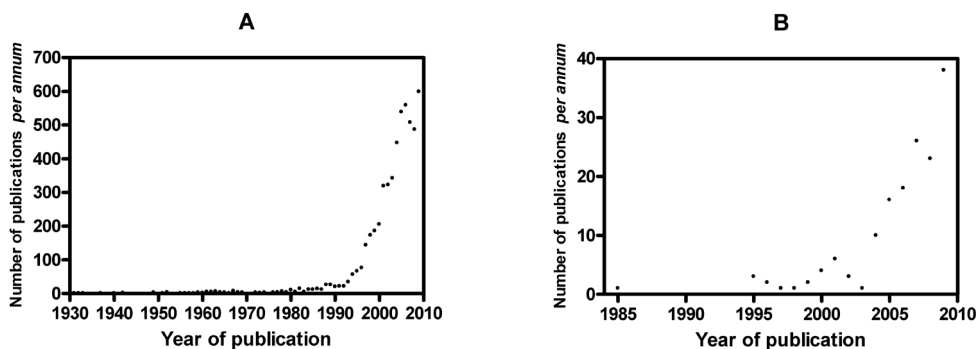
Figure 2. (A) The number of publications within the field of molecular imprinting science and technology per annum for the period 1931 – 2009 (adapted from [2] supplemented by data from [15]). (B) Number of research papers on biomacromolecular imprinting per annum for the period 1985 – 2009.

Till 2003, less than 10 research papers on imprinting of biomacromolecules were published per year, which reflects the difficulties faced when trying to imprint large and sensitive biomolecules[16, 17]. Firstly, for low molecular weight compounds, highly crosslinked gels are used to ensure preservation of the imprint cavity after removal of the template. However, for large template molecules, high crosslink densities seriously hinder mass transfer of the template, leading to slow template removal and rebinding kinetics or, in the worst case, permanent entrapment of the template in the polymer network due to physical immobilization. Additionally, crosslinking of the template to the network can also lead to chemical immobilization[18]. Secondly, due to the solubility properties and sensitive structural nature of biomacromolecules, imprinting can generally only be performed in aqueous environment, which limits the choice of monomers. Moreover, hydrogen bonding interactions strongly contribute to the affinity of molecularly imprinted polymers (MIPs) for low molecular weight compounds in organic, aprotic solvents, but are seriously hampered in water. Thirdly, biomacromolecules are highly complex. Physicochemical properties such as charge or hydrophobicity can strongly vary in different regions of e.g. the protein template, whereas similar regions may be present in other templates. This could lead to high nonspecific binding and cross-reactivity of the imprinted polymer. Despite the challenges, after an initial lag in biomacromolecule imprinting relative to the rest of the field (Figure 2), the number of papers has now begun to increase. Interestingly, Figure 3 shows that in recent years (2005-2009) the model proteins albumin, hemoglobin, and lysozyme are being used more frequently (54%) than in the period up to 2006 (44%). This is opposed to what can be expected from an emerging research field and illustrates that molecular imprinting

of proteins is still in its initial phase of development, where research is mostly focused on proof of concept using well defined, relatively stable and inexpensive model proteins.
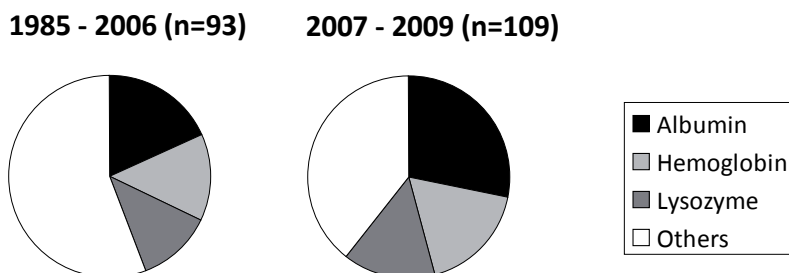
1985 - 2006 (n=93)   2007 - 2009 (n=109)

■ Albumin
▨ Hemoglobin
▨ Lysozyme
☐ Others

Figure 3. Relative frequency of the templates used in molecular imprinting of protein over the periods 1985 – 2006 and 2007 – 2009.

We believe that especially in this time of increasing research intensity, proof of concept, and setting of standards for future research, it is important to subject the published data to a critical review. Therefore, the aim of this paper is to critically analyze published data and conclusions in relation to our own experimental data. The articles discussed are selected on the basis of an extensive literature study on papers published between 2001 and 2009. We focused on the publications that contained sufficient data to allow proper analysis and recalculations. We would like to emphasize that the points raised in this chapter are only meant to initiate debate and it is not our intention to discredit anyone.

EXPERIMENTAL BASIS

Materials

Acrylamide (AAm, ultra pure) and *N,N'*-methylene-bis-acrylamide (MBA, ultra pure) were purchased from MP Biomedicals, methacrylic acid (MA, 99%), *N,N'*-bis(acryloyl) cystamine, fluorescein isothiocyanate (FITC), lysozyme from hen egg white (96381 U/mg), cytochrome C from bovine heart (purity >95%), hemoglobin from bovine blood (purity >90%), myoglobin from horse heart (purity >90%) and *N*-octyl β-D-glucopyranoside (OG) from Sigma-Aldrich. Acetic acid (AcOH), acrylic acid (AAc, synthesis grade) and *N,N*-dimethylformamide p.a. were obtained from Merck. *N,N,N',N'*-tetramethylethylenediamine (TEMED), ammonium peroxodisulfate (APS) and sodium dodecylsulfate (SDS) were obtained from Fluka. *N,N*-dimethylaminoethyl-

methacrylamide (DMAEMA) was obtained from Polysciences Europe GmbH. The Bio-Rad *DC* protein assay was purchased from Bio-Rad Labs. Dioleoylphosphatidylcholine (DOPC) was purchased from Lipoid GmbH, Triton X-100 (TX100) from BDH Laboratory Supplies, and Irgacure 2959 from Ciba Specialty Chemicals. Lipid II, a bacterial membrane-associated peptidoglycan precursor[19], was kindly provided by Dr. E. Breukink (Utrecht University). FITC labeled lysozyme was synthesized as described before[20]. In detail: 300 mg lysozyme was dissolved in 50 mL borate buffer (100 mM, pH 9). While stirring, 0.28 mL FITC solution (10 mg/mL in DMF, FITC:lysine mol ratio 1:20) was added drop-wise to the lysozyme solution and the resulting mixture was stirred for one hour at room temperature. Next, the pH was adjusted to 7.2 by adding boric acid and the protein solution was filtered (0.2 μm). Finally, the solution was extensively dialyzed against water (1 week, at 4°C) to remove unreacted FITC and the FITC-lysozyme was collected after freeze-drying.

Surfaces coated with a lysozyme imprinted polyacrylamide hydrogel layer

The method was adopted from Matsunaga *et al.*[21]. First, the gold surface of surface plasmon resonance (SPR) chips (1 by 1 cm, Biacore) was modified with vinylgroups by incubation for 30 minutes with 5 mM bisacryloylcystamine in methanol. Next, chips were washed five times with methanol and RO-water. The pre-polymer mixture was prepared by dissolving 72.2 mg AAm, 13.6 mg MBA, 12 μL AAc (10% w/w in 10 mM HEPES, pH adjusted to pH 7.4, molar ratio AAm:MBA:AAc = 11:1:0.2) and 50 mg lysozyme in a total volume of 1 mL 10 mM HEPES (pH 7.4). Neutral pre-polymer mixtures were prepared without adding AAc. After flushing with nitrogen for five minutes, 10 μL APS (10 % w/w) was added. The components were mixed and 50 μL of the mixture was pipetted onto the gold surface, and allowed to polymerize for three hours at 37°C. The surfaces were washed with three times 5 mL 1 M NaCl and three times 5 mL RO-water to remove the template. Non-imprinted polymers were prepared in the same way, without adding lysozyme. Rebinding was studied by adding 40 μL of a 30 mg/mL FITC-lysozyme solution in 10 mM HEPES pH 7.4 to the surfaces. After 1.5 h incubation at room temperature, the surfaces were rinsed three times with 10 mM HEPES (pH 7.4) to remove unbound protein. Bound FITC-lysozyme was visualized using a Nikon TE-2000 inverted fluorescence microscope (Nikon Europe).

Preparation and analysis of cytochrome C imprinted hydrogels

The synthesis was done according to Kimhi and Bianco-Peled[22]. In detail, 0.86 g AAm, 0.2 g MBA, 1.025 mL MA and 2.05 mL DMAEMA (molar ratio AAm:MBA:MA:DMAEMA =10:1:10:10) and 0.2 g cytochrome C were dissolved in 10 mM HEPES buffer (final volume 10 mL, pH adjusted to 7.4). The pre-polymer mixture was flushed with nitrogen for 10 minutes to remove oxygen. Next, 0.70 mL APS (1.5% w/w in RO-water) and 0.56 mL TEMED (3.75% in 10 mM HEPES buffer, pH adjusted to 7.4) were added to initiate polymerization. The gels were allowed to polymerize overnight at room temperature and subsequently ground by using an IKA® Ultra-turrax tube drive, and wet-sieved through a 80 µm sieve. The template was removed from the granulated gel particles by successive washing with 100 mL RO-water, 100 mL 1 M NaCl, 100 mL 10% SDS:AcOH and 200 mL RO-water. The protein concentration in the wash fractions was determined with the Bio-Rad *DC* protein assay, using the microplate-assay procedure[23]. Next, the particles were freeze-dried and stored at room temperature. Non-imprinted polymers were prepared in the same way without adding cytochrome C.

The rebinding was done with 50 mg dry particles, which were hydrated with 1 mL TRIS buffer pH 8, prior to the addition of 4 mL cytochrome C or lysozyme solution (final concentration ranging from 0.5 to 4 mg/mL). After overnight incubation on a roller bench at room temperature, the particles were allowed to sediment (visually completely sedimented within 10 minutes) and the protein remaining in the supernatant was determined spectrophotometrically after filtration (0.2 µm), using a calibration curve (A_{410} cytochrome C, $E^1_1 = 86$[24], A_{280} lysozyme $E^1_1 = 2.7$[25]).

Myoglobin recovery after incubation and centrifugation

As a control experiment, the effect of experimental conditions on the protein concentration in solutions not containing any polymer was assessed. Eppendorf tubes containing 200 µL myoglobin solutions (0.05, 0.15, 0.25, 0.35 and 0.45 mg/mL) in 10 mM HEPES pH 7.4 were incubated on a roller bench for six hours at room temperature. Samples were centrifuged at 22.000 g for 15 minutes and the concentration of myoglobin in the supernatant was determined by measuring the absorbance at 410 nm, using a calibration curve ($E^1_1 = 157$[26]).

Preparation and analysis of hemoglobin imprinted hydrogels

Neutral protein imprinted polyacrylamide hydrogels were synthesized essentially as described previously[27, 28]. In detail, 270 mg AAm, 30 mg MBA (molar ratio 19:1) and 40 mg bovine hemoglobin were dissolved in 5 mL RO-water. The pre-polymer mixture was flushed with nitrogen for 10 minutes to remove oxygen. Next, 50 µL APS (20% w/w in RO-water, pH adjusted to 7.4) and 50 µL TEMED (10% v/v in RO-water, pH adjusted to 7.4) were added to initiate the polymerization. The gels were allowed to polymerize overnight at room temperature and subsequently ground by using an IKA® Ultra-turrax tube drive and wet-sieved through a 80 µm sieve. The template was removed from the granulated gel particles by successive washing with 100 mL RO-water, 100 mL 10% SDS and 300 mL RO-water. The hemoglobin concentration in the wash fractions was determined spectrophotometrically (A_{410}, hemoglobin calibration curves were made in RO-water and in 10% SDS). The removal of SDS was verified by adding potassium chloride to the wash fractions. Non-imprinted (control) polymers were prepared in the same manner without adding the template protein.

After template extraction, the gel particles were conditioned with phosphate buffer (PB, 10 mM, pH 6.8). The dry weight of the obtained particle suspension was determined by incubation in a vacuum oven for two hours at 40°C. Subsequently, fixed amounts of the MIP and NIP suspension corresponding to 20 mg of dry polymer (~300 mg wet) were transferred to 2 mL tubes and PB buffer pH 6.8 was added to a total weight of 0.5 g. Subsequently, hemoglobin in PB pH 6.8 was added, the final concentration ranging from 0.125 mg/mL to 1.0 mg/mL, (total volume of 1.65 mL). Since the volume of wet particles was not exactly the same for MIP and NIP, the exact concentration of hemoglobin was determined immediately after addition (C_0). After overnight incubation, samples were centrifuged (15.000 g, two minutes), and filtered (0.2 µm) to remove remaining gel particles. The protein concentration in the filtered supernatant was then determined spectrophotometrically (A_{410}).

Lipid II surface-imprinted nanoparticles

Crosslinked polyacrylamide nanoparticles (10% w/v total monomer, AAm:MBA:AAc 32:8:1 w/w/w, molar ratio 9.6:1:0.27) were synthesized using a liposomal nanoreactor as reported earlier[29], except using extrusion to prepare DOPC liposomes. Lipid II (LII) was incorporated in the liposomal bilayer in a ratio of 1 mol LII per 1333 mol phospholipids. In short, DOPC (2 µmol) and

LII (1.5 nmol) were dissolved in chloroform in a round-bottom flask. A lipid film was prepared under reduced pressure using a rotary evaporator and dried further under a stream of nitrogen. Next, 0.8 mL monomer solution in 10 mM HEPES pH 7.4 was added to yield a final phospholipid concentration of 2.5 mM. Irgacure 2959 (photoinitiator) was added to a concentration of 0.01% (w/v). Subsequently, the formed multilamellar liposomes were extruded using a hand extruder (Avanti Polar Lipids) through polycarbonate filters with a pore size of 0.1 µm. To prevent polymerization of the monomers outside the liposomes, 200 µL ascorbic acid dissolved in HEPES (130 mg/mL, pH adjusted to 7.4) was added to the liposome dispersion immediately before illumination. Photopolymerization was initiated by illumination for 90 seconds under a N_2 atmosphere using a Bluepoint 4 UVC mercury lamp (150 W, λ-range 230-600 nm, Honle UV Technology). After polymerization, the lipid bilayer and the LII-template molecules were removed from the particles by addition of Triton X100, followed by four ultracentrifugal cycles (250.000 g, one hour) and removal of the supernatant. Removal of DOPC was confirmed by a phosphate determination according to Rouser after destruction with perchloric acid[30]. The size and size distribution of the obtained particles were measured by dynamic light scattering (DLS) using a Malvern CGS-3 multiangle goniometer (Malvern Ltd.).

Surface plasmon resonance

The rebinding of the imprinted nanoparticles (MIP) to the LII-template was determined by surface plasmon resonance (SPR) using a Biacore3000 (Biacore). LII-containing DOPC monolayers were immobilized (flowcell 2) on a HPP chip (XanTec bioanalytics GmbH) according to the protocol provided by Biacore (for DMPC monolayers on a HPA chip). In short, LII-containing DOPC liposomes (2 mM phospholipids, molar ratio DOPC:LII = 333:1) in 10 mM HEPES pH 7.4 containing 2 mM $CaCl_2$ were prepared by extrusion. After cleaning the HPP-chip surface by an injection (25 µL, flow 5 µL/min) of N-octyl-β-D-glucopyranoside (40 mM in H_2O), monolayers were formed by an injection (30 µL, flow 2 µL/min) of liposomes, followed by a pulse (30 µL, flow 50 µL/min) of 10 mM NaOH to remove loosely bound vesicles. DOPC monolayers without LII where used a reference surface (flowcell 1). After the immobilization, sensorgrams were recorded in running buffer (10 mM HEPES, pH 7.4, filtered and degassed) until a stable baseline was reached. Different concentrations of MIP and control nanoparticles were injected with a flow of 10 µL/min during six minutes. Dissociation in running buffer was followed for five minutes, followed by regeneration of the surface with 10 mM NaOH.

POLYMER COMPOSITION: THE FIRST CRITICAL PARAMETER

After selecting a protein as target template for molecular imprinting, the next step is the selection of an appropriate polymer matrix, in which high affinity binding sites can be created, ideally without introducing nonspecific interactions. Proteins are very complex and possess many potential recognition sites at their surface, such as charged amino acids and hydrophobic/hydrophilic regions. This makes the creation of molecular imprinted polymers with high selectivity challenging, due to possible cross-reactivity with proteins with similar charge or hydrophobic/hydrophilic structure as the imprinted template protein. It has been proposed, in contrast to small molecules in aprotic organic solvents, where a few strong bonds are responsible for the selective interaction between template and polymer, multiple weak interactions are necessary for the generation of a strong protein binding polymer network in aqueous environment[31, 32]. Hjertén and co-workers, introduced acrylamide (AAm) and *N,N'*-methylene-bisacrylamide (MBA) for the design of imprinted hydrogels of several proteins, e.g. cytochrome C[33], hemoglobine[33], ribonuclease[31], human growth hormone[31] and human serum albumin[34]. They typically used hydrogels with a relatively low crosslink density, i.e. 3% (w/w) relative to the total monomer amount. The polyacrylamide matrix is non-charged and multiple weak interactions, like hydrogen bonds and dipole-dipole interactions are assumed to be responsible for the polymer-template interactions[35]. Additionally, the polymerization of monomers in the vicinity of a template protein leads to the formation of a cavity with the shape and size of the imprinted template, and with the sites of interaction in a pre-determined orientation[31, 34]. Theoretically, electrostatic interactions due to introduction of charged monomers in the polymer network can contribute to more specific and stronger template-imprint interactions. However, charged residues can also cause nonspecific binding of the template, resulting in a decreased imprint effect. Hjertén and co-workers indeed observed that introducing acrylic acid (AAc) as negatively charged monomer at neutral pH in the polymer matrix, led to a decreased selectivity towards hemoglobin and they concluded that the use of functional (charged) monomers should be avoided. High nonspecific interactions, due to the presence of charged monomers were also observed by our group. We prepared lysozyme imprinted and non-imprinted polyacrylamide gels without and with 1.5 mol% AAc (AAc:lysozyme molar ratio = 5:1), with a crosslink density of 15.5% (w/w), as described in the Experimental Basis section. The rebinding of FITC-labeled lysozyme was evaluated with fluorescence microscopy. In order to make comparison possible

between the different samples, the microscope settings (exposure time and gain) were kept constant for all the formulations. As can be seen in Figure 4, the (bright green) fluorescence intensity (FITC-lysozyme) of the AAc-containing MIP is substantially higher than that of the neutral MIP, where almost no fluorescence is observed (black to slightly green). However, this is also the case for the non-imprinted polymer (NIP), which indicates that this effect is mostly the result of nonspecific binding. Although both charged and neutral MIPs seemed to bind more FITC-lysozyme than the non-imprinted counterparts, experiments with bulk imprinted hydrogels of the same composition where the rebinding was assessed by the depletion of protein from the supernatant did not confirm an imprint effect. Also in this experiment the negatively charged bulk imprinted hydrogels showed quantitative rebinding of lysozyme for both the MIP and NIP. These results clearly illustrate the nonspecific binding caused by electrostatic interaction between positively charged lysozyme and the negatively charged networks.
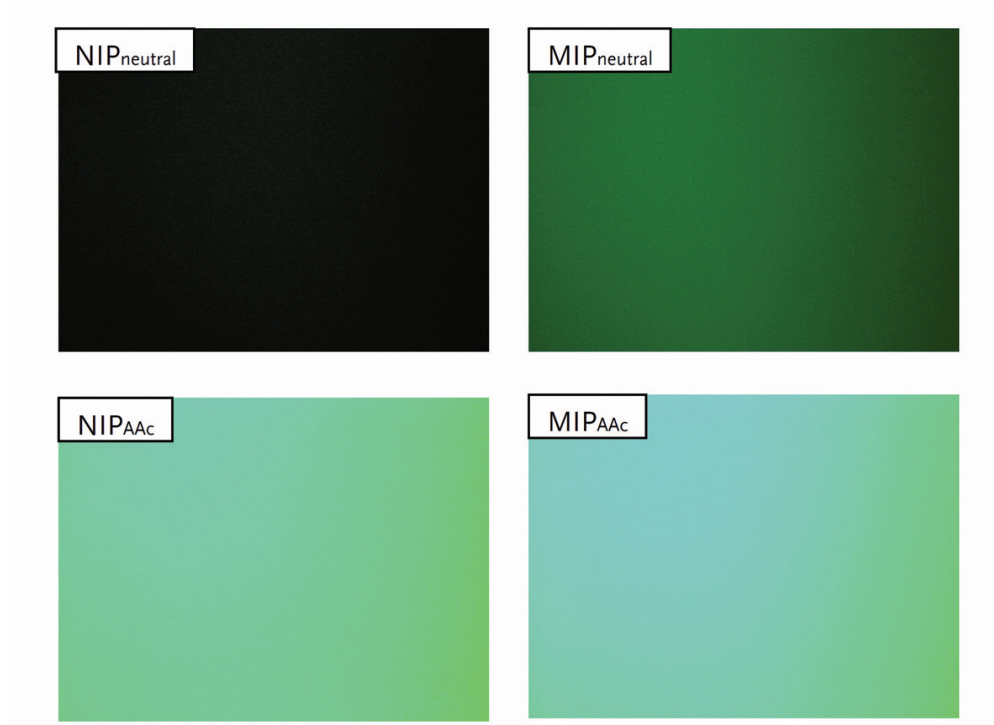

Figure 4. Fluorescent images of neutral (top) and negatively charged (bottom) MIP and NIP after rebinding with FITC-lysozyme (green) (50% of the initially imprinted amount) in 10 mM HEPES, pH 7.4. These figures clearly illustrate the nonspecific binding of lysozyme to acrylic acid (AAc)-containing polyacrylamide hydrogels. The exposure time and gain were kept constant for all the samples.

3-Aminophenylboronic acid (APBA) has been frequently used as functional monomer for the preparation of protein imprinted polymers, with varying results[36-39]. APBA possesses several functional groups (hydroxyl, secondary amine and an aromatic ring), which can interact with different amino acids present in proteins [40, 41]. As observed by Bonini *et al.*, these multiple interaction points can sometimes result in high nonspecific binding[37]. They used aminopropyl silica beads coated with APBA as functional monomer for imprinting of human serum albumin (HSA). The protein was first covalently bound to an aldehyde-modified aminopropyl silica surface (2 mg HSA/g beads). Thereafter, a thin film of pAPBA was deposited on the particle surface (15.2 mg/g beads, thickness of the layer not specified). The template was removed by washing the beads with RO-water and 1 M oxalic acid. The strong acidic solution breaks the covalent bond between the protein and the modified silica surface. From the release profile presented by the authors, it is clear that only ~50 µg was removed from the beads, whereas initially 2 mg HSA was added to derivatize the beads. This suggests that there is still a considerable amount of template present on the beads (97.5%, assuming quantitative immobilization of HSA on the beads), which could be due to either strong interaction between the aminopropyl silica and HSA[42], or to permanent entrapment of HSA between the silica surface and the deposited pABPA layer. Beads were conditioned with phosphate buffer (PB, 10 mM, pH 8) before rebinding. We would like to point out that the pABPA is a linear polymer deposited on the silica surface. In our view, the absence of permanent (covalent) crosslinks makes the creation of stable imprint cavities very unlikely. Rebinding studies were performed with different protein amounts (0.02 up to 2.4 mg/g beads). Only at high rebinding protein concentrations (> 1.56 mg HSA/g beads), a significant difference in binding behavior was observed between the imprinted and non-imprinted beads (imprint factor = 1.4, Figure 5). At lower concentrations, both MIP and NIP adsorbed the loaded HSA quantitatively. This observation is contrary to what is expected for specific protein (re)binding, where one would expect a difference in adsorption at low protein concentrations until all specific binding sites on the MIP are occupied, whereas at higher concentrations nonspecific protein binding to the surface of both MIP and NIP would occur. Additionally, the difference in binding between MIP and NIP (~500 µg/g) beads was 10 times higher than the removed amount of template (50 µg/g beads). Therefore it is likely that the difference in binding between the MIP and NIP observed at high concentrations is caused by a difference in exposed surface area per g particles, which could originate from the presence of the protein during the polymerization.
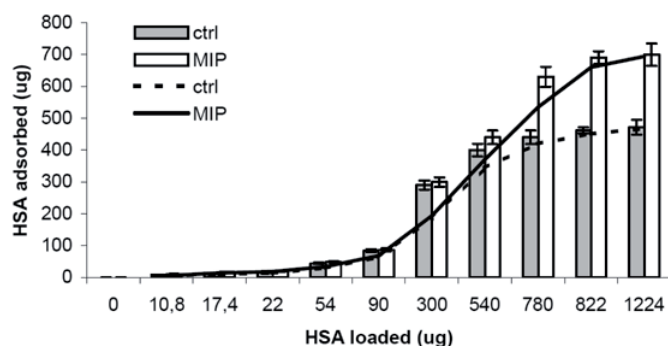
Figure 5. Binding capacity for control (solid) and MIP beads (open). The amount in micrograms bound to the beads is plotted as function of amount in micrograms added to 0.5 g particles for rebinding. Rebinding is done with different amounts of proteins in phosphate buffer (10 mM pH 8). Reprinted with permission from [37].

Even though it is clear that functional (charged) monomers can induce nonspecific binding of the template to the polymers, it has been shown that the charge density of the network[43], as well as the pH[44] and ionic strength of the buffers used for imprinting and rebinding[21, 36] have an effect on the experimentally determined imprint specificity. Matsunaga *et al*. presented a detailed study on the effect of salt concentration on both the imprinting process and rebinding to negatively charged polyacrylamide hydrogels[21]. They synthesized lysozyme imprinted and non-imprinted polymers on SPR-chips with AAc as negatively charged monomer. The effect of ionic strength (0, 20 and 40 mM NaCl) of the buffer (HEPES, pH 7.4) during the polymerization and the rebinding assay was evaluated with SPR. AAc was added to provide negatively charged binding sites for the positively charged lysozyme. The template was removed by washing with 1 M NaCl (the amount of template removed was not quantified). When rebinding was conducted in absence of NaCl, high nonspecific binding of lysozyme was observed for both the MIP and NIP, likely caused by the electrostatic interaction between the template and the polymer (control experiments using polymers without AAc were not performed). Rebinding to the lysozyme-MIP and NIP was also done with other proteins (cytochrome C, RNAse, myoglobin and lactalbumin) to examine the selectivity of the imprints. Cytochrome C and RNAse (both positively charged at pH 7.4) bound to a high extent to both MIP and NIP, whereas no adsorption was observed for myoglobin (neutral) and lactalbumin (negatively charged). Interestingly, when the rebinding of lysozyme and the different control proteins was done in the presence of NaCl (20 or 40 mM), the nonspecific binding to both MIP and NIP decreased, but this did not result in an increased imprint factor for lysozyme. In case the preparation of the MIPs was done in

absence of salt (50 mM HEPES, pH 7.4), no specific adsorption of lysozyme to the MIP was observed (imprinting factor = 1.0). On the other hand, when imprinting was done in presence of salt, 20 or 40 mM, the imprint factor for lysozyme in 20 mM NaCl increased to 1.2 and 3.4, respectively. However, when rebinding was done with these gels in presence of 40 mM instead of 20 mM NaCl the rebinding efficiency decreased. This can be attributed to the interference of the salt ions with the specific charged binding sites, thereby masking the charges and resulting again in loss of rebinding efficiency.

It is clear that the selection of proper monomers is critical for the performance of the imprinted polymer. One has to take into account that strong interactions, either electrostatic or hydrophobic, between monomers and template can lead to nonspecific binding. Moreover, the imprinting and rebinding conditions (pH, salt concentration) have a clear effect on the experimental results, which makes it even more challenging to develop standardized protocols for the design and evaluation of protein imprinted polymers.

THE ESSENCE OF TEMPLATE REMOVAL

An important step in the process of creating imprints with high selectivity and absorption capacity is the removal of the imprinted template, especially because the imprint cavities of interest, i.e. those with the highest binding affinity, will most strongly retain the template molecules during template extraction. Moreover, removal of proteins from imprinted polymers is challenging due to their high molecular weights, which retards diffusion through the dense polymer network. In the past decade, several washing methods have been developed and optimized for protein/template extraction. The pioneering work by Hjertén and co-workers has been used as a starting point by other research groups[31, 33, 35]. In order to remove the template from (neutral) polyacrylamide hydrogels, they used several methods, depending on the protein properties (size and *pI*). For example, cytochrome C was removed by washing with a solution of high salt (0.5 M), whereas for hemoglobin, albumin and myoglobin 10% SDS/10% AcOH was needed and even then traces of the proteins were permanently entrapped (the gels remained slightly red colored after washing)[33]. Nowadays, these methods are still frequently used for template removal. For smaller proteins like cytochrome C and lysozyme, washing with RO-water and solutions with high salt concentrations is sufficient to remove 73 up to 92% of the template molecule, depending on the polymer composition[22, 45, 46]. At present, the

combination of acetic acid (AcOH) with a detergent (SDS or Tween®-20) is the most frequently used washing procedure, however this harsh method does not guaranty complete template removal either; results varying from 50% up to 95% have been published[27, 36, 37, 47, 48]. In 2005, Hawkins *et al*. evaluated the use of a mixture of SDS/AcOH and trypsin as washing solutions for the removal of hemoglobin from polyacrylamide hydrogels[27]. They polymerized acrylamide and bisacrylamide in presence of hemoglobin (12 mg/g polymer). After polymerization, the hydrogels were granulated by sieving and washed with different solutions, and subsequently the rebinding efficiency was determined by incubating the imprinted and control particles with 6 mg hemoglobin/g polymer. The best imprint effect was obtained with 10% SDS/10% AcOH (45% of the initially imprinted amount rebound), even though only approximately 50% of the template was removed. By increasing the SDS/AcOH concentration to 15%:15%, more template was removed (~70%), but the rebinding decreased to ~35%, which Hawkins *et al*. assigned to changes of the network structure, caused by the high SDS:AcOH concentrations. When trypsin was used, up to 87.4% of template was removed from the imprinted network; however, only 20% of the amount initially used for imprinting was rebound. This was explained by the blocking of imprinted sites with residual protein fragments.

Although the results of Hawkins *et al*.[27] look promising, some issues need to be addressed. First, the time used for template removal is not specified, nor do the authors state whether the last wash fraction still contained protein. Therefore it is not certain whether the template that was not removed (up to 50%) did not continue to leak out during rebinding studies. Second, the template rebinding was allowed for only 10 minutes, which is too short to reach equilibrium (vide infra). Third, a bias is observed in the data presented on the hemoglobin recovery after rebinding. According to the described method, 12 mg hemoglobin was used for the imprinting process, whereas the rebinding to the MIP and NIP was done with 6 mg hemoglobin (because only ~50% of the template was removed). However, based on the presented results, the amount of protein recovered in the different wash fractions after rebinding for the NIP, was 7.25-7.75 mg, which is 20-30% more than the initial amount used for rebinding (Figure 6). On the other hand, in case of the MIP, the total amount of protein recovered during the washing steps after rebinding (4.5-5.9 mg) is less than the amount used for rebinding, suggesting some irreversible rebinding of the protein to the MIP. These uneven mass balances were not addressed by the authors. Therefore, given the inaccuracy of the method used to assess rebinding, the

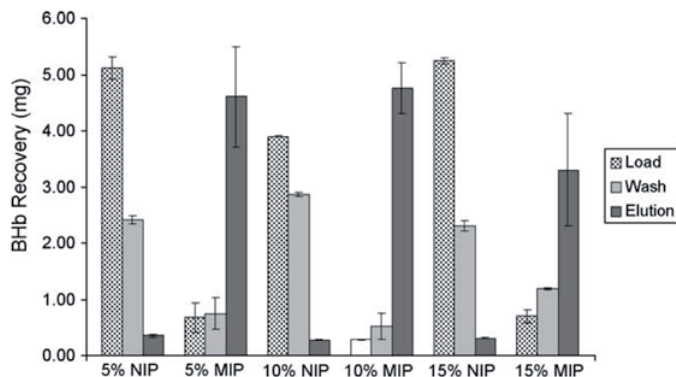author's conclusion that 10% SDS/10% AcOH would be the best template removal method is probably not justified.

Figure 6. Effect of washing method (SDS/AcOH 5%:5%, 10%:10% and 15%:15%) on the rebinding to MIP and NIP. The figure shows the amount of hemoglobin present in the different wash fractions after rebinding. (Load fraction = unbound protein remaining in the supernatant after rebinding, Wash: low affinity bound protein removed by washing with water, Elution: strong affinity bound protein eluted with SDS/AcOH). All values are means of duplicate experiments and the error bars represent the two "actual" results for each data set groups. In case of the NIPs, accumulation of the protein recovered in the different wash fractions, resulted in a higher amount of protein than originally added to the polymers. Reprinted with permission from [27]

In a second paper, the same authors evaluated the efficiency of the SDS/AcOH washing method with confocal microscopy[48]. Fluorescently labeled (FITC) albumin was imprinted in a polyacrylamide hydrogel and visualized by confocal microscopy. After addition of 50 µL 10% SDS/10% AcOH to the MIP an immediate and almost complete decrease in fluorescence signal was observed. This observation was ascribed to the structural denaturation of the FITC-labeled protein and subsequent extraction from the hydrogel network. However, fluorescein (and also FITC) is a pH-sensitive fluorescent probe and has been used e.g. as pH sensor to measure the intracellular pH[49, 50]. The fluorescence intensity of fluorescein has a maximum above pH 7 and a minimum below pH 5. Consequently, the observed instant loss of the fluorescence signal is more likely caused by the decrease of the pH after adding SDS/AcOH (pH ~2.8), rather than due to denaturation and removal of FITC-albumin from the gel network. Moreover, immediate release is highly unlikely because of the low diffusion rates of proteins in highly crosslinked hydrogel matrices. Despite the above mentioned concerns, many researchers adopted this method to remove protein templates from MIPs[28, 47, 51-54].

As demonstrated by Fu *et al*., template removal by SDS and AcOH can be associated with another artifact[47]. They synthesized BSA imprinted chitosan-polyacrylamide gels by graft

copolymerization of acrylamide on chitosan in presence of bisacrylamide. The gels were sieved (70-mesh sieve) and the obtained granules were washed with 10% SDS/10% AcOH to remove the template. When performing a rebinding experiment (acetate buffer pH 4.6 in which BSA has no net charge), they observed that the MIP had a binding capacity exceeding the theoretical capacity at least twice, whereas the template binding to NIP was very low[47]. In a later publication they verified that the mixture of SDS/AcOH, used to remove the imprinted template, was responsible for this extremely high absorption by the MIP[55]: when non-imprinted polymers were washed with the same solution (10% SDS/10% AcOH), a comparable amount of template (hemoglobin) was bound to the NIP as to the MIP (Figure 7).
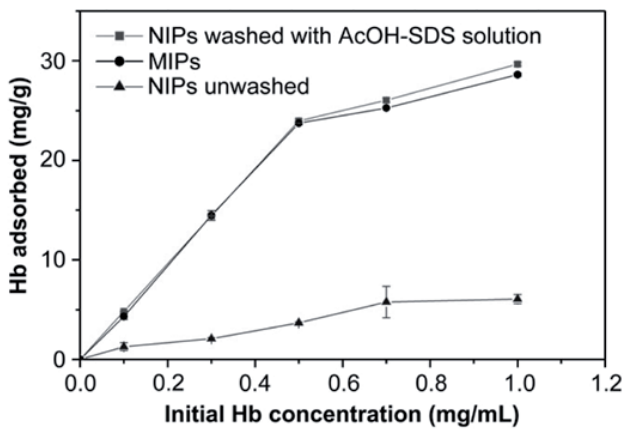

Figure 7. Hemoglobin binding isotherms for imprinted hydrogels based on polyacrylamide-chitosan semi-interpenetrating network, and for the NIP-washed or unwashed with the AcOH/SDS solution. Binding conditions: temperature 25°C, time 8 h, Particles 0.1 g, volume 5 mL, 20 mM phosphate buffer pH 6.8. All values are means of three measurements. Reprinted with permission from [55].

In a control experiment, using crosslinked chitosan beads, high nonspecific protein adsorption to the beads occurred when they were washed with a combination of SDS and AcOH, whereas after washing with only AcOH or SDS, a much lower protein sorption was observed (Figure 8). It is possible that anionic SDS binds electrostatically to the positively charged chitosan surface, which is more pronounced at the low pH (~2.8) of the SDS/AcOH solution. The SDS molecules may remain adsorbed to the surface after washing and can thereby cause nonspecific hydrophobic interactions with BSA and hemoglobin (both neutral at pH 4.6 and pH 6.8, respectively). These results indicate that nonspecific sorption induced by the washing step with SDS/AcOH, rather than the creation of imprinted sites, is responsible for the very high

binding capacity. As suggested by the authors, it is very important to treat the MIP and NIP in exactly the same way during the whole imprinting process.
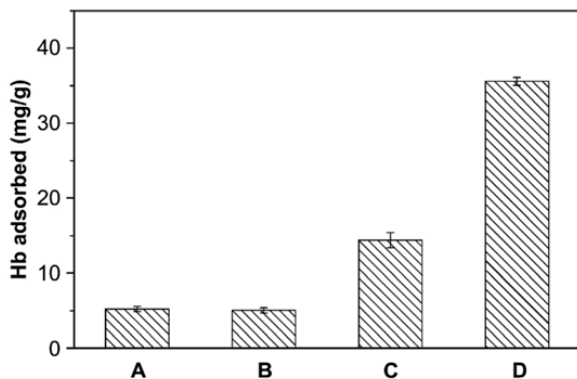

Figure 8. Hemoglobin binding to bare crosslinked chitosan beads treated differently. (A) Original crosslinked chitosan beads; (B) beads washed with 10% (v/v) AcOH; (C) washed with 10% (w/v) SDS solution; and (D) washed with the AcOH/SDS solution. Binding conditions: temperature 25°C, time 18 h, polymer mass 0.1 g, rebinding volume 5 mL, Initial concentration (C_0) 1.0 mg/mL, and 20 mM phosphate buffer pH 6.8. All values are means of three measurements. Reprinted with permission from [55].

Tan and Tong also reported extremely high adsorption capacities for a protein imprinted methylmethacrylate polymer crosslinked with ethylene glycol dimethacrylate, up to 100-fold of the theoretical maximum binding capacity, however, this was not addressed in their discussion[53, 56, 57]. In a comment on one of their papers, the washing step with SDS/AcOH was proposed to be responsible for this exceptionally high rebinding capacity. Moreover it was suggested that the MIP and NIP were treated differently during the washing steps[58]. Tan and Tong replied and assured that both MIP and NIP were treated in a similar way and explained the unrealistic high adsorption capacity by means of the general mechanism of protein adsorption to hydrophobic surfaces[59]. The authors argued that the presence of binding sites in the imprinted polymer would create a stable layer of adsorbed proteins, onto which other proteins can be adsorbed, leading to multiple layers of proteins. In absence of these binding sites, the adsorbed layer is not stable and can be desorbed again. However, the explanation is based on hypothesises and not supported by experimental data. Moreover, multi-layer protein adsorption has only been observed with some protein-surface combinations, and there is still a lot of controversy on this topic[60, 61].

Recently, Janiak *et al*. also discussed the problems they encountered with the use of SDS/AcOH to remove imprinted protein molecules from charged polyacrylamide hydrogels[28, 62].

Like Fu *et al.*[55], they observed that the presence of SDS in the wash solution, in particular in combination with AcOH, led to an increased nonspecific binding to the imprinted and non-imprinted polymers.

Also in our work we observed high nonspecific rebinding due to insufficient washing after removal of the template with 10% SDS/10% AcOH. Cytochrome C imprinted and non-imprinted neutral polyacrylamide hydrogels (containing equal amounts of negatively (MA) and positively (DMAEMA) charged monomers) were prepared according to Kimhi and Bianco-Peled[22], as described in the Experimental Basis section. The template was removed (85 % ± 5 %) by washing of the granulated gels with 10% SDS/10% AcOH, comparable with results reported by Kimhi *et al.*[22]. After washing, the gels were equilibrated in TRIS buffer pH 8. To assess the selectivity of the imprinted polymers, rebinding was performed with cytochrome C and lysozyme, which are similar with respect to their size and isoelectric point (*pI*; lysozyme = 14.3 kDa, *pI* = 9; cytochrome C = 12.6 kDa, *pI* = 11). The rebinding was done by incubation of 50 mg MIP and NIP (dry weight) with different amounts of both proteins (2.5, 5, 10, 15 and 20 mg) for 14 hours. Based on the initial template concentration, the maximum rebinding capacity of the MIP was 50 mg/g. After sedimentation of the particles, the unbound protein in the supernatant was determined spectrophotometrically. Surprisingly, for all initial rebinding concentrations used (0.5 mg/mL – 4 mg/mL), no protein was detected in the supernatant of solutions incubated with both MIP and NIP. The absence of a red color in the supernatant after rebinding with cytochrome C confirmed this finding. However, a closer examination of the MIP and NIP after rebinding revealed that the protein molecules had neither penetrated into nor adsorbed onto the polymers, but were precipitated on top of the polymers, as shown for lysozyme in Figure 9.
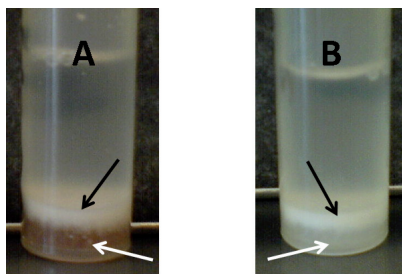

Figure 9. Precipitation of lysozyme after rebinding to cytochrome C imprinted particles (A) and non-imprinted particles (B). Lysozyme (3 mg/mL in TRIS pH 8) was added to 0.5 gram dry particles and incubated overnight. Black arrows: protein precipitate, white arrows: sedimented particles (slightly red colored in the case of the imprinted particles (A)).

The MIP was still slightly red colored, indicating the presence of cytochrome C that was permanently entrapped in the hydrogel network after imprinting (Figure 9A). For all lysozyme concentrations used, quantitative precipitation occurred for both MIP and NIP. Determination of the pH revealed that the solution was slightly acidic (pH 5), even though they were washed with H_2O, and TRIS-buffer (pH 8) was used during hydration of the polymer particles and during rebinding. This suggests that AcOH, and likely also SDS, used for template removal were not extracted quantitatively from the gels. Therefore, the stability of lysozyme and cytochrome C was assessed in 10% SDS, 10% AcOH and a mixture of 10% SDS/10% AcOH. Only the combination of SDS and AcOH caused precipitation of the proteins, which confirms the hypothesis that traces SDS and AcOH were still present in the gels during the rebinding, causing precipitation of the proteins.

Based on the examples mentioned above, it has become clear that a harsh washing method, like SDS/AcOH, may improve the removal of imprinted template proteins, but care must be taken to avoid nonspecific interactions or protein precipitation by e.g. residual SDS molecules present in the polymer network. As shown, such artifacts might lead to false positive results. First of all, imprinted and non-imprinted polymers should be subjected to identical procedures used for the template removal and washing of the polymers. This way, nonspecific interaction introduced by the washing procedure can be identified. Second, one should ensure that washing compounds are removed completely prior to the rebinding step. In case of SDS and AcOH, this can be done easily by measuring the pH of the supernatant (AcOH) and by adding potassium chloride to the supernatant which will cause precipitation of KDS. Nevertheless, SDS entrapped inside the gel matrix may still cause artifacts.

ASSESSMENT OF TEMPLATE REBINDING

Incubation time/equilibrium

Affinity is a parameter that describes the binding of substances (e.g. ligand and receptor) in equilibrium. Logically, in order to assess the affinity of a MIP for the template, one has to be sure that equilibrium has been reached. It is well-known that the diffusivity of proteins in a highly crosslinked polymer matrix is rather slow. Polymer geometry, polymer hydration, crosslink density, protein size and temperature all play a role in the time needed for a protein

to diffuse into the polymer matrix and to reach equilibrium. As a result, the required incubation time needs to be validated before affinity can be properly assessed. Surprisingly, in many articles on protein imprinting the incubation time is not accounted for. For example, Ou *et al*. reported on lysozyme imprinted polyacrylamide beads (solid content up to 40% w/w) of 105–149 μm using an incubation time of 30 minutes[45]. Their formulation and incubation time were adopted by Kimhi and Bianco-Peled[22], but in a later paper by the same group it was stated that it took at least two hours to reach equilibrium, and the incubation time was adjusted to five hours[63]. Even more striking are the papers on hemoglobin imprinted polyacrylamide gels (6% w/w total monomers, 10% crosslinker), by Hawkins *et al*.[27] (sieved through a 75 μm sieve) and Janiak *et al*.[28] (granulated, dimensions not specified), where an incubation time of only 10 minutes was used. Judging from the time-dependent adsorption curves shown by others for similar hydrogel compositions[64-66], it can be stated with certainty that equilibrium was not reached.

Also when the time needed to reach equilibrium is determined, the results should be analyzed critically. For example, Lu *et al*. showed that the concentration of BSA and lysozyme upon incubation with their corresponding polyacrylamide MIP beads (25% w/w total monomer, 10% crosslinker) decreased with the same kinetics[38]. This is contradictive to what is expected, considering that the molecular weight of BSA is approximately six times higher than that of lysozyme. The difference in size leads to much slower movement of BSA in the crosslinked polyacrylamide matrix and therefore one would expect that more time is needed to reach equilibrium for BSA. The finding that equilibrium was reached within the same time interval raises the question whether the change in concentration was indeed caused by specific binding to imprint cavities in the polymer matrix, or that it was rather caused for example by protein aggregation or nonspecific binding to the polymer surface or test tube.

Quantification of rebinding

In the majority of papers the indirect method of template depletion from solution is used to quantify template rebinding. MIP and template are mixed and the concentration of unbound protein in the solution is determined after a certain incubation period (when equilibrium is reached). A major shortcoming of the template depletion method is that it does not confirm that the template is in fact bound to the polymer. The drop in concentration of protein in the supernatant can have other causes, such as the SDS/AcOH combination (vide supra). Also other unexpected effects could lead to serious artifacts, as is illustrated with some of our own data

shown in Figure 10. Figure 10A shows the relative amount of myoglobin measured in 10 mM HEPES buffer, pH 7.4, after incubation in eppendorf tubes without MIP/NIP for six hours at room temperature followed by centrifugation. It becomes clear that ~90% of the myoglobin remained in the solution, independent of the original concentration. When this picture is converted into a Langmuir curve (Figure 10B) it seems that significant "binding" occurred. This background binding could result from adsorption of protein to the test tube and loss of protein (aggregates) as a result of centrifugation. Solid surfaces can adsorb up to 1 μg protein/cm^2 (monolayer of globular protein)[67]. The surface of an eppendorf tube is ~10 cm^2, which means that approximately 10 μg of protein can adsorb to it and this could indeed explain the observed decrease of protein ($\Delta C = 0.05$ μg/mL, V = 200 μL). If MIP/NIP would have been present, such phenomena could lead to false positive results. Therefore, when indirect measurements are used to show template rebinding, samples not containing MIP/NIP should be included as an extra control, additional to the normal non-imprinted polymer.
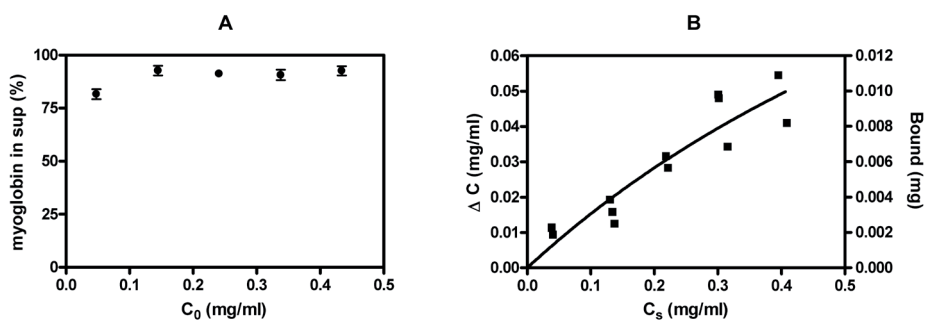

Figure 10. Depletion of myoglobin from solution after 6 h incubation (10 mM Hepes buffer pH 7.4) and subsequent centrifugation. The concentration was determined by A410 and expressed as % of the original amount (A, n = 3), and the resulting Langmuir isotherm expressed as both decrease in concentration (left y-axis) and amount bound (right y-axis) vs. equilibrium concentration (B). Individual triplicates are shown because the x-coordinate (equilibrium concentration) is a sample-dependent value. The line in Figure B represents the fit using a one site binding model.

It should be noted that in some papers protein rebinding is quantified by determining the bound protein directly, for example by ELISA[68] or using a quartz crystal microbalance (QCM)[69-71]. Also for these methods it is essential that they are validated, to be able to make the distinction between rebinding and for example change of the availability or conformation of epitopes in the case of ELISA, and polymer swelling and deswelling in the case of QCM. To our knowledge, no papers have been published in which the affinity of a MIP for the template protein is assessed using equilibrium dialysis, a method commonly used in pharmacology, immunology

and biochemistry to assess the affinity of ligand/protein complexes[72, 73]. In this method, the distribution of a radiolabeled ligand is determined over two compartments separated by a semipermeable membrane. Only one of the compartments contains the receptor (MIP), while the ligand (template) can freely diffuse over the membrane. Ligand binding to the receptor results in an increased amount of total radioactive ligand in the receptor compartment. This method has several advantages. First, there is no need to separate the unbound template from the MIP by centrifugation or filtration, which could lead to unwanted loss of ligand. Second, artifacts due to protein aggregation or adsorption to the compartment walls do not affect the outcome in such an experimental set-up, since those phenomena occur to the same extent in both compartments. Third, a proper mass balance of the ligand is obtained, which strengthens the power of the experiment. Therefore, adopting this method would be an improvement to the field of protein imprinting.

The most common method for determination of protein concentration in solution after rebinding to MIPs or NIPs is UV-VIS spectrometry, using either absorption of the aromatic amino acids (at 280 nm)[45, 52, 54, 65, 66, 74-78], the absorption maximum of the heme group at ~410 nm in case of hemoglobin, cytochrome C or myoglobin[28], or a colorimetric protein assay such as Bradford[46, 79]. In most papers, results are converted to represent the amount of protein bound per weight of MIP/NIP. Presented this way many results look quite convincing. However, the raw data should always be considered in order to judge whether the proposed imprinting effects are significant. For example, Bolisay *et al*. reported that mosaic virus imprinted polymers rebound 8.82 mg virus/g MIP while NIP bound 4.22 mg/g[12]. The binding was assessed by indirect measurement of virus concentration, using UV-VIS spectrometry after removal of the polymer with a 0.45 μm filter from samples containing a ratio of 1 mg polymer per 1 mg/mL virus. Using these data, it can be calculated that the ΔC measured for MIP and NIP were 0.00882 and 0.00422 mg/mL, respectively. It can be calculated that the concentration in the supernatant was 99.1% and 99.6% of the original, respectively, which is without doubt within the margin of error of the assay. Silvestri *et al*. reported that when α-amylase was passed through a poly(ethylene-co-vinyl alcohol)/dextran MIP/NIP membrane, the imprinted membrane retained 0.41 μmol/g more than the control (MIP 0.60 μmol/g, NIP 0.19 μmol/g)[76]. With a Mw of 51 kDa and knowing that the imprinted membrane was prepared using a protein concentration of 2% w/w, (= 0.39 μmol/g), this translates into an imprint efficiency of 105%. However, the difference in non-adsorbed α-amylase was 8% of the original α-amylase concentration (0.15 mg/mL), which

is 0.012 mg/mL. Using ε = 5925 $M^{-1}cm^{-1}$ [80, 81], it can be calculated that this results in a difference of A_{280} between MIP and NIP of only 0.022.

Hua *et al*. showed Scatchard plots of BSA rebinding to MIP and NIP disks (Figures 11A and B, respectively)[74]. Solutions of various concentrations of BSA were incubated for 24 h with 5 mg polymer and the concentration of BSA was determined using A_{280}. They found that the MIP exhibited two binding sites, one with high and one with low affinity, while the NIP only had one binding site with low affinity. An interesting point not mentioned by the authors is that the maximum amount of bound protein to the high affinity site (Q_{max}), which can be deducted from the plot by extrapolation of the line to the x-axis, is ~4.5 µmol/g dry polymer. According to their Materials and Methods section, the MIPs were prepared with 229 mg BSA/g monomer, which leads to a theoretical maximum of 3.5 µmol/g dry polymer. Taking into account that template removal was 93.4%; reduces Q_{max} to 3.2 µmol/g. The equilibrium concentration C (µmol/L) can be calculated from the points in Figure 11 by C = x/y (Q/(Q/C). The approximate A_{280} can then be calculated using ε = 43800 $M^{-1}cm^{-1}$ for BSA, and assuming a 1 cm path length. The results of this calculation are shown in Table 1. Considering the small differences in A_{280} between the MIPs and the NIPs, the likely error in weighing 5 mg polymer, the general error in absorbance measurements and the fact that no standard deviations are given, it is questionable whether these measurements show an imprinting effect.

Table 1. The original concentrations (C_0) (given in material and methods) and the equilibrium concentrations (C_{eq}) and corresponding A_{280} values recalculated from Figure 11. A_{280} values were calculated using ε = 43800 $M^{-1}cm^{-1}$, assuming a path length of 1 cm, and not considering dilution of the samples.

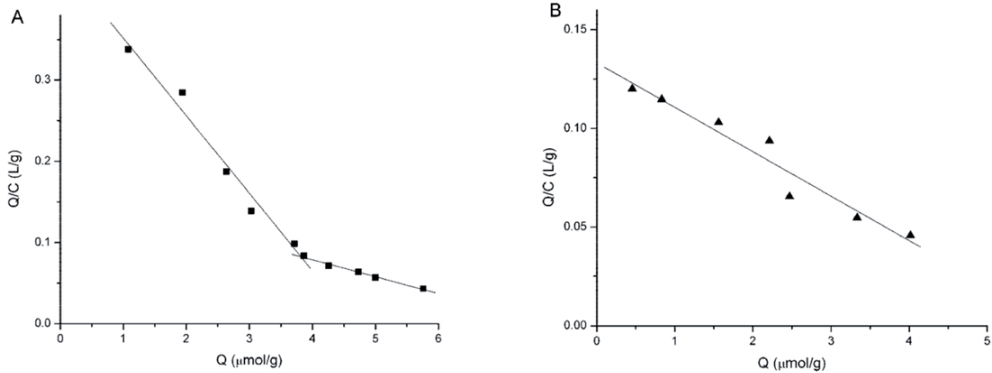| C_0 (mg/mL)	C_{eq} (mg/mL)		A_{280}	
	MIP	NIP	MIP	NIP
2.27				
4.55	3.25	3.76	0.14	0.17
7.58	6.82	7.28	0.30	0.32
15.2	14.3	15.3	0.63	0.67
22.7	21.6	23.6	0.94	1.03
30.3				
37.9	37.4	37.7	1.64	1.65
45.5	45.1		1.98	
60.6	58.0	61.1	2.54	2.68
75.8	75.2		3.29	
	89.2	86.9	3.91	3.81
	134		5.88	

Figure 11. Scatchard plot of the BSA readsorption assay of MIP (A) and NIP (B) presented by Hua *et al*.[74]. 5 mg MIP and NIP composed of N-Isopropylacrylamide (3.5 mmol), N-[3-(dimethylamino)propyl]-methacrylamide (0.085 mmol), AAm (0.070 mmol) and MBA (0.117 mmol) were incubated in 8 mL BSA solutions in 10 mM Tris pH 7.4 containing 1 mM NaCl for 24 h. Reprinted with permission.

When nonspecific and error sensitive indirect measurements are used, especially when the amount of protein bound is just a fraction of the total amount of protein offered, standard deviations or duplicates/triplicates are essential to judge the significance of the presented data. However, standard deviations are often missing in papers on molecular imprinting of proteins. This is illustrated further by a paper by Guo *et al*.[77], in which rebinding of hemoglobin to polyacrylamide MIP beads was studied using A_{280} (Figure 12).
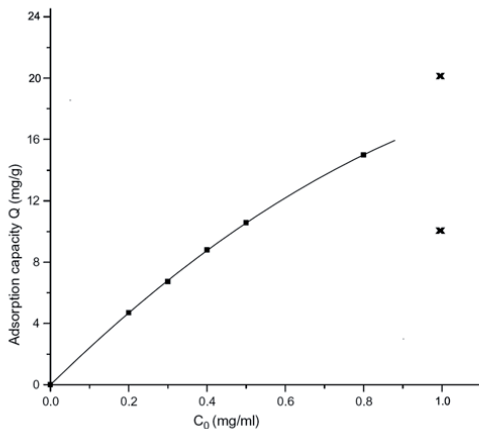
Figure 12. Adsorption isotherm of hemoglobin on MIP beads as presented by Guo et al. (Reprinted with permission from [77]), supplemented with data showing the calculated values for $C_0 = 1.0$ mg/mL (depicted as X). Hemoglobin (600 mg) imprints were prepared using 1.9 g AAm and 0.1 g MBA graft polymerized to 16 g (wet) porous crosslinked chitosan beads. Template removal was not quantified. Rebinding studies were performed at 25°C for 16-17 h using 0.5 g wet beads and 10 mL (= max 10 mg) of hemoglobin solution.

When the adsorption isotherm was linearly converted according to the Langmuir equation they found a correlation coefficient of 0.9989, suggesting an excellent fit. However, it is interesting to note that in the same paper, from another experiment at the same conditions, the adsorption capacity (Q-value) at C_0 = 1.0 mg/mL was determined to be 20.4 mg/g, which deviates substantially from the curve presented in Figure 12. Yet another Q value at C_0 = 1.0 mg/mL can be calculated from the reported K_D value of 23.2. Given that K_D = Cp/C_s (Cp = concentration of protein in the MIP in mg/g, C^s = concentration in the solution in mg/mL), C_0 =1.0 mg/mL, V = 10 mL and the amount of beads is 0.5 g, Q is 10.8 mg/g. Adding these two additional values for Q to Figure 12 (depicted in the figure as X) it becomes clear that there is an enormous deviation from the presented curve. Besides that, the authors did not show the adsorption isotherm to the NIP.

According to our own experience, reproducibility is a difficult issue in protein imprinting. Figure 13A shows the A410 values of the supernatant after hemoglobin rebinding to MIP and NIP (crushed polyacrylamide gels with 6% (w/v) total monomer, AAm:MBA = 9:1, 40 mg hemoglobin/g dry polymer, template removal 55 ± 3%). The differences in absorption are minimal but significant (paired t-test, p = 0.0234), and when these data are converted to a Langmuir plot (Figure 13B) there seems to be a clear imprinting effect. However, the imprints were prepared using 200 mg hemoglobin/g dry polymer, while the maximum amount of hemoglobin bound to MIP was only 17 mg/g dry polymer (= 8.5% of the imprinted amount). Moreover, the reproducibility of these data was poor: an imprint effect was observed in less than 50% of our repeated experiments.
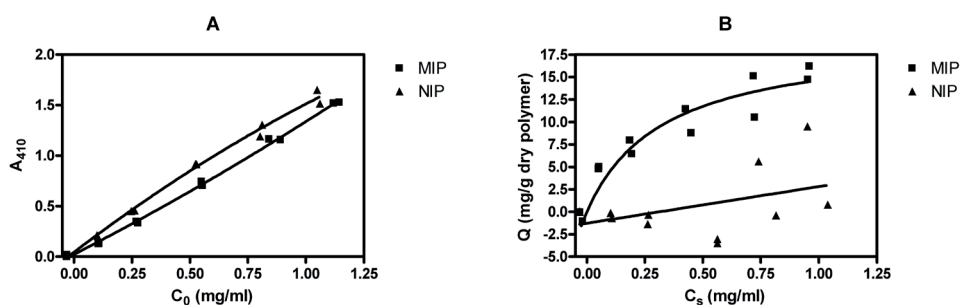
Figure 13. The raw A410 data (A) and corresponding Langmuir representation (B) of hemoglobin binding to crush sieved MIP and NIP (n = 2). Hemoglobin was incubated with fixed amount of polymer particles in phosphate buffer (pH 6.8) for 14 h. Particles were pelleted by centrifugation, and the supernatant was filtered (0.2 μm) before determination of the A_{410}. Individual duplicates are shown because the x-coordinate is sample-dependent (in Figure A, C_0 was determined for each sample immediately after addition of the wet polymer particles, and in Figure B, Cs is an experimental outcome).

Poor reproducibility is also illustrated by another example from our own experiments on surface-imprinting of the bacterial membrane-anchored cell wall precursor lipid II (LII), aiming for bacteria recognizing MIPs. The bacterial cell wall comprises of a biopolymer of alternating amino sugars, *N*-acetylglucosamine (GlcNAc) and *N*-acetylmuramic acid (MurNAc), crosslinked by a pentapeptide (*L*-alanyl-*D*-glutamyl-diaminopimelyl-*D*-alanyl-*D*-alanine). The cell wall is synthesized from LII, which consists of the hydrophilic pentapeptide, GlcNAc and MurNAc, linked to the lipid anchor bactoprenyl-phosphate[82]. LII-surface-imprinted nanoparticles were prepared by the formation of a polymer network inside the aqueous inner compartment of liposomes. LII was immobilized in the liposomal bilayer in order to create surface-imprints of the hydrophilic part of LII directed towards the liposomal interior. The rebinding of surface-imprinted particles to their LII-template was determined by surface plasmon resonance. The hydrodynamic particle size and polydispersity index of the isolated LII-imprinted and non-imprinted particles as determined by dynamic light scattering are shown in table 2.

Table 2. Z-average diameter and polydispersity index (PDI) of LII-imprinted (MIP) and non-imprinted (NIP) polyacrylamide nanoparticles.

	Z-Avg (nm)	PDI
MIP	217	0.176
NIP	251	0.205

Figure 14 shows the sensorgrams of LII-imprinted and non-imprinted particles (NIP) flown over the SPR chip on which the LII was immobilized. Upon injection of MIP (at the time point marked by (A) a strong increase in signal was observed. The increase in response was dependent on particle concentration; a higher concentration led to a higher association level. Injection of NIP led to much lower association, which was concentration independent. After the injection of particles was finished (time point B), the amount of immobilized material remained constant, i.e. no dissociation of bound particles was observed. The data in Figure 14 suggest that MIP specifically bound to the LII-template and imprinting is therefore successful. Furthermore, the absence of dissociation implies a very strong interaction between template and MIP. Unfortunately, attempts to reproduce these data with a new batch of particles and with a new batch of LII were unsuccessful. The poor reproducibility raises the question whether there are some minor and obviously uncontrollable and unknown experimental details that

have an important influence on the successful formation of imprints, or whether the observed effect were merely a result of experimental errors or artifacts. To say the least, the exact factors that determine whether imprinting is successful are currently poorly understood.
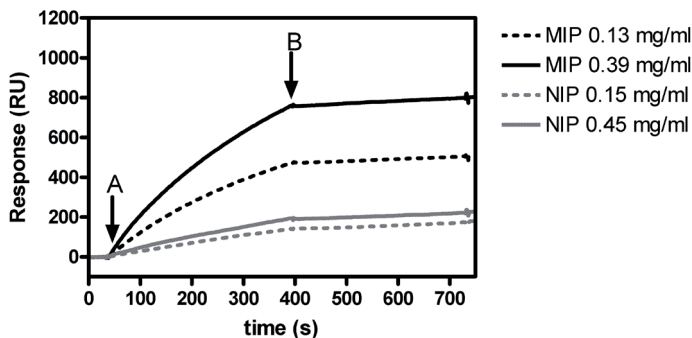

Figure 14. Binding of LII-imprinted particles (MIP) and non-imprinted particles (NIP) to LII immobilized in a DOPC monolayer on a SPR chip. The sensorgrams were corrected for the signal of a reference DOPC surface without LII (flowcell 1).

CONCLUSIONS AND RECOMMENDATIONS

Despite the increase in the number of publications per year, our analysis of data presented by other authors and our own experiments has shown that molecular imprinting of proteins still faces fundamental challenges. A substantial part of the literature contains data that seemingly confirm an imprinting effect, but lack convincing evidence when subjected to a critical analysis. Based on our findings we would like to conclude with some recommendations that in our view will help to avoid the common pitfalls.

Strong electrostatic interactions between monomers and template can lead to very high nonspecific binding. The use of charged monomers should therefore be considered carefully. Up till now, it has not been convincingly shown that they lead to better imprinting results. Additionally, factors such as pH and ionic strength seriously complicate the eventual effects. On the other hand, it remains to be seen whether non-charged hydrophilic matrices currently used for imprinting are suitable to form high affinity polymers. In nature, high affinity between for example antibody and antigen or ligand and receptor does not only result from hydrogen bonding. Electrostatic and hydrophobic interactions also play a major role. Interestingly, in a recent series of papers on peptide (melittin) imprinting in aqueous environment, imprinted

polymer particles were prepared from *N*-isopropylacrylamide crosslinked with *N,N'*-methylene-bisacrylamide, supplemented with functional monomers for electrostatic and hydrophobic interactions (AAc and *N*-t-butylacrylamide, respectively) [83-85]. This example illustrates that for imprinting of biomolecules in aqueous media, hydrophobic and electrostatic interactions may substantially contribute to an imprinting effect.

The combination of SDS and AcOH is commonly used for template removal. However, the evidence that this leads to the best results can be seriously doubted. To mention, it has become clear that this combination can also lead to experimental artifacts, and should ideally be avoided. When it is used, MIP and NIP should undergo exactly the same washing protocol and extensive rinsing should ensure complete removal of remainders of AcOH and SDS, which should be checked by pH measurements and addition of KCl, respectively. For validation, destructive analysis of the polymer could be used to rule out minute amounts remaining in the polymer.

Template removal and rebinding should be quantified by validated methods. Proper controls should ensure that changes in concentration are actually the result of binding to the polymer and not due to e.g. protein aggregation/adsorption. The raw data should be presented, either as separate duplicates/triplicates or with error bars, to show convincing differences between MIP and NIP, and reproducibility should be confirmed with different batches. Kinetic measurements should always be employed to determine the time needed to reach binding equilibrium. Rebinding studies should be done with amounts equal to that used for the preparation of MIP to ensure that the measured effects are a plausible result of the formation of specific binding sites.

At present, it can be argued that in numerous publications, the scientific evidence of molecular imprinting of proteins is not convincing. Further studies with improved and solid experimental designs, critical data analysis, and clear presentation and interpretation are needed to make protein imprinting fit for the future.

REFERENCES

1. Polyakov, M. V. Adsorption properties and structure of silica gel, *Zhur. Fiz. Khim.,* 2 **(1931)**, 799-805.
2. Alexander, C.; Andersson, H. S.; Andersson, L. I.; Ansell, R. J.; Kirsch, N.; Nicholls, I. A.; O'Mahony, J.; Whitcombe, M. J. Molecular imprinting science and technology: A survey of the literature for the years up to and including 2003, *J Mol Recognit,* 19 **(2006)**, 106-80.
3. van Nostrum, C. F. Molecular imprinting: A new tool for drug innovation, *Drug Discov Today: Technol,* 2 **(2005)**, 119-124.
4. Hilt, J. Z.; Byrne, M. E. Configurational biomimesis in drug delivery: Molecular imprinting of biologically significant molecules, *Adv Drug Del Rev,* 56 **(2004)**, 1599-620.
5. Ye, L.; Mosbach, K. The technique of molecular imprinting - principle, state of the art, and future aspects, *J Incl Phen Macrocycl Chem,* 41 **(2001)**, 107-113.
6. Byrne, M. E.; Park, K.; Peppas, N. A. Molecular imprinting within hydrogels, *Adv Drug Del Rev,* 54 **(2002)**, 149-161.
7. Flavin, K.; Resmini, M. Imprinted nanomaterials: A new class of synthetic receptors, *Anal Bioanal Chem,* 393 **(2009)**, 437-444.
8. Huang, Y. P.; Liu, Z. S.; Zheng, C.; Gao, R. Y. Recent developments of molecularly imprinted polymer in CEC, *Electrophoresis,* 30 **(2009)**, 155-162.
9. Lee, W. C.; Cheng, C. H.; Pan, H. H.; Chung, T. H.; Hwang, C. C. Chromatographic characterization of molecularly imprinted polymers, *Anal Bioanal Chem,* 390 **(2008)**, 1101-1109.
10. Maier, N. M.; Lindner, W. Chiral recognition applications of molecularly imprinted polymers: A critical review, *Anal Bioanal Chem,* 389 **(2007)**, 377-397.
11. Takatsy, A.; Vegvari, A.; Hjerten, S.; Kilar, F. Universal method for synthesis of artificial gel antibodies by the imprinting approach combined with a unique electrophoresis technique for detection of minute structural differences of proteins viruses and cells, (bacteria). Lb. Gel antibodies against proteins (hemoglobins), *Electrophoresis,* 28 **(2007)**, 2345-2350.
12. Bolisay, L. D.; Culver, J. N.; Kofinas, P. Molecularly imprinted polymers for tobacco mosaic virus recognition, *Biomaterials,* 27 **(2006)**, 4165-4168.
13. Seidler, K.; Lieberzeit, P. A.; Dickert, F. L. Application of yeast imprinting in biotechnology and process control, *Analyst,* 134 **(2009)**, 361-366.
14. Spivak, D. A.; Shea, K. J. Investigation into the scope and limitations of molecular imprinting with DNA molecules, *Anal Chim Acta,* 435 **(2001)**, 65-74.
15. Whitcombe, M. J., http://mipdatabase.com/database.html. Accessed *29-07-2010.*
16. Turner, N. W.; Jeans, C. W.; Brain, K. R.; Allender, C. J.; Hlady, V.; Britt, D. W. From 3D to 2D: A review of the molecular imprinting of proteins, *Biotechnol Prog,* 22 **(2006)**, 1474-1489.
17. Takeuchi, T.; Hishiya, T. Molecular imprinting of proteins emerging as a tool for protein recognition, *Org Biomol Chem,* 6 **(2008)**, 2459-2467.
18. Valdebenito, A.; Espinoza, P.; Lissi, E. A.; Encinas, M. V. Bovine serum albumin as chain transfer agent in the acrylamide polymerization. Protein-polymer conjugates, *Polymer,* 51 **(2010)**, 2503-2507.
19. Breukink, E.; van Heusden, H. E.; Vollmerhaus, P. J.; Swiezewska, E.; Brunner, L.; Walker, S.; Heck, A. J. R.; de Kruijff, B. Lipid ii is an intrinsic component of the pore induced by nisin in bacterial membranes, *J Biol Chem,* 278 **(2003)**, 19898-19903.
20. Kok, R. J.; Grijpstra, F.; Nederhoed, K. H.; Moolenaar, F.; Zeeuw, D. D.; Meijer, D. K. F. Renal drug delivery with low-molecular-weight proteins: The effect of charge modifications on the body distribution of drug-lysozyme conjugates, *Drug Del,* 6 **(1999)**, 1-8.
21. Matsunaga, T.; Hishiya, T.; Takeuchi, T. Surface plasmon resonance sensor for lysozyme based on molecularly imprinted thin films, *Anal Chim Acta,* 591 **(2007)**, 63-67.
22. Kimhi, O.; Bianco-Peled, H. Study of the interactions between protein-imprinted hydrogels and their templates, *Langmuir,* 23 **(2007)**, 6329-6335.

23. Lowry, O. H.; Rosebrough, N. J.; Farr, A. L.; Randall, R. J. Protein measurement with the folin phenol reagent, *J Biol Chem,* 193 **(1951)**, 265-275.

24. Dong, A. C.; Jones, L. S.; Kerwin, B. A.; Krishnan, S.; Carpenter, J. F. Secondary structures of proteins adsorbed onto aluminum hydroxide: Infrared spectroscopic analysis of proteins from low solution concentrations, *Anal Biochem,* 351 **(2006)**, 282-289.

25. Kelly, S. M.; Jess, T. J.; Price, N. C. How to study proteins by circular dichroism, *Biochim Biophys Acta - Prot Proteomics,* 1751 **(2005)**, 119-139.

26. Hardman, K. D.; Eylar, E. H.; Ray, D. K.; Banaszak, L. J.; Gurd, F. R. N. Isolation of sperm whale myoglobin by low temperature fractionation with ethanol and metallic ions, *J Biol Chem,* 241 **(1966)**, 432-442.

27. Hawkins, D. M.; Stevenson, D.; Reddy, S. M. Investigation of protein imprinting in hydrogel-based molecularly imprinted polymers (hydromips), *Anal Chim Acta,* 542 **(2005)**, 61-65.

28. Janiak, D. S.; Ayyub, O. B.; Kofinas, P. Effects of charge density on the recognition properties of molecularly imprinted polymeric hydrogels, *Macromolecules,* 42 **(2009)**, 1703-1709.

29. Schillemans, J. P.; Flesch, F. M.; Hennink, W. E.; van Nostrum, C. F. Synthesis of bilayer-coated nanogels by selective cross-linking of monomers inside liposomes, *Macromolecules,* 39 **(2006)**, 5885-5890.

30. Rouser, G.; Fkeischer, S.; Yamamoto, A. Two dimensional then layer chromatographic separation of polar lipids and determination of phospholipids by phosphorus analysis of spots, *Lipids,* 5 **(1970)**, 494-6.

31. Hjerten, S.; Liao, J. L.; Nakazato, K.; Wang, Y.; Zamaratskaia, G.; Zhang, H. X. Gels mimicking antibodies in their selective recognition of proteins, *Chromatographia,* 44 **(1997)**, 227-234.

32. Sellergren, B., The non-covalent approach to molecular imprinting. In *Molecularly imprinted polymers: Man-made mimics of antibodies and their applications in analytical chemistry*, Sellergren, B., Ed. Elsevier: Amsterdam, 2001; pp 113-183.

33. Liao, J.; Wang, Y.; Hjertén, S. A novel support with artificially created recognition for the selective removal of proteins and for affinity chromatography, *Chromatographia,* 42 **(1996)**, 259-262.

34. Ghasemzadeh, N.; Nyberg, F.; Hjerten, S. Highly selective artificial gel antibodies for detection and quantification of biomarkers in clinical samples. I. Spectrophotometric approach to design the calibration curve for the quantification, *J Sep Sci,* 31 **(2008)**, 3945-3953.

35. Tong, D.; Heényi, C.; Bikádi, Z.; Gao, J.; Hjertén, S. Some studies of the chromatographic properties of gels ('artificial antibodies/receptors') for selective adsorption of proteins, *Chromatographia,* 54 **(2001)**, 7-14.

36. Bossi, A.; Piletsky, S. A.; Piletska, E. V.; Righetti, P. G.; Turner, A. P. Surface-grafted molecularly imprinted polymers for protein recognition, *Anal Chem,* 73 **(2001)**, 5281-6.

37. Bonini, F.; Piletsky, S.; Turner, A. P.; Speghini, A.; Bossi, A. Surface imprinted beads for the recognition of human serum albumin, *Biosens Bioelectron,* 22 **(2007)**, 2322-8.

38. Lu, Y.; Yan, C. L.; Gao, S. Y. Preparation and recognition of surface molecularly imprinted core-shell microbeads for protein in aqueous solutions, *Appl Surf Sci,* 255 **(2009)**, 6061-6066.

39. Rick, J.; Chou, T.-C. Using protein templates to direct the formation of thin-film polymer surfaces, *Biosens Bioelectron,* 22 **(2006)**, 544-549.

40. Piletsky, S. A.; Piletska, E. V.; Chen, B.; Karim, K.; Weston, D.; Barrett, G.; Lowe, P.; Turner, A. P. F. Chemical grafting of molecularly imprinted homopolymers to the surface of microplates. Application of artificial adrenergic receptor in enzyme-linked assay for β-agonists determination, *Anal Chem,* 72 **(2000)**, 4381-4385.

41. Turner, N. W.; Liu, X.; Piletsky, S. A.; Hlady, V.; Britt, D. W. Recognition of conformational changes in beta-lactoglobulin by molecularly imprinted thin films, *Biomacromolecules,* 8 **(2007)**, 2781-2787.

42. Kulikova, G. A.; Ryabinina, I. V.; Guseynov, S. S.; Parfenyuk, E. V. Calorimetric study of adsorption of human serum albumin onto silica powders, *Thermochim Acta,* 503 **(2010)**, 65-69.

43. Hirayama, K.; Sakai, Y.; Kameoka, K. Synthesis of polymer particles with specific lysozyme recognition sites by a molecular imprinting technique, *J Appl Pol Sci,* 81 **(2001)**, 3378-3387.

44. Uysal, A.; Demirel, G.; Turan, E.; Caykara, T. Hemoglobin recognition of molecularly imprinted hydrogels prepared at different pHs, *Anal Chim Acta,* 625 **(2008)**, 110-115.

45. Ou, S. H.; Wu, M. C.; Chou, T. C.; Liu, C. C. Polyacrylamide gels with electrostatic functional groups for the molecular imprinting of lysozyme, *Anal Chim Acta,* 504 **(2004)**, 163-166.

46. Odabasi, M.; Say, R.; Denizli, A. Molecular imprinted particles for lysozyme purification, *Mater Sci Eng C,* 27 **(2007)**, 90-99.

47. Fu, G. Q.; Zhao, J. C.; Yu, H.; Liu, L.; He, B. L. Bovine serum albumin-imprinted polymer gels prepared by graft copolymerization of acrylamide on chitosan, *React Funct Pol,* 67 **(2007)**, 442-450.

48. Hawkins, D. M.; Trache, A.; Ellis, E. A.; Stevenson, D.; Holzenburg, A.; Meininger, G. A.; Reddy, S. M. Quantification and confocal imaging of protein specific molecularly imprinted polymers, *Biomacromolecules,* 7 **(2006)**, 2560-2564.

49. Lanz, E.; Gregor, M.; Slavík, J.; Kotyk, A. Use of FITC as a fluorescent probe for intracellular pH measurement, *J Fluoresc,* 7 **(1997)**, 317-319.

50. Ma, L. Y.; Wang, H. Y.; Xie, H.; Xu, L. X. A long lifetime chemical sensor: Study on fluorescence property of fluorescein isothiocyanate and preparation of pH chemical sensor, *Spectrochim Acta A Mol Biomol Spectrosc,* 60 **(2004)**, 1865-1872.

51. Guo, T. Y.; Xia, Y. Q.; Hao, G. J.; Song, M. D.; Zhang, B. H. Adsorptive separation of hemoglobin by molecularly imprinted chitosan beads, *Biomaterials,* 25 **(2004)**, 5905-12.

52. Pang, X. S.; Cheng, G. X.; Zhang, Y. H.; Lu, S. L. Soft-wet polyacrylamide gel beads with the imprinting of bovine serum albumin, *React Funct Pol,* 66 **(2006)**, 1182-1188.

53. Tan, C. J.; Tong, Y. W. The effect of protein structural conformation on nanoparticle molecular imprinting of ribonuclease A using miniemulsion polymerization, *Langmuir,* 23 **(2007)**, 2722-2730.

54. Xia, Y. Q.; Guo, T. Y.; Song, M. D.; Zhang, B. H.; Zhang, B. L. Hemoglobin recognition by imprinting in semi-interpenetrating polymer network hydrogel based on polyacrylamide and chitosan, *Biomacromolecules,* 6 **(2005)**, 2601-2606.

55. Fu, G.-Q.; Yu, H.; Zhu, J. Imprinting effect of protein-imprinted polymers composed of chitosan and polyacrylamide: A re-examination, *Biomaterials,* 29 **(2008)**, 2138-2142.

56. Tan, C. J.; Chua, M. G.; Ker, K. H.; Tong, Y. W. Preparation of bovine serum albumin surface-imprinted submicrometer particles with magnetic susceptibility through core-shell miniemulsion polymerization, *Anal Chem,* 80 **(2008)**, 683-692.

57. Tan, C. J.; Wangrangsimakul, S.; Bai, R.; Tong, Y. W. Defining the interactions between proteins and surfactants for nanoparticle surface imprinting through miniemulsion polymerization, *Chem Mater,* 20 **(2008)**, 118-127.

58. Fu, G.; Zhu, J.; Jiang, Y. Comment on "Preparation of superparamagnetic ribonuclease A surface-imprinted submicrometer particles for protein recognition in aqueous media", *Anal Chem,* 80 **(2008)**, 2634-2635.

59. Tan, C. J.; Wangrangsimakul, S.; Sankarakumar, N.; Tong, Y. W. Response to comment on "Preparation of superparamagnetic ribonuclease a surface-imprinted submicrometer particles for protein recognition in aqueous media", *Anal Chem,* 80 **(2008)**, 9375-9376.

60. Young, B. R.; Pitt, W. G.; Cooper, S. L. Protein adsorption on polymeric biomaterials : Ii. Adsorption kinetics, *J Colloid Interface Sci,* 125 **(1988)**, 246-260.

61. Holmberg, M.; Hou, X. Competitive protein adsorption - multilayer adsorption and surface induced protein aggregation, *Langmuir,* 25 **(2009)**, 2081-2089.

62. Janiak, D. S.; Ayyub, O. B.; Kofinas, P. Effects of charge density on the recognition properties of molecularly imprinted polyampholyte hydrogels, *Polymer,* 51 **(2010)**, 665-670.

63. Tov, O. Y.; Luvitch, S.; Bianco-Peled, H. Molecularly imprinted hydrogel displaying reduced non-specific binding and improved protein recognition, *J Sep Sci,* 33 **(2010)**, 1673-1681.

64. Lu, S. L.; Cheng, G. X.; Pang, X. S. Protein-imprinted soft-wet gel composite microspheres with magnetic susceptibility. Ii. Characteristics, *J Appl Pol Sci,* 99 **(2006)**, 2401-2407.

65. Pang, X. S.; Cheng, G. X.; Li, R. S.; Lu, S. L.; Zhang, Y. H. Bovine serum albumin-imprinted polyacrylamide gel beads prepared via inverse-phase seed suspension polymerization, *Anal Chim Acta,* 550 **(2005)**, 13-17.

66. Pang, X. S.; Cheng, G. X.; Lu, S. L.; Tang, E. J. Synthesis of polyacrylamide gel beads with electrostatic functional groups for the molecular imprinting of bovine serum albumin, *Anal Bioanal Chem,* 384 **(2006)**, 225-230.

67. Nicolau Jr, D. V.; Nicolau, D. V. Towards a theory of protein adsorption: Predicting the adsorption of proteins on surfaced using a piecewise linear model validated using the biomolecular adsorption database, *2nd Asia-Pacific Bioinformatics Conference; Conferences in Research and Practice in Information Technology,* 29 **(2004)**.

68. Lin, H.-Y.; Hsu, C.-Y.; Thomas, J. L.; Wang, S.-E.; Chen, H.-C.; Chou, T.-C. The microcontact imprinting of proteins: The effect of cross-linking monomers for lysozyme, ribonuclease A and myoglobin, *Biosens Bioelectron,* 22 **(2006)**, 534-543.

69. Turner, N. W.; Wright, B. E.; Hlady, V.; Britt, D. W. Formation of protein molecular imprints within langmuir monolayers: A quartz crystal microbalance study, *J Colloid Interface Sci,* 308 **(2007)**, 71-80.

70. Hayden, O.; Haderspock, C.; Krassnig, S.; Chen, X. H.; Dickert, F. L. Surface imprinting strategies for the detection of trypsin, *Analyst,* 131 **(2006)**, 1044-1050.

71. Lin, T. Y.; Hu, C. H.; Chou, T. C. Determination of albumin concentration by MIP-QCM sensor, *Biosens Bioelectron,* 20 **(2004)**, 75-81.

72. Honore, B. Protein-binding studies with radiolabeled compounds containing radiochemical impurities - equilibrium dialysis versus dialysis rate determination, *Anal Biochem,* 162 **(1987)**, 80-88.

73. Limbird, L. E., *Cell surface receptors: A short course on theory and methods*. 3rd ed.; Springer: New York, **2005**.

74. Hua, Z.; Chen, Z.; Li, Y.; Zhao, M. Thermosensitive and salt-sensitive molecularly imprinted hydrogel for bovine serum albumin, *Langmuir,* 24 **(2008)**, 5773-5780.

75. Silvestri, D.; Barbani, N.; Coluccio, M. L.; Pegoraro, C.; Giusti, P.; Cristallini, C.; Ciardelli, G. Poly(ethylene-co-vinyl alcohol) membranes with specific adsorption properties for potential clinical application, *Sep Sci Technol,* 42 **(2007)**, 2829-2847.

76. Silvestri, D.; Barbani, N.; Cristallini, C.; Giusti, P.; Ciardelli, G. Molecularly imprinted membranes for an improved recognition of biomolecules in aqueous medium, *J Membrane Sci,* 282 **(2006)**, 284-295.

77. Guo, T. Y.; Xia, Y. Q.; Hao, G. J.; Zhang, B. H.; Fu, G. Q.; Yuan, Z.; He, B. L.; Kennedy, J. F. Chemically modified chitosan beads as matrices for adsorptive separation of proteins by molecularly imprinted polymer, *Carbohydrate Pol,* 62 **(2005)**, 214-221.

78. Yan, C.-L.; Yan, Y.; Gao, S.-Y. Coating lysozyme molecularly imprinted thin films on the surface of microspheres in aqueous solutions, *J Polym Sci A,* **(2007)**, 1911-1919.

79. Shiomi, T.; Matsui, M.; Mizukami, F.; Sakaguchi, K. A method for the molecular imprinting of hemoglobin on silica surfaces using silanes, *Biomaterials,* 26 **(2005)**, 5564-5571.

80. Gasteiger, E.; Hoogland, C.; Gattiker, A.; Duvaud, S.; Wilkins, M. R.; Appel, R. D.; Bairoch, A., *Protein identification and analysis tools on the expasy server*. Humana Press **2005**.

81. Bethesda, M. D. The ncbi handbook [internet] chapter 17, the reference sequence (refseq) project. Available from http://www.ncbi.nlm.nih.gov/entrez/query.fcgi?db=Books (**23-07-2010**),

82. Breukink, E.; de Kruijff, B. Lipid ii as a target for antibiotics, *Nat Rev Drug Discov,* 5 **(2006)**, 321-332.

83. Hoshino, Y.; Kodama, T.; Okahata, Y.; Shea, K. J. Peptide imprinted polymer nanoparticles: A plastic antibody, *J Am Chem Soc,* 130 **(2008)**, 15242-15243.

84. Hoshino, Y.; Koide, H.; Urakami, T.; Kanazawa, H.; Kodama, T.; Oku, N.; Shea, K. J. Recognition, neutralization, and clearance of target peptides in the bloodstream of living mice by molecularly imprinted polymer nanoparticles: A plastic antibody, *J Am Chem Soc,* 132 **(2010)**, 6644-6645.

85. Hoshino, Y.; Urakami, T.; Kodama, T.; Koide, H.; Oku, N.; Okahata, Y.; Shea, K. Design of synthetic polymer nanoparticles that capture and neutralize a toxic peptide, *Small,* **(2009)**, 1562-1568.

CONJUGATION OF METHACRYLAMIDE GROUPS
TO A MODEL PROTEIN
VIA A REDUCIBLE LINKER FOR IMMOBILIZATION
AND SUBSEQUENT TRIGGERED RELEASE FROM HYDROGELS

- ELLEN VERHEYEN - LISE DELAIN-BIOTON - STEFFEN VAN DER WAL - NAJIM EL MORABIT -

- ARJAN BARENDREGT - WIM E. HENNINK - CORNELUS F. VAN NOSTRUM -

ABSTRACT

We report an efficient strategy to introduce methacrylamide groups on the lysine residues of a model protein (lysozyme) for immobilization and triggered release from a hydrogel network. A novel spacer unit was designed, containing a disulfide bond, such that the release of the protein can be triggered by reduction. The lysozyme modification was performed in two steps in aqueous media. First, the protein was thiolated and subsequently reacted with the novel linker molecule (2-(2-pyridin-2-yldisulfanyl)ethyl 2-(methacrylamido)acetate) via disulfide exchange to obtain the desired methacrylated protein. The modified lysozymes with different degrees of methacrylate substitution were characterized by MALDI-TOF MS and titration of free NH_2 residues, whereas possible structural changes of the protein were investigated by spectral analysis. The modification reaction is well controlled and the number of introduced functions can be tailored by changing the reaction conditions. The protein conformation was not significantly influenced up to an average of three modifications per lysozyme. Gel electrophoresis experiments showed that the methacrylamide modified protein can be immobilized in a polyacrylamide hydrogel and subsequently released by reduction of the spacer by which the protein was grafted to the polymeric network.

INTRODUCTION

Chemical derivatization of proteins to form bioconjugates has become increasingly important in the field of biotechnology[1-3]. Chemical modification is carried out for a number of reasons, for example to improve the bioavailability[4], to increase the stability[5], or to modify the biological activity[6, 7]. A successful and widely used strategy is the attachment of PEG to therapeutic proteins, resulting in a decreased immunogenicity, an increased stability and prolonged circulation time[8-10]. Also the temperature-sensitive poly(N-isopropyl acrylamide) (pNIPAAM) has been conjugated to proteins and peptides for enzyme immobilization[11-13], affinity separation[14] and immunosensors[15, 16].

On the other hand, chemically modified proteins and enzymes can be used for immobilization on surfaces or within polymer networks, which serves some interesting purposes, e.g. increased stability of the protein/enzyme, easy work up of reaction mixtures and reuse of the biocatalysts[17]. One approach for the covalent immobilization of proteins is the synthesis of protein-macromers, which can be co-polymerized in hydrogel networks. This technique is used for enzyme immobilization[18-20], as well for drug delivery purposes. For the latter application, protein-polymer conjugates were polymerized to form hydrogels which can be used for the controlled delivery of entrapped drug molecules[21, 22]. More precisely, Iemma *et al*. conjugated methacrylate groups directly to bovine serum albumin (BSA) for subsequent use as biodegradable crosslinker in pNIPAAm hydrogel microspheres[21]. On the other hand, King *et al*. conjugated PEG-diacrylates to calmodulin (CaM), a dynamic protein which undergoes a reversible conformational change upon binding of ligands. Crosslinking of PEG-CaM resulted in hydrogels that showed reversible volume change upon binding of ligands (i.e. trifluoperazine), resulting in release of an entrapped therapeutic protein (i.e. vascular endothelial growth factor)[22].

In this paper we add a novel concept as we present the covalent, yet transient immobilization of a model protein in a hydrogel network, eventually aiming at the triggered intracellular release of the protein. During the past decades the design and synthesis of carrier systems for triggered release of biomacromolecules, e.g. proteins, peptides or DNA, has received increasing attention[23-26]. This comes together with the increasing development of biomacromolecules to be used as therapeutic agents for various diseases, including cancer. Many of these biopharmaceuticals have their therapeutic targets inside the cell, and should therefore be taken

up by cells in order to be effective. However, the intracellular delivery is often hampered because they have a poor stability in vivo, are susceptible to extra- and intracellular degradation, and show poor cellular uptake[25]. Hydrogel nanoparticles are very suitable materials for the delivery of macromolecules like proteins, due to their biocompatibility[27-29]. However, due to the large surface area and short diffusion distances in nanoparticles, entrapped proteins are released extremely rapidly. By altering the gel properties, one can tailor the release kinetics[22, 30, 31]. For instance, one can increase the network density to prevent premature rapid release from the nanogels. As a drawback of this approach, however, incomplete release of protein molecules may happen[32, 33], or the slow release could be a disadvantage once the nanogels have reached their target site. Recently, many stimuli responsive hydrogels have been developed to address this issue[30, 34, 35]. These hydrogels respond to physiological variations in, e.g. temperature[36] or pH[37-39]. Also systems responding to the presence of biomolecules like glucose[40, 41], as well as hydrogels containing reduction sensitive disulfide crosslinks[15, 42] have been developed to obtain a controlled release of biotherapeutics.

Here we introduce an alternative approach for triggered intracellular release of proteins from the protective environment of a hydrogel. A specially designed linker molecule containing a methacrylamide group was conjugated to a model protein to allow its co-polymerization in a hydrogel network. The linker molecule contains biodegradable units, i.e. a disulfide bond that is susceptible to reduction by e.g. glutathione present in the cytosol[43] and an ester bond which can be hydrolyzed. This makes the linker highly attractive in applications such as intracellular delivery of protein[15, 43]. The challenge is to introduce a maximum number of linker molecules to the protein without modification of the 3D-structure and biological activity.

In this paper, we used hen egg white lysozyme as a well known and well described model protein[44-46]. Lysozyme has six amine groups in the side chains of the lysine residues and one amine at its N-terminus. The reactivity of these seven groups is different and well documented in the literature[47]. Three of them, localized on the surface of the macromolecule, are the most reactive and readily available to be functionalized, the other three are buried inside the ternary protein structure. Lysozyme, modified with different amounts of linkers, was characterized by MALDI-TOF MS, titration of free amines, spectral analysis and the remaining biological activity was determined. Furthermore, the reactivity of the methacrylamide moieties was tested by co-polymerization in a polyacrylamide gel.

MATERIALS AND METHODS

Materials

All chemicals were used as received. Chicken egg white lysozyme (LZM), N,N'-dicyclohexylcarbodiimide (DCC), 4-(Dimethylamino)pyridine (DMAP), dimethylsulfoxide (DMSO), β-mercaptoethanol, and sinapinic acid were purchased from Fluka (Zwijndrecht, The Netherlands). N-Succinimidyl S-Acetylthioacetate (SATA), dialysis cassettes, and Micro BCA Protein Assay kit were obtained from PIERCE (Perbio Science BV, Etten-leur, The Netherlands). Disodium hydrogen phosphate, ethylenediaminetetraacetic acid disodium salt (EDTA), hydrindantin, hydrochloric acid (HCl), hydroxylamine hydrochloride, mercaptopyridine, 2-methoxyethanol, Micrococcus Lysodeikticus, ninhydrin, ammonium peroxodisulfate (APS), sodium dihydrogen phosphate, 3-(N-morpholino)propanesulfonic acid (MOPS), tetrahydrofurane (THF), N,N,N',N'-tetramethylethylenediamine (TEMED), and trifluoroacetic acid (TFA) were purchased from Sigma-Aldrich (Zwijndrecht, The Netherlands). Acetonitril, dichloromethane (DCM), ethyl acetate and methanol were obtained from Biosolve (Valkenswaard, The Netherlands). Acetic acid, ethanol, glycine, hexane, silica gel 60 (0.040-0.063 mm), sodium acetate, sodium chloride, sodium hydroxide and Tris(hydroxymethyl)-aminomethane were purchased from Merck (Darmstadt, Germany). N-Methacryloyl glycine was obtained from SynChem OHG (Altenburg, Germany). SimplyBlue™ SafeStain was purchased from Invitrogen Ltd (Breda, The Netherlands). 2-(2-Pyridin-2-yldisulfanyl)ethanol was synthesized as described elsewhere[48].

Synthesis of 2-(2-Pyridin-2-yldisulfanyl)ethyl 2-(methacrylamido)acetate

A dried round bottom flask placed under a dry nitrogen atmosphere was loaded with N-methacryloyl glycine (3.592 g, 25.1 mmol), 2-(2-pyridin-2-yldisulfanyl)ethanol (4.7 g, 25.1 mmol) and DMAP (0.305 g, 2.5 mmol), in 100 mL dry THF. The solution was cooled to -10°C and a solution of DCC (5.565 g, 25.1 mmol) in 5 mL of THF was added dropwise. The mixture was stirred for 48 hours at room temperature under nitrogen atmosphere. Next, the crude product was filtered over a glass filter to remove the formed dicyclohexylurea (DCU) and the white precipitate was washed twice with 100 mL dichoromethane. Subsequently, the filtrate was evaporated to dryness under vacuum. The product was dissolved in ethylacetate and purified by column chromatography with hexane/ethylacetate (50/50) as the eluent (Rf=

0.18). After purification and evaporation of the solvent, 1.4 g product was obtained as yellow-orange oil (yield 30 %). IR (KBr): v= 3340, 3048, 2950, 1755, 1664, 1623, 1528, 1450, 1418, 1194, 763 cm^{-1}. ESI-MS: m/z (%)= 313 (M+H, 100), 170 (12), 142 (32). ^{1}H NMR (300 MHz, CDCl$_3$): δ = 1.98 (t, ^{3}J^{HH}= 7 Hz, 3H, CH$_3$), 3.06 (t, ^{3}J^{HH}= 6 Hz, 2H, OCH$_2$CH$_2$S), 4.07 (d, ^{3}D^{HH}= 5 Hz, 2H, NHCH$_2$C=O), 4.43 (t, ^{3}J^{HH}= 6 Hz, 2H, OCH$_2$CH$_2$S), 5.38 (1H, CH=C), 5.76 (1H, CH=C), 6.15 (1H, NH), 7.09 (m, 1H, Hpyr), 7.65 (m, 2H, Hpyr), 8.46 (m, 1H, Hpyr). ^{13}C NMR (75.4 MHz, CDCl$_3$): δ = 19.0 (CH$_3$), 37.6 (CH$_2$S), 41.9 (CH$_2$N), 63.6 (CH$_2$O), 120.4 (CH$_2$=C), 120.9, 124.6 (2C, C2, 4pyr), 137.7 (C3pyr), 139.7 (CH$_2$=C), 150.2 (C5pyr), 159.9 (C2pyr), 168.9, 170.2 (2C, C=O).

Modification of Lysozyme with Succinimidyl S-acetylthioacetate (SATA)

A stock solution of lysozyme (5 mg/mL) was prepared by dissolving 100 mg lysozyme (7.0 μmol; 49 μmol NH$_2$) in 20 mL PBS Buffer (0.1 M phosphate, 0.15 M NaCl, pH 7.2). SATA[49] (5.0 mg, 21.5 μmol) was dissolved in 0.5 mL dry DMSO and added to 2.0 mL of lysozyme solutions with molar ratios 1/7 to 10/7 of SATA/NH$_2$ (0.24, 0.48, 0.71, 0.95, 1.19 and 2.376 mg respectively). The mixtures were incubated at room temperature for 30 minutes. Next, the modified lysozyme (LSx, where x stands for the equivalents of SATA used) was dialyzed against PBS buffer (pH 5) for 24 hours to remove the excess of SATA as well as low molecular weight reaction products. The mass of the different modified proteins was analyzed with MALDI-TOF MS (vide infra) and the number of modified lysine residues was calculated by using the ninhydrin assay described below.

Deprotection of SATA-modified lysozyme and conjugation of 2-mercaptoethyl (methacrylamido)acetate

The SATA-modified lysozyme solution (3.5 mg/mL in PBS pH 5), was purged with nitrogen for 15 minutes. A deacetylation solution was prepared by dissolving 1.74 g of hydroxylamine hydrochloride, 0.365 g of EDTA in 50 mL PBS buffer (pH 7.2). Next 250 μL of this solution was added to the 2.5 mL protein solution under mild stirring. Subsequently, a solution of 2-(2-pyridin-2-yldisulfanyl)ethyl 2-(methacrylamido)acetate (5 equiv. with respect SH) in DMSO was added (0.92, 1.43, 1.67, 2.06, 3.13 and 4.38 mg for LS1-LS5 and LS10, respectively). The mixture was incubated at room temperature for 12 hours. The modified lysozyme was filtered (0.2 μm) and then purified by dialysis against PBS buffer (pH 5) for 48 hours at room temperature and stored

at 4°C. The mass of the different modified proteins was analyzed with MALDI-TOF MS (vide infra) and the number of modified lysine residues was calculated by using the ninhydrin assay as described below.

Mass spectrometry (MALDI-TOF MS)

For MALDI-TOF MS analysis of LSx and LMAx, a Kratos Axima CFR apparatus was used with cytochrome C (Mw = 12360 Da) as the internal reference and sinapinic acid as the matrix. The different lysozyme samples were diluted in a solution of water/CH_3CN (95/5) + 0.1 vol% of TFA to obtain a concentration of 0.1 mg/mL. Five µL of this solution was mixed with 10 µL solution of matrix (10 mg/mL) in water/CH_3CN containing 0.1 vol% TFA and spotted on the MALDI plate. For each sample two independent spectra were obtained for mass analysis. The relative amount of each modified protein species was calculated using ratios of the peak heights[50].

Determination of free amine groups in LSx and LMAx

The concentration of free amine groups in the different samples was determined spectrophotometrically by the use of ninhydrin[51]. The protein samples were diluted to ± 0.2 µmol/mL in 1 M sodium acetate buffer (pH 5.5). Next, 1 mL of freshly prepared ninhydrin solution (2.0 g ninhydrin and 0.3 g hydrindantin dissolved in 75 mL of 2-methoxyethanol and 25 mL of 4 M sodium acetate buffer, pH 5.5) was added to 1 mL protein solution. The solutions were mixed and incubated for 15 min at 100°C. After being cooled to room temperature, the samples were diluted with 5 mL of 50 vol% ethanol in water, and the absorbance was read at 570 nm with a Shimadzu UV-2450 UV/VIS spectrophotometer. Glycine (in 1 M acetate buffer) was used for calibration.

Spectral analysis of methacrylamide modified lysozyme (LMAx)

UV-VIS spectroscopy was carried out with a Shimadzu UV-2450 UV/VIS spectrophotometer with a 6-cell holder and UV-Probe software (Shimadzu Corporation, Kyoto, Japan). The absorbance spectra were recorded in the range of 200-350 nm. The concentration of the samples was fixed at 0.20 mg/mL lysozyme in PBS buffer.

CD measurements were performed with a dual beam DSM 1000 CD spectropolarimeter (On-Line Instruments Systems, Bogart, GA) using cuvettes with a path length of 0.20 mm. The

samples were diluted in PBS to obtain a concentration of 0.50 mg/mL lysozyme. Far UV-CD spectra were recorded from 250 to 195 nm at 25°C. For each sample, an average of 10 spectra was calculated.

Fluorescence measurements were carried out with Horiba Fluorolog fluorometer FL3-21 (Horiba Jobin Yvon, Longjumeau Cedex, France) using quartz cuvettes (Hellma, Müllheim, Germany). The excitation wavelength was set at 295 nm and the emission spectra were recorded in the range of 300-450 nm. An integration time of 1 s was used, and the excitation and emission band slits were set at 5 nm. The concentration was fixed at 0.05 mg/mL lysozyme in PBS buffer.

Determination of the enzymatic activity of lysozyme

The enzymatic activity assay is based on the hydrolysis of the outer cell membrane of *M. Lysodeikticus*, resulting in lysis of the bacteria and consequently a decrease of light scattering[52]. In short, a 0.2 mg/mL substrate cell suspension was prepared in 66 mM phosphate buffer pH 6.2. Next, 10 µL of a sample of modified lysozyme (0.1 mg/mL) was mixed with 1.3 mL of substrate solution and the decrease in turbidity at 450 nm was measured for 180 seconds. The enzymatic activity of the modified lysozyme is expressed as a percentage of activity of a reference lysozyme solution.

Immobilization of methacrylamide lysozyme in polyacrylamide hydrogels and gel electrophoresis under non-reducing and reducing conditions

The experimental set-up is based on the method described by Xiao and Tolbert[20]. In detail, 75 µL of modified (LMA3) or non-modified lysozyme solution (4.25 mg/mL) was mixed with 100 µL of a 30 wt% acrylamide:bisacrylamide solution (29:1 w/w), 75 µL sample buffer (60 mM Tris-HCl, 25 vol% glycerol, 4 vol% SDS, 0.1 wt% bromophenol, pH 6.8) and 50 µL PBS pH 5. To 250 µL of this mixture, 2.5 µL TEMED (20 vol% in PBS, pH adjusted to 5 with 6 M HCl) and 2.5 µL APS (10 wt% in PBS) were added to initiate the free radical polymerization. Immediately after mixing, 20 µL of the mixture was transferred into the slots of a SDS-PAGE gel and incubated for one hour at room temperature. For comparison, 20 µL unpolymerized protein-monomer mixture was added to the remaining empty slots and the gel was electrophoresed with SDS running buffer (50 mM MOPS, 50 mM TRIS, 0.1 vol% SDS). The proteins were stained with

coomassie brilliant blue[53]. The experimental set-up for SDS-PAGE under reducing conditions is similar, except the sample buffer contained 1.25 vol% β-mercaptoethanol. The migrated and immobilized fractions were quantified by gel densitometry using TotalLab Quant software (TotalLab, Newcastle, UK). The percentage of immobilized protein was calculated by the following equation:

$$\% \text{ LZM}_{immobile} = \text{immobilized density/(immobilized + migrated density)} \qquad (1)$$

RESULTS AND DISCUSSION

Synthesis and chemical characterization of methacrylamide lysozyme

The novel linker molecule 2-(2-pyridin-2-yldisulfanyl)ethyl 2-(methacrylamido)acetate was synthesized by esterification of N-methacryloyl glycine with 2-(2-pyridin-2-yldisulfanyl) ethanol in 30% yield (Scheme 1). The synthesis of methacrylamide-modified lysozyme was performed in two steps. First, lysine groups of the protein were modified with protected thiol functions using SATA reagent. Subsequently, the thiol groups were deprotected and coupled to the linker molecule via thiol-disulfide exchange to introduce methacrylamide groups into lysozyme (Scheme 2). To determine the maximum number of lysines that can be modified without affecting the protein conformation, lysozyme was reacted with different amounts of SATA to obtain LS1 to LS10, i.e. one to ten equivalents SATA per lysozyme which contains 7 NH_2 groups. The reaction was carried out at a protein concentration of 5 mg/mL, since precipitation occurred during the reaction at higher concentrations.

Scheme 1. Synthesis of 2-(2-Pyridin-2-yldisulfanyl)ethyl 2-(Methacrylamido)Acetate
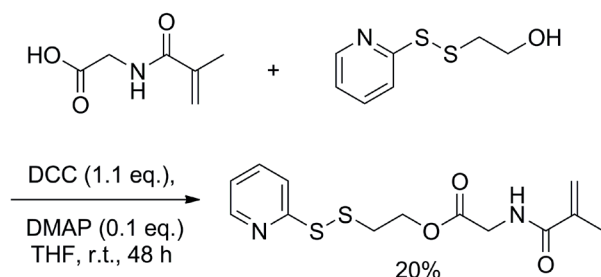
Scheme 2. Reaction scheme for the synthesis of methacrylamide modified lysozyme
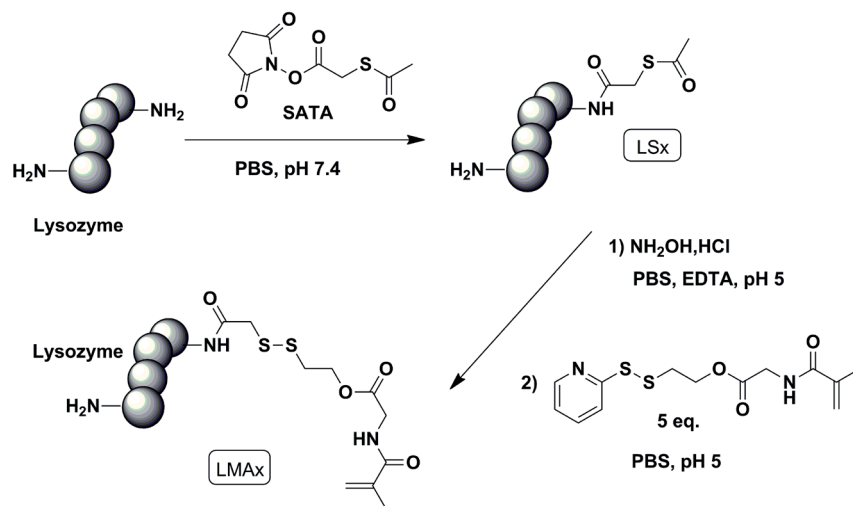
A typical MALDI-TOF spectrum of SATA modified lysozyme (LS3) is shown in Figure 1A. Several peaks are visible, and the difference between individual peaks is 116 Da, which is equal to the mass of one S-acetylthioacetate (ATA) unit. For each SATA to protein ratio an overview of the abundance of the different species is given in Table 1. As expected, a higher ratio of SATA to protein resulted in a higher degree of modification. When reacted with one, two and three equivalents SATA, residual native lysozyme was still present, with on average 1.5, 2.2 and 2.3 coupled ATA groups per protein molecule, respectively. Four and five equivalents resulted in an average of 2.4 and 2.8 modifications per lysozyme, respectively, and no unmodified lysozyme could be detected. In all cases, predominantly, up to three ATA groups were coupled to the protein. This is in correspondence with the fact that the six lysine amine groups and the N-terminus ε-amine have different reactivity and different location in the protein[47]. Three of them, the most reactive ones, are surface-exposed and consequently readily available for modification. The other three are buried in the molecular structure and should not be modified to prevent a major structural and conformational change of the protein[47]. Indeed, in the case that 10 equivalents of SATA reagent (LS10) were added to the protein, the MALDI-TOF spectrum showed a high level of modifications, up to 7 ATA groups per protein, which resulted in excessive precipitation of the protein most likely caused by a change of the net charge and increase of hydrophobicity of the protein. Since MALDI-TOF MS is not an absolute method to quantify the number of modifications, the number of ATA groups coupled to lysozyme was quantified

by use of the ninhydrin assay. The average number of ATA groups per lysozyme molecule was calculated using unmodified lysozyme as reference. As shown in Table 2, with an increasing SATA/NH_2 feed ratio, increasing numbers of amine groups are modified, in accordance to the MALDI-TOF mass spectra.
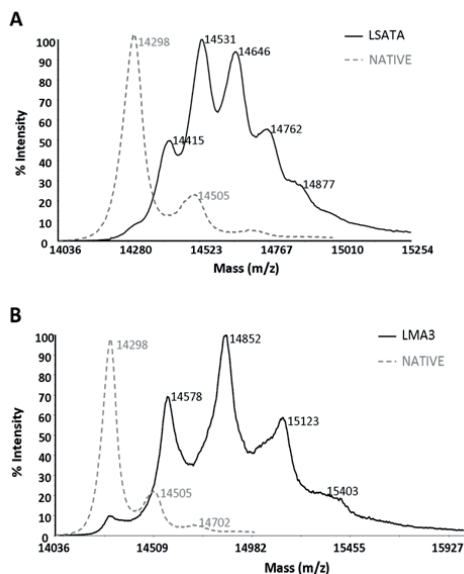

Figure 1. (A) MALDI-TOF MS spectrum of LS3 (i.e. SATA modified lysozyme prepared with 3:1 ratio SATA:LZM) (B) MALDI-TOF MS spectrum of LMA3 (i.e. MA-modified lysozyme prepared with 3:1 ratio SATA:LZM)

Table 1. Relative abundance of the different species in ATA/MA modified lysozyme

# equivalents ATA/MA	Relative abundance of different species[a]								
	LS1	LS2	LS3	LS4	LS5	LS10	LMA3	LMA4	LMA5
0	0.16	0.04	0.05				0.05		
1	0.36	0.20	0.22	0.15	0.05		0.31	0.12	0.05
2	0.31	0.37	0.29	0.42	0.34		0.32	0.42	0.28
3	0.17	0.30	0.27	0.30	0.42	0.12	0.21	0.31	0.45
4		0.09	0.20	0.13	0.19	0.39	0.12	0.15	0.22
5						0.32			
6						0.12			
7						0.05			
# equiv per LZM[b]	1.5	2.2	2.4	2.4	2.8	4.6	2.0	2.5	2.9

[a]Based on individual peak heights in MALDI-TOF mass spectrum; [b]Average number of ATA/MA moieties introduced per lysozyme, calculated from relative abundance of each species.

Table 2. Number of free NH$_2$ groups after modification of lysozyme (LZM) with 0-10 equivalents of SATA (LSx) and subsequent conjugation of the methacrylamide groups, as determined by ninhydrin assay. Also the calculated number of ATA and MA modifications for the different samples are given.

	After SATA modification		After MA conjugation	
# SATA equivalents/ LZM	# Free NH$_2$ groups LSx	# ATA groups per lysozyme	# Free NH$_2$ groups LSx	# MA groups per lysozyme
0 (native)	7.0 ± 0.2	0.0	7.0 ± 0.2	0.0
1	5.9 ± 0.2	1.1	5.7 ± 0.3	1.3
2	5.4 ± 0.2	1.6	5.2 ± 0.2	1.8
3	4.6 ± 0.1	2.4	4.3 ± 0.1	2.7
4	4.5 ± 0.2	2.5	4.5 ± 0.2	2.5
5	3.7 ± 0.1	3.3	3.4 ± 0.1	3.6
10	2.3 ± 0.1	4.7	1.8 ± 0.0	5.2

The deprotection of the SH groups was performed by adding hydroxylamine dissolved in a PBS/EDTA buffer. Next, the designed linker molecule (2-(2-pyridin-2-yldisulfanyl)ethyl 2-(methacrylamido)acetate) was conjugated to the thiol groups of modified lysozyme by thiol-disulfide exchange. Since thiol groups can be readily oxidized by molecular oxygen, the coupling reaction was done simultaneously with the deprotection step. The reaction was carried out at room temperature during 12 hours, with a five times molar excess of reagent with respect to thiol groups, at pH 5. This low pH is beneficial towards the thiol-disulfide exchange reaction for two reasons. First, protonation of the nitrogen of the pyridine ring provides a good leaving group for the thiol-disulfide exchange reaction, resulting in an increased conjugation rate[54]. Additionally, this low pH prevents the formation of a thiolate anion which suppresses the occurrence of a Michael addition reaction between the thiol group and the methacrylamide[55]. Furthermore, lysozyme has eight cysteines which could participate in the thiol-disulfide exchange reaction[56]. However, these cysteines are all paired and buried inside the protein structure. Even after treatment with urea, the cysteines are hardly available for reduction by dithiothreitol[57], so it is very unlikely that the cysteines of lysozyme participate in the thiol-disulfide reaction.

MALDI-TOF mass spectra of lysozyme-methacrylamide conjugates show similar distributions of modifications as the spectra of the intermediate protected thiol derivatives (Figure 1B and Table 1). The spectra of lysozyme previously modified with 3 equivalents of SATA, showed no ATA modified lysozyme and a mixture of species with 1 to 4 methacrylamide groups per lysozyme was detected. The number of introduced methacrylamide groups, as calculated from peak heights of the MALDI-TOF spectra, was comparable to the number of thiol groups

that were introduced in the first step (Table 2). Also quantification with the ninhydrin assay showed that the degree of modification was comparable for both LSx and LMA (Table 2). These results suggest a quantitative coupling of the linker molecule to the thiol groups introduced in lysozyme.

Structural analysis of methacrylamide modified lysozyme

UV spectroscopy was used to study possible aggregation of lysozyme during the reactions. Representative UV-VIS spectra for lysozyme modified with four ATA or four MA units are shown in Figure 2 (LS4 and LMA4). No difference in the spectra was observed between the modified lysozyme (1 to 4 equivalents ATA and MA) and the native one, indicating that no aggregation has occurred during the different reaction steps and subsequent work-up[58]. On the other hand, the spectrum of lysozyme modified with 10 equivalents of SATA (LS10) showed a clear increase in absorbance above 300 nm, indicating aggregation of the modified proteins[58] (Figure 2).
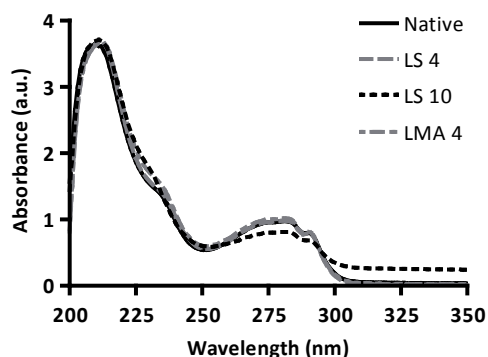

Figure 2. UV-VIS spectra of different variants of lysozyme. LS4, LS10: SATA modified LZM (with 4 and 10 equiv. of SATA); LMA4: methacrylamide modified LZM (obtained from intermediate LS4)

Circular dichroism (CD) and fluorescence spectroscopy were used to study possible changes in the secondary and tertiary structure after modification with SATA and the subsequent coupling of the methacrylamide groups. The overall shape of the far-UV CD spectra did not show significant changes for the samples modified with one up to four equivalents of SATA (Figure 3A). Also after coupling methacrylamide moieties to these intermediates no significant changes in the far-UV CD spectra were observed (Figure 3B). This indicates that up to three amine groups in lysozyme can be modified with ATA/MA moieties while maintaining the secondary protein structure (β-sheets). However, a clear change in the CD signal appeared for

lysozyme when more than 5 ATA groups were introduced (LS10), indicating moderate changes in the secondary protein structure[59]. By extensively modifying lysine residues, the net positive charge of the protein is reduced such that the protein folding is affected[60].
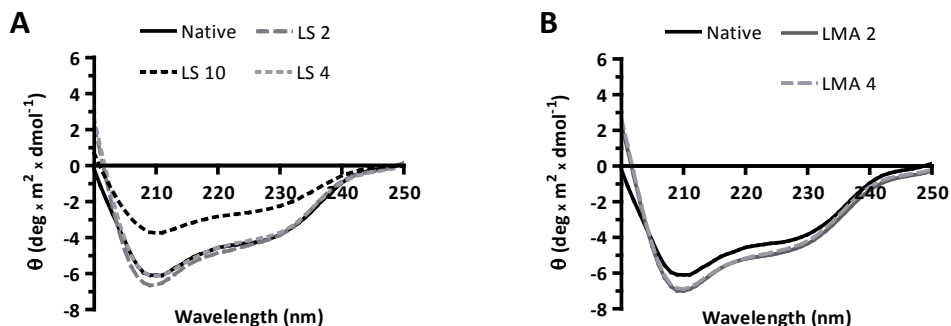

Figure 3. (A) Far-UV CD spectra of SATA modified lysozyme samples (Ratio SATA:LZM 2, 4, 10). (B) Far-UV CD spectra of methacrylamide modified lysozyme samples (Ratio SATA:LZM 2, 4). Spectra (average of 10) were taken of lysozyme samples at a concentration of 0.50 mg/mL in PBS pH 5.

The fluorescence spectrum of proteins is sensitive to small changes in their secondary and tertiary structure[61]. Hen egg white lysozyme contains six tryptophans which are predominantly responsible for its fluorescent properties[62, 63]. The tryptophan fluorescence spectra of the different lysozyme samples (0.05 mg/mL in PBS) are shown in Figure 4. The spectra have a similar band shape, however, large differences in fluorescence intensity are found. An increasing degree of modification, lead to a decrease in fluorescence intensity. This is probably caused by a decreased net charge of the protein which can affect the protein folding, and thus result in quenching of the tryptophans[64]. The decrease in fluorescence was more pronounced for methacrylamide modified (LMAx) than for SATA modified lysozyme (LSx). It is known that tryptophan fluorescence can be quenched if the tryptophans are in the vicinity of intermolecular disulfide bridges[65, 66]. Therefore, in case 2-(2-pyridin-2-yldisulfanyl)ethyl 2-(methacrylamido) acetate is conjugated with lysozyme (i.e. LMAx), additional quenching of the fluorescence intensity can be caused by the introduction of disulfide bridges. Since four of the (modified) lysine groups are located within a distance of 0.6 nm from one or two tryptophans[67], it is possible that the disulfide bridge interacts with tryptophan, resulting in quenching of the fluorescence signal. The spectra of the different modified species also show a subtle blue shift of the emission maximum (1 to 6 nm). This can be due to an increase in hydrophobicity of the tryphophans environment upon conjugation of the ATA and methacrylamide groups[68].
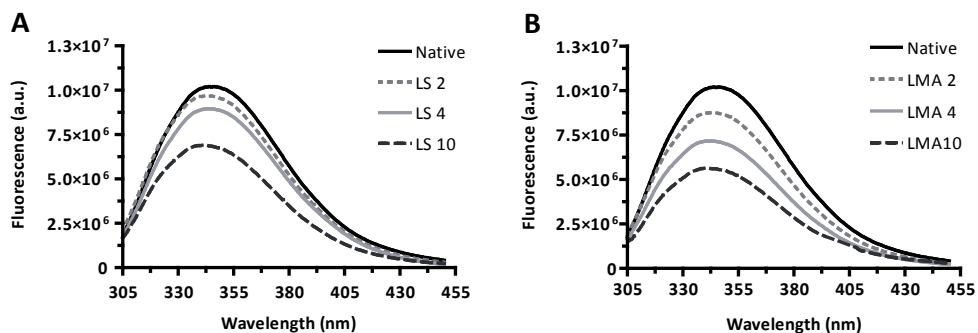
Figure 4. (A) Fluorescence spectra of SATA modified lysozyme samples (Ratio SATA:LZM 2, 4, 10). (B) Fluorescence spectra of methacrylamide modified lysozyme samples (Ratio SATA:LZM 2, 4 10). Spectra (average of 10) were taken of lysozyme samples at a concentration of 0.05 mg/mL in PBS pH 5.

Enzymatic activity

The enzymatic activity of the different modified lysozymes was measured and compared with that of native lysozyme (Figure 5). A decrease of the enzymatic activity was observed with increasing average number of modifications per lysozyme. It has been reported that some of the lysine residues are important for the catalytic activity of lysozyme and modification of the amine groups can result in a decrease of the activity[60, 69]. Also steric hindrance by the conjugated linker molecules might prevent binding of the substrate to the active site of the enzyme. Since the observed enzymatic activities are comparable for ATA-modified and methacrylated lysozymes, the decreased activity is most likely caused by change in surface charge of the protein, rather than by steric hindrance of the linker molecule. Interestingly, lysozyme LMA4, which was modified with an average of 2.3 methacrylamide moieties, is still for 60% active despite the absence of native lysozyme in this sample. Only a higher degree of modification results in an almost complete loss of lytic activity (LMA10: 14% remaining activity).
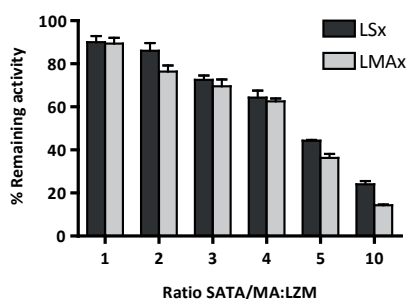

Figure 5. Enzymatic activity of the different lysozyme species after modification with SATA and methacrylamide moieties.

Immobilization of methacrylamide lysozyme in hydrogels and triggered release

SDS-PAGE analysis of LMA3 (Figure 6A, lane 2) showed that during the modification of the protein minute lysozyme dimerization had occurred (< 10%). Since these dimers are absent in the reducing gel (Figure 6B, lane 2), this is probably due to minor disulfide formation after deprotection of the thiol groups. To investigate whether the modified lysozyme can be immobilized in a hydrogel network, an aqueous solution of acrylamide and bisacrylamide was subjected to a free radical induced polymerization in the presence of native (LZM) or modified lysozyme (LMA3). The release of both native and modified lysozyme from the resulting polyacrylamide (PAA) gels was investigated by SDS-PAGE. At non-reducing conditions only 5% of the methacrylamide modified lysozyme was able to freely migrate into the gel (Figure 6A, lane 5), whereas the unmodified lysozyme (lane 4) almost completely (96%) migrated into the gel. These results indicate that almost 95% of the methacrylamide lysozyme was copolymerized in the gel network. The small amount of modified lysozyme that still migrated is probably unmodified lysozyme, which was still present in lysozyme modified with 3 equivalents (see Table 1).
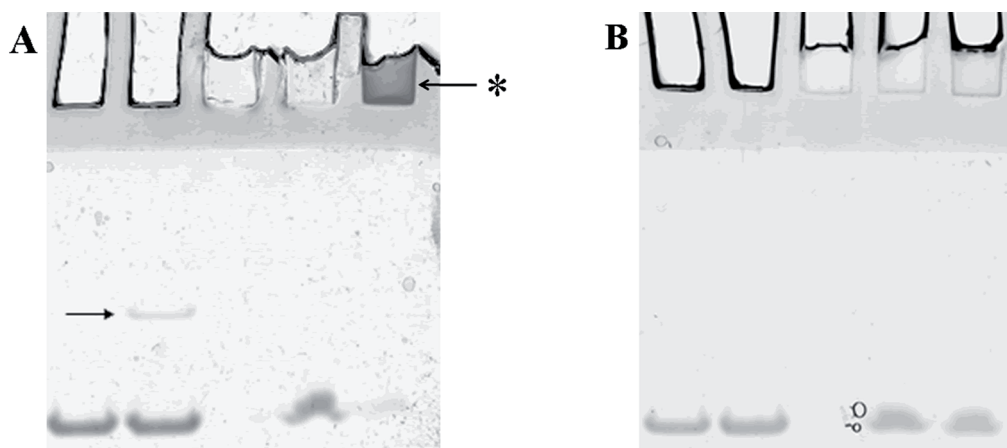
Figure 6. Immobilization and release of lysozyme from polyacrylamide (PAA) hydrogels visualized by coomassie staining and quantified by gel densitometry (given in % according to equation (1)). (A) SDS-page under non reducing conditions. Lane 1: Native LZM; 2: Non-polymerized LMA3 (arrow indicates LZM dimers (7%); 3 Control (empty) PAA hydrogel; 4: Native LZM in a polymerized gel (4% immobilized in slot); 5: immobilized LMA3 (95% in slot, indicated by *) (B) SDS-page under reducing conditions. Lane 1: Native LZM; 2: Non-polymerized LMA3; 3 Control (empty) PAA hydrogel; 4: Native LZM in a polymerized gel (6% immobilized in slot); 5: Immobilized LMA3 (9% in slot)

Since the spacer between the modified lysozyme and the polymer network can be split by reduction of the disulfide bond, electrophoresis was repeated in presence of β-mercaptoethanol as reducing agent. Under reducing conditions, both native and modified lysozyme migrated almost completely (± 90%) from the polymerized gel into the running gel (Figure 6B, lane 4 and 5, respectively). These results show that the disulfide linkages by which lysozyme is grafted to the hydrogel network are broken after exposure to β-mercaptoethanol and indicates that methacrylamide modified lysozyme can be reversibly immobilized in a hydrogel. Detailed data on the release kinetics and enzymatic activity of released lysozyme are presently under investigation and will be reported in a forthcoming report.

CONCLUSION

The objective of this study was to develop a method to functionalize lysozyme with methacrylamide functions, for subsequent immobilization and controlled release from a hydrogel network. The modification reaction is well controlled and the number of linkers introduced per protein molecule can be tailored by changing the reaction conditions. The first step is the most critical one as it determines the corresponding reaction sites for the following steps of the synthesis. After deprotection of the conjugated sulfhydryl groups, the methacrylamide moieties are introduced in a quantitative way. Lysozyme can be modified with up to three methacrylamide moieties without major conformational changes, as shown by spectral analysis. The lytic activity was still 60% after introducing an average of 2.3 methacrylamide units. The modified lysozyme was successfully immobilized into a hydrogel network and subsequently released by reduction of the degradable linker. Therefore it can be concluded that our approach is not only suitable for immobilization of proteins, but also highly promising for intracellular delivery of proteins. For example, when immobilized into a nanogel that can be internalized, the disulfide bond present in the linker molecule may be cleaved by glutathione present in the cytosol of cells, upon which the protein is released[70].

Acknowledgements:

REFERENCES

1. Duncan, R. The dawning era of polymer therapeutics, *Nat Rev Drug Discov,* 2 **(2003)**, 347-360.
2. Heredia, K. L.; Maynard, H. D. Synthesis of protein-polymer conjugates, *Org Biomol Chem,* 5 **(2007)**, 45-53.
3. Lutz, J.-F.; Börner, H. G. Modern trends in polymer bioconjugates design, *Prog Polym Sci,* 33 **(2008)**, 1-39.
4. Mahato, R. I.; Narang, A. S.; Thoma, L.; Miller, D. D. Emerging trends in oral delivery of peptide and protein drugs, *Crit Rev Ther Drug Carrier Syst,* 5 **(2003)**, 45-53.
5. Veronese, F. M.; Pasut, G. Pegylation, successful approach to drug delivery, *Drug Discovery Today,* 10 **(2005)**, 1451-1458.
6. Wenck, K.; Koch, S.; Renner, C.; Sun, W.; Schrader, T. A noncovalent switch for lysozyme, *J Am Chem Soc,* 129 **(2007)**, 16015-16019.
7. Bernkop-Schnürch, A.; Krist, S.; Vehabovic, M.; Valenta, C. Synthesis and evaluation of lysozyme derivatives exhibiting an enhanced antimicrobial action, *Eur J Pharm Sci,* 6 **(1998)**, 301-306.
8. Bailon, P.; Berthold, W. Polyethylene glycol-conjugated pharmaceutical proteins, *Pharm Sci Technol To,* 1 **(1998)**, 352-356.
9. Harris, J. M.; Chess, R. B. Effect of pegylation on pharmaceuticals, *Nat Rev Drug Discov,* 2 **(2003)**, 214.
10. Abuchowski, A.; McCoy, J. R.; Palczuk, N. C. Effect of covalent attachment of polyethylene glycol on immunogenicity and circulating life of bovine liver catalase, *J Biol Chem,* 252 **(1977)**, 3582-3586.
11. Heredia, K. L.; Bontempo, D.; Ly, T.; Byers, J. T.; Halstenberg, S.; Maynard, H. D. In situ preparation of protein-"Smart" Polymer conjugates with retention of bioactivity, *J Am Chem Soc,* 127 **(2005)**, 16955-16960.
12. Ding, Z.; Chen, G.; Hoffman, A. S. Unusual properties of thermally sensitive oligomer-enzyme conjugates of poly(*N*-isopropylacrylamide)-trypsin, *J Biomed Mater Res A,* 39 **(1998)**, 498-505.
13. Arica, M. Y.; Öktem, H. A.; Öktem, Z.; Tuncel, S. A. Immobilization of catalase in poly(isopropylacrylamide-co-hydroxyethylmethacrylate) thermally reversible hydrogels, *Polymer International,* 48 **(1999)**, 879-884.
14. Chen, J. P.; Huffman, A. S. Polymer-protein conjugates: Ii. Affinity precipitation separation of human immunogammaglobulin by a poly(*N*-isopropylacrylamide)-protein a conjugate, *Biomaterials,* 11 **(1990)**, 631-634.
15. Liu, Y.; Meng, S.; Mu, L.; Jin, G.; Zhong, W.; Kong, J. Novel renewable immunosensors based on temperature-sensitive pnipaam bioconjugates, *Biosens Bioelectron,* 24 **(2008)**, 710-715.
16. Monji, N.; Hoffman, A. A novel immunoassay system and bioseparation process based on thermal phase separating polymers, *Appl Biochem Biotechnol,* 14 **(1987)**, 107-120.
17. Bornscheuer, U. T. Immobilizing enzymes: How to create more suitable biocatalysts, *Angew Chem Int Ed,* 42 **(2003)**, 3336-3337.
18. Brueggemeier, S. B.; Kron, S. J.; Palecek, S. P. Use of protein-acrylamide copolymer hydrogels for measuring protein concentration and activity, *Anal Biochem,* 329 **(2004)**, 180-189.
19. Brueggemeier, S. B.; Wu, D.; Kron, S. J.; Palecek, S. P. Protein-acrylamide copolymer hydrogels for array-based detection of tyrosine kinase activity from cell lysates, *Biomacromolecules,* 6 **(2005)**, 2765-2775.
20. Xiao, J.; Tolbert, T. J. Synthesis of polymerizable protein monomers for protein-acrylamide hydrogel formation, *Biomacromolecules,* 10 **(2009)**, 1939-1946.
21. Iemma, F.; Spizzirri, U.; Puoci, F.; Cirillo, G.; Curcio, M.; Parisi, O.; Picci, N. Synthesis and release profile analysis of thermo-sensitive albumin hydrogels, *Colloid Polym Sci,* 287 **(2009)**, 779-787.
22. King, W. J.; Mohammed, J. S.; Murphy, W. L. Modulating growth factor release from hydrogels via a protein conformational change, *Soft Matter,* 5 **(2009)**, 2399-2406.

23. Koo, O. M.; Rubinstein, I.; Onyuksel, H. Role of nanotechnology in targeted drug delivery and imaging: A concise review, *Nanomed: Nanotech Biol Med,* 1 **(2005)**, 193-212.

24. Hamidi, M.; Azadi, A.; Rafiei, P. Hydrogel nanoparticles in drug delivery, *Adv Drug Del Rev,* 60 **(2008)**, 1638-1649.

25. Allen, T. M.; Cullis, P. R. Drug discovery systems: Entering the mainstream, *Science,* 303 **(2004)**, 1818-1822.

26. Crommelin, D. J. A.; Storm, G.; Jiskoot, W.; Stenekes, R.; Mastrobattista, E.; Hennink, W. E. Nanotechnological approaches for the delivery of macromolecules, *J Control Release,* 87 **(2003)**, 81-88.

27. Kashyap, N.; Kumar, N.; Ravikumar, M. Hydrogels for pharmceutical and biomedical applications, *Crit Rev Ther Drug Carrier Syst,* 22 **(2005)**, 107-150.

28. Peppas, N. A.; Bures, P.; Leobandung, W.; Ichikawa, H. Hydrogels in pharmaceutical formulations, *Eur J Pharm Biopharm,* 50 **(2000)**, 27-46.

29. Hoffman, A. S. Hydrogels for biomedical applications, *Adv Drug Del Rev,* 54 **(2002)**, 3-12.

30. Caldorera-Moore, M.; Peppas, N. A. Micro- and nanotechnologies for intelligent and responsive biomaterial-based medical systems, *Adv Drug Del Rev,* 61 **(2009)**, 1391-1401.

31. Bajpai, A. K.; Shukla, S. K.; Bhanu, S.; Kankane, S. Responsive polymers in controlled drug delivery, *Prog Polym Sci,* 33 **(2008)**, 1088-1118.

32. Hennink, W. E.; Talsma, H.; Borchert, J. C. H.; De Smedt, S. C.; Demeester, Controlled release of proteins from dextran hydrogels, *J Control Release,* 39 **(1996)**, 47-55.

33. Stenekes, R. J. H.; De Smedt, S. C.; Demeester, J.; Sun, G.; Zhang, Z.; Hennink, W. E. Pore sizes in hydrated dextran microspheres, *Biomacromolecules,* 1 **(2000)**, 696-703.

34. Qiu, Y.; Park, K. Environment-sensitive hydrogels for drug delivery, *Adv Drug Del Rev,* 53 **(2001)**, 321-339.

35. Langer, R.; Peppas, N. A. Advances in biomaterials, drug delivery, and bionanotechnology, *AIChE Journal,* 49 **(2003)**, 2990-3006.

36. Bromberg, L. E.; Ron, E. S. Temperature-responsive gels and thermogelling polymer matrices for protein and peptide delivery, *Adv Drug Del Rev,* 31 **(1998)**, 197-221.

37. Dong, L.-C.; Hoffman, A. S. Synthesis and application of thermally reversible heterogels for drug delivery, *J Control Release,* 13 **(1990)**, 21-31.

38. Franssen, O.; Vandervennet, L.; Roders, P.; Hennink, W. E. Degradable dextran hydrogels: Controlled release of a model protein from cylinders and microspheres, *J Control Release,* 60 **(1999)**, 211-221.

39. Chen, G.; Hoffman, A. S. Graft polymers that exhibit temperature-induced phase transitions over a wide range of pH, *Nature,* 373 **(1995)**, 49.

40. Obaidat, A. A.; Park, K. Characterization of protein release through glucose-sensitive hydrogel membranes, *Biomaterials,* 18 **(1997)**, 801-806.

41. Miyata, T.; Uragami, T.; Nakamae, K. Biomolecule-sensitive hydrogels, *Adv Drug Del Rev,* 54 **(2002)**, 79-98.

42. Lihua, L.; Xulin, J.; Renxi, Z. Synthesis and characterization of thermoresponsive polymers containing reduction-sensitive disulfide linkage, *J Polym Sci Part A: Polym Chem,* 47 **(2009)**, 5989-5997.

43. Saito, G.; Swanson, J. A.; Lee, K.-D. Drug delivery strategy utilizing conjugation via reversible disulfide linkages: Role and site of cellular reducing activities, *Adv Drug Del Rev,* 55 **(2003)**, 199-215.

44. Phillips, D. C. The hen egg-white lysozyme molecule, *Proc Natl Acad Sci U S A,* 57 **(1967)**, 483-495.

45. Smith, L. J.; Sutcliffe, M. J.; Redfield, C.; Dobson, C. M. Structure of hen lysozyme in solution, *J Mol Biol,* 229 **(1993)**, 930-944.

46. Blake, C. C. F.; Koenig, D. F.; Mair, G. A.; North, A. C. T.; Phillips, D. C.; Sarma, V. R. Structure of hen egg-white lysozyme: A three-dimensional fourier synthesis at 2 å resolution, *Nature,* 206 **(1965)**, 757-761.

47. Kleopina, G. V.; Kravchenko, N. A.; Kaverzneva, E. D. Role of the 6-amino groups of lysine in lysozyme, *Russ Chem Bull,* 14 **(1965)**, 806-812.

48. Henne, W. A.; Doorneweerd, D. D.; Hilgenbrink, A. R.; Kularatne, S. A.; Low, P. S. Synthesis and activity of a folate peptide camptothecin prodrug, *Bioorg Med Chem Lett,* 16 **(2006)**, 5350-5355.

49. Duncan, R. J. S.; Weston, P. D.; Wrigglesworth, R. A new reagent which may be used to introduce sulfhydryl groups into proteins, and its use in the preparation of conjugates for immunoassay, *Anal Biochem,* 132 **(1983)**, 68-73.

50. Xu, H.; Kaar, J. L.; Russell, A. J.; Wagner, W. R. Characterizing the modification of surface proteins with poly(ethylene glycol) to interrupt platelet adhesion, *Biomaterials,* 27 **(2006)**, 3125-3135.

51. Prochazkova, S.; Vårum, K. M.; Ostgaard, K. Quantitative determination of chitosans by ninhydrin, *Carbohydr Polym,* 38 **(1999)**, 115-122.

52. Shugar, D. The measurement of lysozyme activity and the ultra-violet inactivation of lysozyme, *Biochim Biophys Acta,* 8 **(1952)**, 302-309.

53. Syrový, I.; Hodný, Z. Staining and quantification of proteins separated by polyacrylamide gel electrophoresis, *J Chromatogr B Biomed Sci Appl,* 569 **(1991)**, 175-196.

54. Wang, L.; Kristensen, J.; Ruffner, D. E. Delivery of antisense oligonucleotides using HPMA polymer: Synthesis of a thiol polymer and its conjugation to water-soluble molecules, *Bioconjug Chem,* 9 **(1998)**, 749-757.

55. Rizzi, S. C.; Hubbell, J. A. Recombinant protein-co-PEG networks as cell-adhesive and proteolytically degradable hydrogel matrixes. Part I: Development and physicochemical characteristics, *Biomacromolecules,* 6 **(2005)**, 1226-1238.

56. Canfield, R. E. The amino acid sequence of egg white lysozyme, *J Biol Chem,* 238 **(1963)**, 2698-2707.

57. Iyer, K. S.; Klee, W. A. Direct spectrophotometric measurement of the rate of reduction of disulfide bonds, *J Biol Chem,* 248 **(1973)**, 707-710.

58. Kueltzo, L. A.; Middaugh, C. R., Ultraviolet absorption spectroscopy. In *Methods for structural analysis of protein pharmaceuticals*, Jiskoot , W.; Crommelin, D. J. A., Eds. AAPS: Arlington, VA, **2005**; Vol. 3, p 678.

59. Greenfield, N. J. Methods to estimate the conformation of proteins and polypeptides from circular dichroism data, *Anal Biochem,* 235 **(1996)**, 1-10.

60. Masuda, T.; Ide, N.; Kitabatake, N. Effects of chemical modification of lysine residues on the sweetness of lysozyme, *Chem. Senses,* 30 **(2005)**, 253-264.

61. Jiskoot , W.; Visser, A. J. W. G.; Herron, J. N.; Sutter, M., Fluorescence spectroscopy. In *Methods for structural analysis of protein pharmaceuticals*, Jiskoot , W.; D.J.A., C., Eds. AAPS Arlington, VA, **2005**; Vol. 3, p 678.

62. Lehrer, S. S.; Fasman, G. D. Fluorescence of lysozyme and lysozyme substrate complexes, *J Biol Chem,* 242 **(1967)**, 4644-4651.

63. Rmoso, C.; Forster, L. S. Tryptophan fluorescence lifetimes in lysozyme, *J Biol Chem,* 250 **(1975)**, 3738-3745.

64. Formoso, C.; Forster, L. S. Tryptophan fluorescence and homology in lysozymes and α-lactalbumins, *BBA - Protein Structure,* 427 **(1976)**, 377-386.

65. Vanhooren, A.; Devreese, B.; Vanhee, K.; Van Beeumen, J.; Hanssens, I. Photoexcitation of tryptophan groups induces reduction of two disulfide bonds in goat lactalbumin, *Biochemistry,* 41 **(2002)**, 11035-11043.

66. Wu, L.-Z.; Sheng, Y.-B.; Xie, J.-B.; Wang, W. Photoexcitation of tryptophan groups induced reduction of disulfide bonds in hen egg white lysozyme, *J Mol Struct,* 882 **(2008)**, 101-106.

67. Atassi, M. Z.; Kazim, A. L. Distance calculation of residues neighbouring to lysozyme antigenic sites. Site-neighbouring residues whose evolutionary substitution can modify the characteristics and binding energy of the sites, *Biophys J,* 187 **(1980)**, 163-172.

68.   Weljie, A. M.; Vogel, H. J. Tryptophan fluorescence of calmodulin binding domain peptides interacting with calmodulin containing unnatural methionine analogues, *Protein Eng.,* 13 **(2000)**, 59-66.

69.   Davies, R. C.; Neuberger, A. Modification of lysine and arginine residues of lysozyme and the effect of enzymatic activity, *BBA-enzymes,* 178 **(1969)**, 306-317.

70.   Saito, G.; Swanson, J. A.; Lee, K. D. Drug delivery strategy utilizing conjugation via reversible disulfide linkages: Role and site of cellular reducing activities, *Adv Drug Del Rev,* 55 **(2003)**, 199-215.

APPENDIX TO CHAPTER 4:   SEMI-COVALENT IMPRINTING OF PROTEINS

INTRODUCTION

Hydrogen bonding interactions strongly contribute to the affinity of molecularly imprinted polymers (MIPs) for low molecular weight compounds in organic, aprotic solvents[1]. However, as discussed in Chapter 3, due to problems of solubility and conformational stability of proteins in organic solvents, synthesis of protein imprinted polymers has to be performed in aqueous environment which seriously hampers the hydrogen bond formation. Nevertheless, successful imprints have been achieved within hydrogels, where it has been proposed that multiple weak interactions are responsible for the strong binding of the protein to the polymer network in aqueous environment[2,3]. To create more specific and stronger template-imprint interactions, one can introduce charged monomers in the polymer network to enable electrostatic interactions. However, it has been shown in Chapter 3 that charged residues can also cause non-specific binding of the template, because part of the residues are randomly distributed throughout the polymer network, resulting in a decreased imprint effect. A strategy to overcome this issue is to precisely position the charged monomers at the site of interaction.

Here we present a new concept to improve the selectivity and the efficiency of protein imprinting in aqueous media, i.e. semi-covalent imprinting. This technique has been first introduced by Whitcombe *et al.* for small template molecules and it involves the covalent attachment of functional monomers to the template molecule[4,5]. The monomers are bound to the template through reversible covalent bonds (e.g. ester bonds, disulfide bonds, Schiff bases). Once the monomer-template conjugate is copolymerized with the matrix-monomer and crosslinker to form the polymer network, the bonds between the template and the polymer are selectively cleaved and the template is removed leaving an imprinted cavity, with the functional groups positioned such that they are able to physically interact with the template molecule upon rebinding. However, this method has not been applied for proteins yet.

For this purpose, we developed an efficient strategy to introduce polymerizable methacrylamide moieties to the lysine residues of proteins, using a novel sacrificial linker (see Chapter 4). The concept is schematically shown in Figure 1. The linker molecule contains a

disulfide bond and an ester bond, which allows easy removal of the template from the polymer network by reduction and/or hydrolysis, respectively. After hydrolysis of the ester bond, carboxylic acid groups are created in the polymer network which can subsequently interact with the basic lysine groups of the native protein for rebinding. Moreover, the template can be reused for imprinting after reduction of the disulfide and subsequent attachment of a new methacrylamide group.
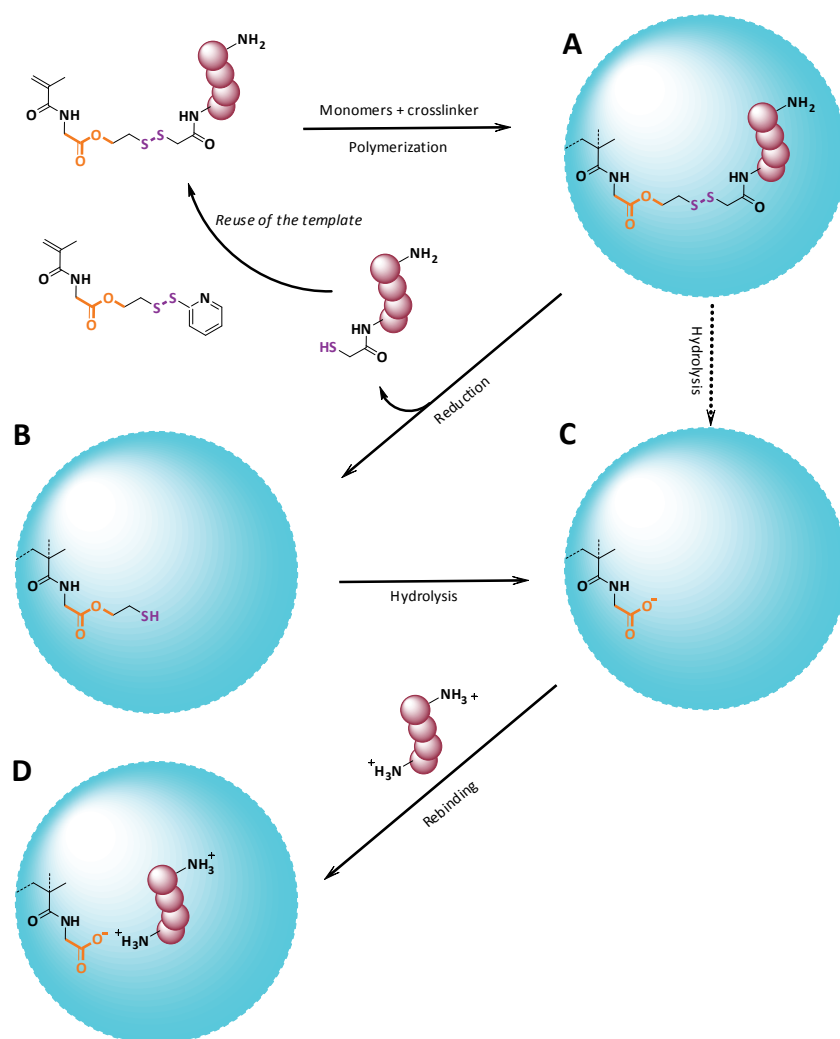

Figure 1. The concept of semi-covalent protein imprinting. Methacrylamide modified proteins are co-polymerized in the hydrogel reduction (B) and/or hydrolysis (C), the template is removed, and an imprint cavity is formed, with carboxylic acid groups positioned such they can interact with the basic lysine groups of the native protein (D).

As described in Chapter 4, we were able to successfully conjugate up to three methacrylamide moieties to the lysine groups of a model protein, lysozyme, with preservation of the protein structure, and maintaining the lytic activity. Moreover, the modified protein could be immobilized in a polyacrylamide hydrogel, and subsequently released upon reduction of the linker molecule that conjugated the protein to the hydrogel network.

NON-COVALENT AND SEMI-COVALENT IMPRINTING OF LYSOZYME

Materials

Ammonium peroxodisulfate (APS), chicken egg white lysozyme (LZM), dextran T40 (from Leuconostoc spp.), glutathione, and N,N,N′,N′-tetramethylethylenediamine (TEMED) were obtained from Fluka (Buchs, Switzerland). Methacrylic acid (MAA) was purchased from Sigma-Aldrich (Zwijndrecht, The Netherlands). Methacrylated dextran (Dex-MA) with a degree of substitution (DS) of 7.9 was synthesized according to Van Dijk-Wolthuis *et al.*[6, 7]. Methacrylated lysozyme (LMA) was synthesized as described in chapter 4 of this thesis.

Synthesis and template extraction

Methacrylated dextran (Dex-MA) was chosen as polymer matrix. Dextran hydrogels with an initial Dex-MA content of 10% (w/w) were prepared in presence of native or modified lysozyme (LZM and LMA, respectively) by free radical polymerization as described previously[8]. In detail, 0.25 g of a Dex-MA buffer solution (DS 7.9, 0.20 g/g total weight, in 10 mM acetate buffer, pH 5) was mixed with 0.2 mL of a protein stock solution (6.25 mg/mL LMA or LZM) in acetate buffer (10 mM acetate, pH 5) (final protein concentration 2.5 mg/g gel). The mixture was purged with nitrogen for five minutes. Next, the polymerization was initiated by adding 25 μL TEMED (10 vol%, in HEPES buffer, pH adjusted to 7.4 with HCl) and 25 μL APS (5 wt% in HEPES buffer). The mixture (final weight 0.5 g) was quickly transferred into a 1 mL syringe (radius 0.23 cm) and allowed to polymerize at room temperature for at least two hours. Non-imprinted hydrogels were prepared without adding a protein solution, but 0.2 mL acetate buffer (10 mM acetate, pH5) instead.

As LMA will be removed from the hydrogel by hydrolysis of the ester bond in the linker that conjugates the lysozyme to the gel network, the final imprinted cavity will contain carboxylic acid groups, available for electrostatic interaction with the template. Therefore we also synthesized a non-imprinted polymer, with methacrylic acid (MAA) to introduce negative charges. The amount of MAA added to the Dex-MA solution, was 4.5 µmol, corresponding to the average amount of methacrylamide groups conjugated to lysozyme (i.e. 2.5 MA/LMA).

After polymerization, the template was removed from the hydrogel network by successive washing. First, the gels were washed four times for two hours and subsequently one time overnight with 3 mL sodium acetate buffer (10 mM acetate, 150 mM NaCl, pH 5) to extract non-immobilized LZM. Next, the removal of immobilized LMA was triggered by adding TRIS buffer (10 mM TRIS, 150 mM NaCl, pH 8.5) or 2.5 mM glutathione in HEPES buffered saline (HBS, 10 mM HEPES, 150 mM NaCl, pH 7), for hydrolysis or reduction of the linker, respectively. The washing procedure was four times two hours, followed by an overnight washing step for all the hydrogels in TRIS buffer (10 mM TRIS, 150 mM NaCl, pH 8.5). The protein concentration in the wash samples was determined using UPLC, as described in Chapter 5.

Rebinding of the template was assessed by adding 2 mL native lysozyme solution (0.5 mg/mL in 10 mM HEPES) to the imprinted and non-imprinted polymers. The gels were incubated for six hours, after which the remaining protein concentration in the supernatant (=unbound fraction) was determined by UPLC.

Results

The total amount of lysozyme extracted in the different wash fractions after preparation of the imprinted network, was determined by UPLC. The cumulative amount of removed protein is presented in Table 1. In acetate buffer (10 mM acetate, 150 mM NaCl, pH 5), native LZM released for 76.5%, whereas modified LZM (LMA) only released for 16.0%, demonstrating that the majority of the methacrylated LZM was successfully immobilized in the Dex-MA gel network. After triggering the release by hydrolysis or reduction, the remaining lysozyme was released up to a total amount of 71%. Both native and modified LZM could not be completely removed from the imprinted polymer, indicating permanent physical[9] or chemical[10] entrapment of approx. 25% of the lysozyme in the gel network. These results are similar to the results reported in chapter 5. As the final washing step for all the hydrogels was done with TRIS buffer

to hydrolyze the ester bonds, it is expected that all the gels were finally functionalized with remaining negatively charged (carboxylic acid) groups for rebinding of the protein.

Table 1. Removal of native lysozyme (LZM) or covalently incorporated lysozyme (LMA) template from the imprinted hydrogels

	Acetate buffer pH 5	TRIS buffer pH 8.5	Glutathione 2.5 mM	Total
LZM	76.5 ± 4.7%	/	/	76.5 ± 4.7%
LMA$_a$	16.0 ± 6.4%	55.4 ± 4.7%	/	71.4 ± 4.9%
LMA$_b$	15.4 ± 5.2%	/	54.9 ± 5.2%	70.3 ± 5.6%

Results are presented as average ± S.D; n=6
LMA$_a$: release of LMA is triggered by hydrolysis
LMA$_b$: release of LMA is triggered by reduction

To assess the ability of the imprinted polymers to rebind the template, the imprinted and non-imprinted (neutral and negatively charged) hydrogels were incubated for six hours with 2 mL native LZM (0.5 mg/mL) in 10 mM HEPES, pH 7.4. In total 1 mg lysozyme was added for rebinding, or 2 mg/g gel, whereas the imprinted polymers were made with 2.5 mg protein/g gel. The results are presented as the amount of lysozyme absorbed per gram polymer (Figure 2). In contrast to what was expected, no significant difference in rebinding was observed for the four polymers used. Both MIP and NIP absorbed ~30 % of the initially added lysozyme, and no significant difference was observed when using the semi-covalent approach. Most likely, the apparent rebinding is the result of nonspecific absorption of the protein into the hydrogel, i.e. partitioning of the protein between the hydrogel and the surrounding buffer (~20%). However, it cannot be ruled out that lysozyme adsorbed on the surface of the polymers in a nonspecific manner. The presence of a small amount (4.5 µmol/g) of negatively charged groups (in NIP$_{charged}$ and MIP$_{LMA}$) did not result in significant higher adsorption. Similar unsatisfying results were obtained when polyacrylamide was used as a gel matrix (results not shown).
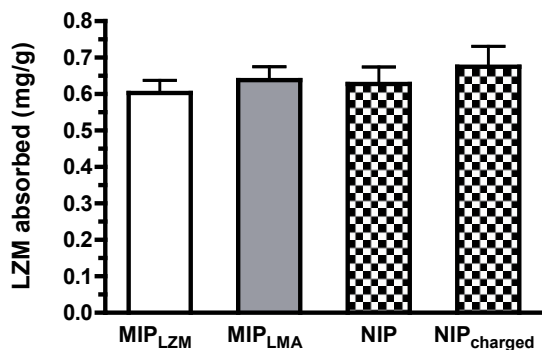
Figure 2. Binding of lysozyme to MIP prepared via non-covalent (MIP$_{LZM}$) and semi-covalent (MIP$_{LMA}$) imprinting. Uncharged Dex-MA (NIP) and negatively charged Dex-MA (NIP$_{charged}$) were used as control. Rebinding conditions: 0.5 g polymer, 2 mL of 0.5 mg/mL LZM in 10 mM HEPES pH 7.4, 6 h incubation. The data show that ~30 % of the initially added amount of lysozyme was absorbed/adsorbed by the different hydrogel networks (1 mg of protein was added and 0.3 mg per gel (0.5 g) was ab(d)sorbed).

Even though the semi-covalent approach would in theory create better defined imprint cavities, with functional groups oriented such that they can interact with the template molecule, the experiment described here did not lead to successful imprinting results. This might be due to the limited amount of functional binding units introduced per imprint cavity, i.e. on average 2.5 units per LZM. However, it was recognized that this semi-covalent approach could be used for another purpose, i.e. controlled triggered release of proteins from hydrogel networks. This was further assessed in Chapter 5.

REFERENCES

1. Ramström, O.; Ansell, R. J. Molecular imprinting technology: Challenges and prospects for the future, Chirality, 10 (**1998**), 195-209.
2. Hjerten, S.; Liao, J. L.; Nakazato, K.; Wang, Y.; Zamaratskaia, G.; Zhang, H. X. Gels mimicking antibodies in their selective recognition of proteins, Chromatographia, 44 (**1997**), 227-234.
3. Sellergren, B., The non-covalent approach to molecular imprinting. In Molecularly imprinted polymers: Man-made mimics of antibodies and their applications in analytical chemistry, Sellergren, B., Ed. Elsevier: Amsterdam, **2001**; pp 113-183.
4. Klein, J. U.; Whitcombe, M. J.; Mulholland, F.; Vulfson, E. N. Template-mediated synthesis of a polymeric receptor specific to amino acid sequences, Angew Chem Int Ed, 38 (1999), 2057-2060.
5. Wulff, G. The use of polymers with enzyme-analogous structures for the resolution of racemates., Angew Chem Int Ed, 11 (**1972**), 341.
6. van Dijk-Wolthuis, W. N. E.; Franssen, O.; Talsma, H.; van Steenbergen, M. J.; Kettenes-van den Bosch, J. J.; Hennink, W. E. Synthesis, characterization, and polymerization of glycidyl methacrylate derivatized dextran, Macromolecules, 28 (**1995**), 6317-6322.
7. van Dijk-Wolthuis, W. N. E.; Kettenes-van den Bosch, J. J.; van der Kerk-van Hoof, A.; Hennink, W. E. Reaction of dextran with glycidyl methacrylate: An unexpected transesterification, Macromolecules, 30 (**1997**), 3411-3413.
8. Hennink, W. E.; Talsma, H.; Borchert, J. C. H.; De Smedt, S. C.; Demeester, Controlled release of proteins from dextran hydrogels, J Control Release, 39 (**1996**), 47-55.
9. Turner, N. W.; Jeans, C. W.; Brain, K. R.; Allender, C. J.; Hlady, V.; Britt, D. W. From 3d to 2d: A review of the molecular imprinting of proteins, Biotechnol Prog, 22 (**2006**), 1474-1489.
10. Valdebenito, A.; Espinoza, P.; Lissi, E. A.; Encinas, M. V. Bovine serum albumin as chain transfer agent in the acrylamide polymerization. Protein-polymer conjugates, Polymer, 51 (**2010**), 2503-2507.

PROTEIN MACROMONOMERS
CONTAINING REDUCTION-SENSITIVE LINKERS
FOR COVALENT IMMOBILIZATION AND GLUTATHIONE
TRIGGERED RELEASE FROM DEXTRAN HYDROGELS

- ELLEN VERHEYEN - STEFFEN VAN DER WAL - HENDRIK DESCHOUT - KEVIN BRAECKMANS -

- STEFAAN DE SMEDT - ARJAN BARENDREGT - WIM E. HENNINK - CORNELUS F. VAN NOSTRUM -

ABSTRACT

We report an efficient strategy to conjugate methacrylamide moieties to the lysine groups of lysozyme for co-polymerization and subsequent triggered release from hydrogels. Two novel linker molecules, containing an ester bond and/or a disulfide bond for reversible immobilization, were synthesized and conjugated to lysozyme. Lysozyme was successfully modified with on average 2.5 linker molecules per protein molecule, as evidenced by MALDI-TOF and by titration of the free amine groups, while spectral analysis verified the preservation of the protein structure. Next, methacrylated dextran (Dex-MA) was polymerized in presence of native or modified lysozyme to yield hydrogels. The release of native and modified lysozyme from Dex-MA hydrogels was studied in acetate buffer (pH 5, in absence of any trigger) and only a minor fraction (~15%) of the modified lysozyme was released, whereas ~74% of the native lysozyme was released. This indicates successful immobilization of the majority of the modified lysozyme in the hydrogel network. Upon hydrolysis of the ester bonds or incubation with glutathione to reduce disulfide bonds of the linker molecules that conjugate the lysozyme to the gel network, the modified lysozyme was mobilized and released from the hydrogel to the same extent as native lysozyme. These data were confirmed by fluorescence recovery after photobleaching experiments. This approach appeared to be highly interesting for temporary immobilization and subsequent glutathione triggered intracellular delivery of proteins from hydrogels.

INTRODUCTION

Many potent biomacromolecular therapeutics such as peptides, proteins and nucleic acids (plasmid DNA, siRNA) have their therapeutic target intracellular, and should therefore be internalized by the cell in order to be effective. Although these macromolecular bio-therapeutics are promising candidates for the treatment of a variety of diseases including cancer, the efficacy of such drugs is often hampered by a poor stability in vivo, due to rapid extra- and intracellular degradation, rapid clearance by the reticuloendothelial system, and poor cellular uptake[1]. To overcome these hurdles, several nanoparticulate delivery systems have been developed, including hydrogel nanoparticles[2, 3], polymeric micelles[4, 5], liposomes[6, 7], protein-polymer conjugates[8] and complexes of soluble polymers with proteins[9], DNA[10] and siRNA[11]. Hydrogel nanoparticles are very attractive systems for the intracellular delivery of macromolecular drugs, due to their biocompatibility and the possibility to control the release kinetics by the network properties. The release of proteins from hydrogels can occur by one or a combination of following three mechanisms: (1) diffusion controlled, (2) swelling controlled and (3) degradation/dissolution controlled[12]. In case of diffusion controlled release, the protein is smaller than the mesh size of the hydrogel network, and it can freely diffuse out of the hydrogel which can result in premature release, for instance already during preparation and storage. In particular for nanoparticles, the release can be extremely rapid due to the large surface area and short diffusion distance. By adjusting the gel properties, e.g. by increasing the crosslink density or the solid content of the gel network, the release kinetics can be retarded[13-19]. This approach, however, is limited since a too dense gel network can lead to permanent protein entrapment[17, 20] or the protein release can be too slow once the intracellular target is reached. To delay the release one can also use hydrogels from which the release is controlled by swelling and/or degradation[21-25]. In these hydrogels, the mesh size of the polymer network is initially smaller than the protein, thus the protein is initially immobilized in the network. Upon swelling or degradation, the mesh size increases and when it exceeds the size of the protein, diffusion and release can take place. The use of these highly crosslinked hydrogels can aid in delaying the release, but spatio-temporal release is difficult to trigger precisely. More recently, bioresponsive nanogels, which sense and respond to environmental changes, have been used for intracellular delivery of biotherapeutics. Among them, pH sensitive nanogels which are stable at physiological pH, but after cellular uptake in the endosomes, where the pH is lower,

they quickly dissolve or dissociate and consequently release their content intracellularly[26-28]. Also interesting for intracellular delivery of macromolecules, are redox-potential sensitive drug delivery systems[29, 30], where the release is controlled by the reduction of disulfide bonds present in the carrier system. These systems rely on the large difference in redox-potential between intracellular (0.5-10 mM glutathione)[31] and extracellular (2-20 µm glutathione) compartments[32]. Redox-sensitive carriers are designed to be relatively stable in the circulation and extracellular compartments. However, once internalized, the disulfide bonds maintaining the structure of the carrier system will be rapidly cleaved in presence of high concentration of glutathione, resulting in the intracellular release of the entrapped drug molecules.

The above described approaches to tailor the intracellular release of proteins are related to alterations of the hydrogel properties. Proteins are initially entrapped inside the crosslinked network and subsequently released by (stimuli-induced) swelling or degradation of the hydrogel. Another approach to deliver proteins intracellularly is to covalently incorporate them in the gel network, and to trigger release not by changes in the hydrogel structure, but by cleavage of the linker connecting the protein to the hydrogel network. In a previous paper we presented a method to functionalize lysozyme with methacrylamide groups for temporary immobilization and subsequent triggered release of proteins from hydrogel networks[33]. In the present work, a novel bio-reducible linker was designed and synthesized (**MA1**, see scheme 1) that contains a disulfide bond, aiming at glutathione triggered delivery. The previous linker molecule (**MA2**) that was conjugated to lysozyme contained, beside a disulfide bond, also an ester bond for extracellular release by hydrolysis. Preliminary results from gel electrophoresis experiments demonstrated that this latter methacrylamide modified lysozyme could indeed be immobilized in a polyacrylamide gel and subsequently liberated from the gel network under reducing conditions. In the present more extensive study, we investigated the following critical parameters aiming at a novel drug delivery system: 1) quantification of immobilization and in vitro triggered release of the modified protein from a biocompatible hydrogel (i.e. dextran hydrogel), under reducing (and hydrolyzing) conditions; 2) mobility of native and modified lysozyme in the hydrogel by fluorescence recovery after photobleaching (FRAP); 3) structural integrity and enzymatic activity of the lysozyme released under different conditions. Hydrogels synthesized from methacrylated dextran (Dex-MA) were chosen, since they are not degradable under physiological conditions[14]. This ensures that the release of the proteins is not influenced by degradation of the hydrogel matrix.

EXPERIMENTAL PROCEDURES

Materials

All chemicals were used as received. Chicken egg white lysozyme (LZM), dextran T40 from *Leuconostoc spp.,* dimethylsulfoxide (DMSO), β-mercaptoethanol, glutathione, HEPES, and sinapinic acid were purchased from Fluka (Zwijndrecht, The Netherlands). *N*-Succinimidyl-*S*-acetylthioacetate (SATA), dialysis cassettes, and Micro BCA Protein Assay kit were obtained from PIERCE (Perbio Science, Etten-leur, The Netherlands). *N*-aminopropyl methacrylamide was obtained from Polyscience (Eppelheim, Germany). Anhydrous magnesium sulphate, cytochrome C, disodium hydrogen phosphate, ethylenediaminetetraacetic acid disodium salt (EDTA), fluorescein isothiocyanate (FITC), hydrindantin, hydrochloric acid (HCl), hydroxylamine hydrochloride, 2-methoxyethanol, *Micrococcus Lysodeikticus*, ninhydrin, ammonium peroxodisulfate (APS), sodium dihydrogen phosphate, sucrose, *N,N,N',N'*-tetramethylethylenediamine (TEMED), triethylamine, and trifluoroacetic acid (TFA) were purchased from Sigma-Aldrich (Zwijndrecht, The Netherlands). Acetonitril, dichloromethane (DCM), ethyl acetate and methanol were obtained from Biosolve (Valkenswaard, The Netherlands). Acetic acid, ethanol, silica gel 60 (0,040-0,063 mm), sodium acetate, sodium chloride, sodium hydroxide and tris(hydroxymethyl)-aminomethane were purchased from Merck (Darmstadt, Germany).

2-(2-pyridin-2-yldisulfanyl)ethyl-2-(methacrylamido)acetate (MA2) was synthesized as described previously[33]. Methacrylated dextran (Dex-MA) with a degree of substitution (DS) of 7.9 was synthesized according to Van Dijk-Wolthuis *et al.*[34, 35]. The DS was determined using ^{1}H NMR. FITC-labeled lysozyme was synthesized as described by Kok *et al.*[36]. On average 1.0 ± 0.2 FITC molecules were introduced per lysozyme, as determined by the ninhydrin assay (vide infra).

NMR spectroscopy

NMR measurements were performed using a Gemini 300 MHz spectrometer (Varian Associates Inc., NMR Instruments, Palo Alto, CA). Chemical shifts were recorded in ppm with reference to the solvent peak (δ = 7.26 ppm and δ =77.3 ppm for $CDCl_3$ in ^{1}H and ^{13}C NMR, respectively).

Synthesis of N-(3-(3-(pyridin-2-yldisulfanyl)propanamido)propyl)methacrylamide (MA1)

A dried round bottom flask was loaded with N-aminopropyl methacrylamide (0.662 g, 4.66 mmol) in 50 mL dioxane:water (1:1) and the pH was adjusted to 8.5 by adding triethylamine (TEA). *N*-Succinimidyl 3-(2-pyridyldithio)-propionate (SPDP) (1 g, 3.11 mmol), dissolved in 10 mL dioxane, was added dropwise to the N-aminopropyl methacrylamide solution under continuous stirring. The pH was maintained at pH 8 - 8.5 by adding TEA. The reaction was stirred for 10 minutes at room temperature and the solvent was subsequently evaporated under vacuum to a ~20 mL volume. The remaining solution was extracted three times with 20 mL ethyl acetate. The combined ethyl acetate fractions were dried by adding anhydrous magnesium sulphate, filtered and evaporated to dryness under vacuum. Next, the product was dissolved in ethyl acetate and purified by column chromatography (silica gel 60) with ethyl acetate/aceton (1.5:1) as the eluent (Rf = 0.27). After purification and evaporation of the solvent, 0.80 g product was obtained as a white powder (yield 76 %). ESI-MS: m/z calculated for $C_{15}H_{21}N_3O_2S_2$ (M+H)$^+$ 340.11, found 340.05. Melting temperature (T_m) = 86.5°C. ^{1}H NMR (300 MHz, CDCl$_3$): δ = 1.68 (m, 2H), 1.98 (s,3H), 2.65 (t, $^3J^{HH}$=7 Hz, 2H), 3.10 (t, $^3J^{HH}$=7 Hz, 2H), 3.34 (m, 4H), 5.35 (m, 1H), 5.78 (s, 1H), 6.78 (m, 1H), 7.09 (m, 2H), 7.65 (m, 2H), 8.46 (m, 1H). ^{13}C NMR (75.4 MHz, CDCl$_3$): δ = 19.2, 30.1, 35.3, 36.3, 36.6, 115.3, 120.5, 120.9, 121.6, 137.7, 140.3, 150.0, 160.0, 169.4, and 172.3.

Conjugation of the monomers to lysozyme

Preparation of the lysozyme conjugates was done in two consecutive steps as described previously[33]. First, lysine groups of the non-labeled or FITC-labeled protein were modified with protected thiol functions using SATA reagent[37]. In detail, a stock solution of lysozyme (5 mg/mL) was prepared by dissolving 250 mg lysozyme (17 µmol; 120 µmol NH$_2$ groups) in 50.0 mL PBS (0.1 M phosphate, 0.15 M NaCl, pH 7.2). SATA (16 mg, 68 µmol) was dissolved in 0.2 mL dry DMSO and added to the lysozyme solution (molar ratio 4/7 of SATA/NH$_2$). The mixture was incubated at room temperature for 30 minutes. Subsequently, the ATA-modified lysozyme (LATA) was dialyzed against acetate buffer (0.1 M acetate, 0.15 M NaCl, pH 5) for 24 hours to remove the excess of SATA as well as low molecular weight reaction products. In a second step, the thiol groups were deprotected and simultaneously coupled to the monomer (MA1 or MA2) via a thiol-disulfide exchange reaction. Therefore the ATA-modified lysozyme solution (4.0 mg/mL in acetate buffer, pH 5), was purged with nitrogen for 15 minutes. A deacetylation solution

was prepared by dissolving 1.74 g of hydroxylamine hydrochloride and 0.365 g of EDTA in 50 mL PBS (pH 7.2). Next, 4.5 mL of this solution was added to the 45 mL protein solution under mild stirring. Subsequently, a solution of the monomer (MA1 or MA2, 5 equiv. with respect to SH) in 0.2 mL DMSO was added. The mixture was incubated at room temperature for 12 hours while gently stirring. The modified lysozyme was filtered (0.2 μm) and then purified by dialysis against acetate buffer pH 5 (LMA2) or PBS buffer pH 7.2 (LMA1) for 48 hours at room temperature and stored in small aliquots at -20°C. The mass of the different modified proteins (LATA, LMA1 and LMA2) was analyzed with MALDI-TOF MS (vide infra) and the number of modified lysine residues was calculated using the ninhydrin assay as described below.

Mass spectrometry (MALDI-TOF MS)

For MALDI-TOF MS analysis of the different modified proteins, a MALDI TOF/TOF 4700 proteomics analyzer (Applied biosystems, California, USA) was used with cytochrome C (Mw 12360 Da) as the internal reference. The different lysozyme samples were diluted in a solution of water/CH_3CN (1/1) + 0.1 vol% of TFA to obtain a concentration of 0.1 mg/mL. Two μL of this solution was mixed with 10 μL matrix solution (5 mg/mL sinapinic acid in water/CH_3CN (1/1) + 0.1 vol% TFA) and spotted on the MALDI plate. For each sample two independent spectra were obtained for mass analysis.

Determination of free amine groups

The concentration of free amine groups in the different samples was determined spectrophotometrically by the use of ninhydrin[38], as described previously[33]. The protein samples were diluted to 0.5 mg/mL lysozyme in acetate buffer (1 M, pH 5) and each sample was measured in triplicate.

Spectral analysis of the modified lysozyme species

UV-VIS spectroscopy was carried out with a Shimadzu UV-2450 UV/VIS spectrophotometer with 6-cell holder and UV-Probe software (Shimadzu Corporation, Kyoto, Japan). The absorbance spectra were recorded in the range of 200-350 nm. The protein samples were diluted to a concentration of 0.20 mg/mL lysozyme in PBS. The protein concentrations were verified by measuring the absorption at 280 nm (OD280, E_1^1 = 2.7[39]).

Circular dichroism measurements were performed with a dual beam DSM 1000 CD spectropolarimeter (On-Line Instruments Systems, Bogart, GA) using cuvettes with a path length of 0.20 cm. The samples were diluted in PBS to obtain a concentration of 0.50 mg/mL lysozyme. Far UV-CD spectra were recorded from 250 to 195 nm at 25°C. For each sample, the average of five spectra was calculated.

Fluorescence measurements were carried out with Horiba Fluorolog fluorometer FL3-21 (Horiba Jobin Yvon, Longjumeau Cedex, France) using quartz cuvettes (Hellma, Müllheim, Germany). The excitation wavelength was set at 295 nm and the emission spectra were recorded in the range of 300-450 nm. An integration time of 1 s was used, and the excitation and emission band slits were set at 5 nm. The concentration was fixed at 0.05 mg/mL lysozyme in PBS buffer. For each sample, the average of three spectra was calculated.

Determination of the enzymatic activity of lysozyme

The enzymatic activity of lysozyme was determined by measuring the decrease in optical density at 450 nm of a *M. Lysodeikticus* suspension as described previously[33]. The activity of each sample was determined six times. The enzymatic activity of the modified lysozyme is expressed as a percentage of the activity of a reference lysozyme solution.

Preparation of the hydrogels

Dextran hydrogels were prepared by free radical polymerization of Dex-MA in acetate buffer (10% w/w) in presence of native or modified (non-labeled or FITC-labeled) lysozyme as described previously[14]. In detail, 0.100 g Dex-MA (DS 7.9, 0.20 g/g total weight) was dissolved in 0.5 mL acetate buffer (10 mM, pH 5) and mixed with 0.45 mL of a protein stock solution (10 mg/mL) in the same buffer (4.5 mg protein/g gel). The mixture was purged with nitrogen for five minutes. Next, the polymerization was initiated by adding 25 μL TEMED (16 vol%, in HEPES buffer, pH adjusted to 7.4 with HCl) and 25 μL APS (8 wt% in HEPES buffer). The solution was quickly transferred into a 1 mL syringe (radius 0.23 cm) and allowed to polymerize at room temperature for at least two hours. Control hydrogels were prepared without adding a protein solution.

In vitro protein release

After polymerization, the cylindrical hydrogels (height of gel 4.5 cm, radius 0.23 cm) were transferred into glass vials and 3 mL acetate buffer (10 mM acetate, 150 M NaCl, pH 5) was added to each vial. A slightly acidic pH was chosen to minimize hydrolysis of the ester bond present in LMA2. The vials were incubated on a roller bench at 37°C. At different time-points, samples (0.2 mL) were taken and replaced by an equal amount of fresh buffer. After four days, the release of the immobilized lysozyme (LMA2) was triggered by replacing the acetate buffer with TRIS buffer (10 mM TRIS, 150 mM NaCl, pH 8.5) to initiate the hydrolysis of the ester bond. A more alkaline environment (pH 8.5) was chosen, instead of pH 7.4, to accelerate the hydrolysis. The release by reduction of the disulfide bond present in the linker (LMA1 and LMA2) was triggered by adding PBS pH 7.4 containing 2.5 mM glutathione, which is within the range of the reported intracellular glutathione concentrations (0.5 -10 mM)[31]. Samples were again taken at different time points during two days.

Determination of the protein concentration and characterization of the released protein

The samples taken from the release study were analyzed for their protein concentration by UPLC (Acquity UPLC®, Waters Corporation, Milford, USA) equipped with a BEH 300 C18 1.7 μm column. A gradient elution method was used with mobile phase A (95% H_2O, 5% ACN and 0.1% TFA) and mobile phase B (100% ACN and 0.1% TFA). The eluent linearly changed from 75:25 (A:B) to 60:40 (A:B) over four minutes and set back to 75:25 (A:B) in 4.5 minutes, with a flow rate of 0.250 mL/min. The injection volume was five μL, and UV absorbance was measured at 210 nm. Lysozyme standards (native or modified lysozyme, 10–250 μg/mL) in different buffers (acetate pH 5, TRIS pH 8.5 and PBS containing 2.5 mM glutathione) were used for calibration. The integrity of the released lysozyme was determined by UV-VIS spectroscopy, far UV-CD spectroscopy and fluorescence spectroscopy (vide supra). In addition, the enzymatic activity in some selected release samples was determined as described above.

Fluorescence Recovery After Photobleaching (FRAP)

A recently developed pixel-based FRAP model was used, that describes the diffusion process after photobleaching of an arbitrary rectangular area (rFRAP) instead of the standard uniform disc model[40]. FRAP measurements were performed using a set-up as described elsewhere[40]. In

detail, a confocal scanning laser microscope (model MRC1024 UV, Bio-Rad, Hemel Hempstead, UK), modified for bleaching arbitrary regions in the hydrogel, was used. The 488 nm line of a 4 W Ar-ion laser (model Stabilite 2017; Spectra-Physics, Darmstadt, Germany) was used for photobleaching and subsequent imaging of the recovery. The microscope was equipped with a 10x objective lens (CFI Plan Apochromat; Nikon, Badhoevedorp, The Netherlands). After the acquisition of one pre-bleach image, a square with a size of 5 x 5 μm or 30 x 30 μm was bleached at a very high laser intensity (2-5 mW) for a very short time (100 to 200 ms), so that the extent of fluorescence recovery during bleaching is negligible[40]. Next, the recovery of the fluorescence in the bleached area was monitored with a highly attenuated laser beam (100 μW) for one to five minutes. The time interval between subsequent images was 2.5 or 10 seconds depending on the expected diffusion coefficient at different time points in the release study. The diffusion coefficient of the FITC-labeled protein can be calculated by fitting the recovery data to the rFRAP model[40].

Sample preparation for FRAP experiments

Dex-MA hydrogels loaded with native or modified FITC-labeled lysozyme were prepared in a 16-well Lab-TEK® chamber slide™ (Nalge Nunc International, NY, USA), essentially in the same way as described above for the bulk hydrogels. The media chamber of the chamber slide was removed and the polymerization mixture (40 μL) was added to the remaining gasket. The gasket was covered with a microscope coverslip and the mixture was allowed to polymerize for at least two hours. Prior to the FRAP measurements, the thin hydrogels (~2 mm) were transferred into a glass bottom petridish (MatTek corporation, Massachusetts, USA). To prevent dehydration of the gel during the measurement, five μL HEPES buffer (10 mM, pH 6) was added on top of the gel and the gel was covered with a cover slip.

After the first FRAP measurement, the gels were transferred into a 24-well plate containing 1 mL acetate buffer (10 mM acetate, 150 mM NaCl, pH 5) to remove non-immobilized lysozyme. The gels were gently shaken and the release medium was replaced completely by fresh buffer two times a day. After 96 hours, FRAP measurements were repeated in the same set-up as described above. Next, 20 μL 5 mM glutathione in HBS (10 mM HEPES, 150 mM NaCl, pH 7.4) or 20 μL 1 mM NaOH was added on top of the gel to induce release due to reduction or hydrolysis, respectively. After three hours incubation, the FRAP measurements were repeated. As a control, the diffusion coefficient of the FITC-labeled lysozyme in a sucrose solution (48 % w/w) was measured.

RESULTS AND DISCUSSION

Synthesis and characterization of methacrylamide modified lysozyme
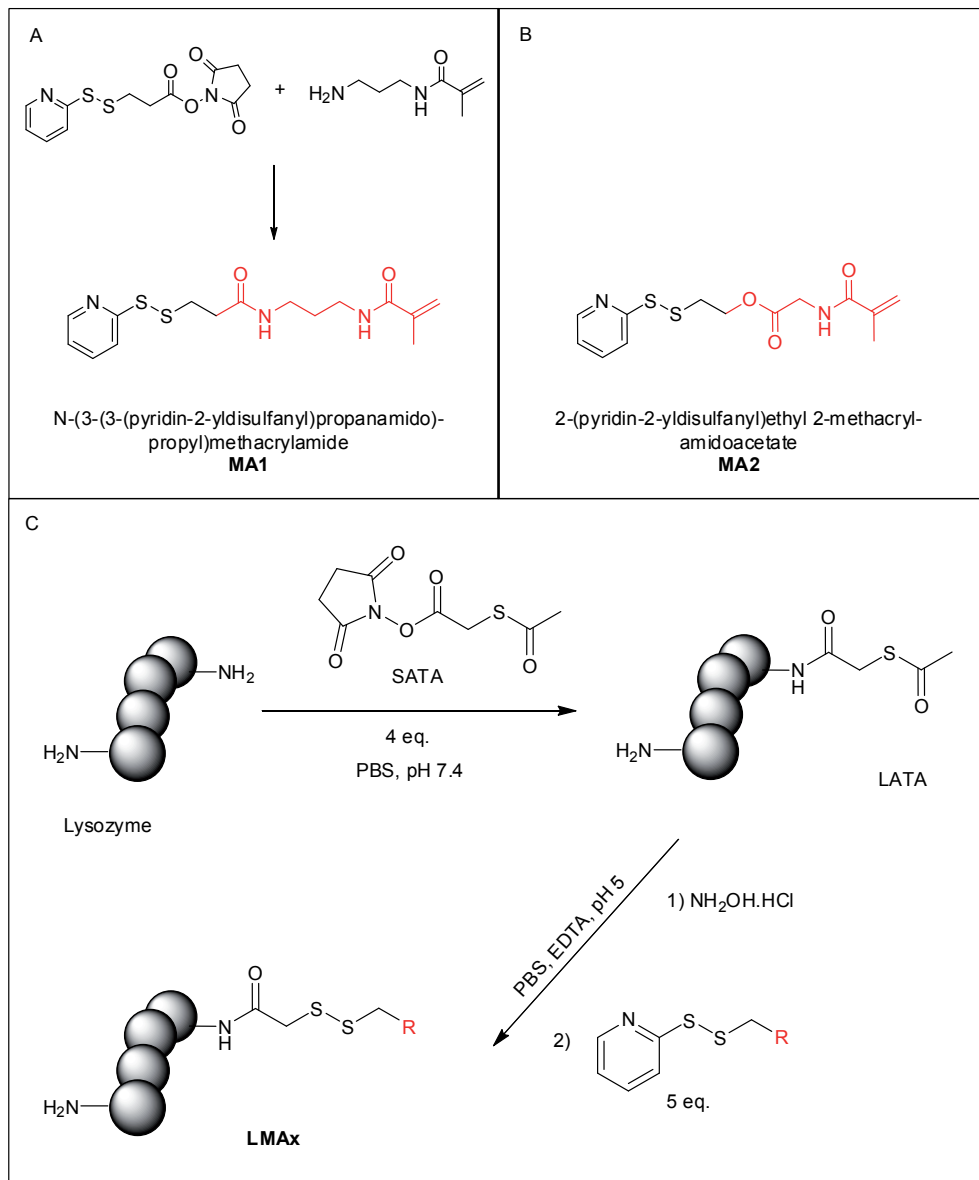
Scheme 1. (A) Synthesis of N-(3-(3-(pyridin-2-yldisulfanyl)propanamido)propyl)methacrylamide (MA1). (B) 2-(2-pyridin-2-yldisulfanyl)ethyl-2-(methacrylamido)acetate (MA2). (C) Reaction scheme for the synthesis of methacrylamide modified lysozyme (LMA1 or LMA2, respectively). R: represents a part of the linker molecule, given in red the molecular structures of MA1 and MA2.

Two monomers with different linkers, to be conjugated to lysozyme, were synthesized; first a known one containing a degradable ester and a reducible disulfide bond (2-(2-pyridin-2-yldisulfanyl)ethyl-2-(methacrylamido)acetate, MA2, Scheme 1B), and second a novel one which can be cleaved by reduction only (MA1, Scheme 1A). MA2 was synthesized as reported previously[33], while the novel linker MA1 was synthesized by amide formation between N-(3-aminopropyl)methacrylamide and the N-hydroxysuccinimide ester of SPDP in a 76% yield. The conjugation of both linkers to lysozyme was done as described before[33]. First, lysozyme was thiolated using SATA (LATA) and subsequently reacted with one of the two linkers via disulfide exchange to obtain the desired methacrylated protein (Scheme 1C, LMA1 or LMA2). The initial ratio of SATA to NH_2 of the protein was 4:7, as optimized earlier, and resulted in the conjugation of ~2.5 methacrylamide moieties per lysozyme, while maintaining ~70% of the enzymatic activity (Table 1). A representative MALDI-TOF spectrum for lysozyme modified with linker MA1 is given in Figure 1. The difference between subsequent peaks is ~303 kDa, which corresponds to the additional mass of one methacrylamide group, using linker MA1. Only a minor fraction of the protein (~3%) remained unmodified, as calculated from the peak height ratios[41]. These results are similar to the spectra obtained for LATA and LMA2 that were presented previously[33].

Table 1. Characteristics different lysozyme species

Lysozyme species	# modifications[a]	Enzymatic activity (%)[b]
Native	0.0 ± 0.2	100.0 ± 2.4
LATA	2.4 ± 0.1	70.1 ± 5.1
LMA1	2.6 ± 0.2	71.6 ± 2.9
LMA2	2.3 ± 0.3	68.2 ± 4.2

[a] Calculated from the number of free amino groups per lysozyme molecule as determined by the ninhydrin assay (average ± SD; n=3)

[b] Expressed as % remaining activity, as compared to the reference solution of native lysozyme (average ± S.D; n=6)
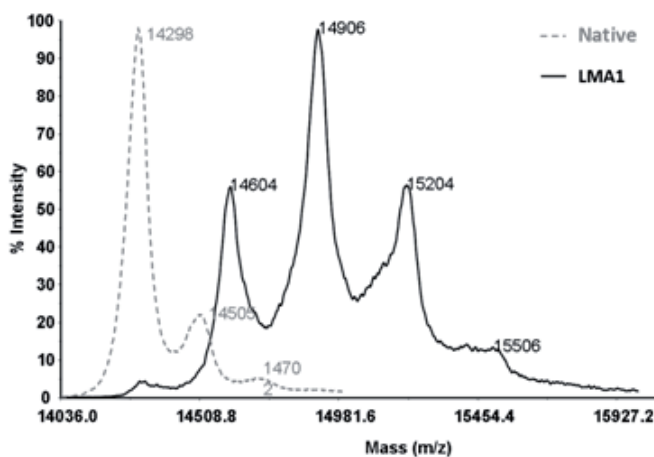
Figure 1. MALDI-TOF MS spectra of native and LMA1 (initial ratio SATA:NH$_2$, 4:7) modified lysozyme

Possible changes in the protein structure due to the conjugation reaction were analyzed with spectroscopic techniques. The UV-VIS spectra of native and both methacrylamide modified lysozyme species are similar, indicating that no aggregation has occurred during the modification reaction and subsequent work-up (Figure 2A). Far UV-CD and fluorescence spectroscopy were used to study changes in secondary and tertiary structure. The far UV-CD spectra of the modified lysozyme species overlapped almost completely with that of native lysozyme, indicating that the secondary structure has been preserved (Figure 2B). Fluorescence emission spectra of the different lysozyme species have a similar band shape, however, modification with both linkers resulted in a decrease of fluorescence intensity (~25%, Figure 2C). Both a decrease of the net positive charge of the protein by modifying the lysines, and the introduction of a disulfide bond in the vicinity of the tryptophans[42, 43], can be responsible for the decrease in fluorescence intensity as is discussed in our previous publication[33]. The spectra of the modified lysozyme also showed a subtle blue shift in the emission maximum (2 nm) caused by an increased hydrophobicity upon conjugation of the linker molecules[44]. Overall, the protein structure and enzymatic activity were only slightly affected by the conjugation of the methacrylamide groups.
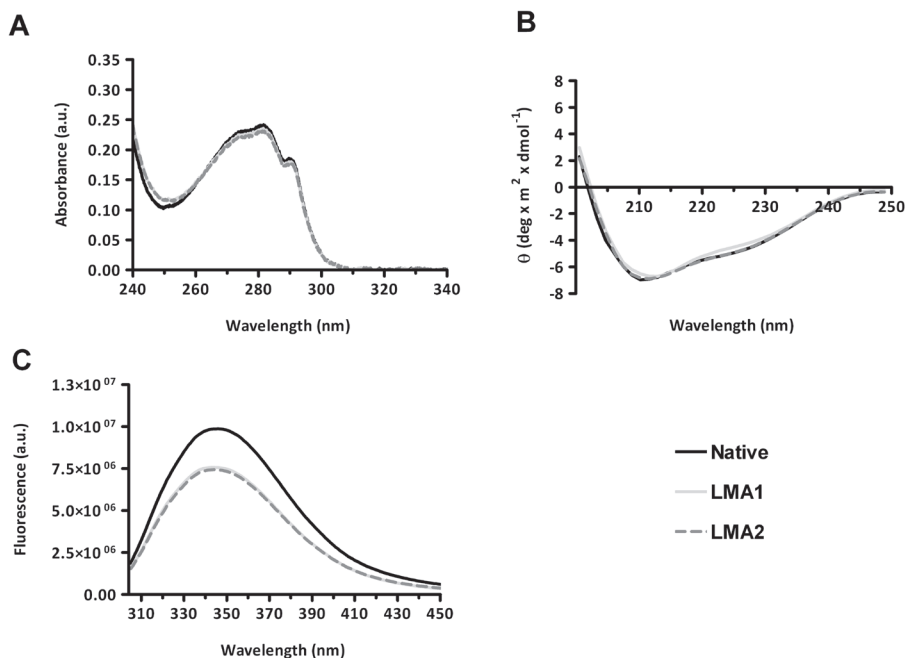
A

B

C

Figure 2. Spectral analysis of the different lysozyme variants. Native lysozyme (black line) and protein modified with linker MA1 (LMA1, grey line) and MA2 (LMA2, dashed grey line). (A) UV absorption spectra (0.2 mg/mL protein), (B) far UV-CD spectra (0.5 mg/mL protein) and (C) Fluorescence emission spectra (0.05 mg/mL protein, λ_{ex} 295 nm).

Immobilization of modified lysozyme in Dex-MA hydrogels

In our previous study[33], we showed by gel electrophoresis that LMA2 could be immobilized in a polyacrylamide gel by polymerization of acrylamide and bisacrylamide in presence of modified lysozyme, and subsequently liberated by breaking the disulfide bonds between protein and polymer network under reducing conditions. In the present work, we used biocompatible Dex-MA hydrogels as the matrix and quantified the reversible immobilization of both methacrylamide-modified lysozymes LMA1 and LMA2. Dex-MA hydrogels are not degradable and release is therefore only mediated by diffusion[14]. To prepare protein loaded hydrogels, Dex-MA (DS 7.9, 10 wt%) was polymerized in presence of native or modified (LMA1 or LMA2) lysozyme. The crosslinking reaction was carried out by free radical polymerization, which results in high conversions of the methacrylate units. Consequently, because each dextran unit contains a multitude of methacrylate units, approx. 90% of Dex-MA chains present in the mixture take part in the polymer network as experimentally verified previously[45]. Dex-

MA hydrogels of the composition used in this study are known not to swell significantly when placed in an aqueous buffer, so possible swelling effects on protein release are excluded[14]. Figure 3 shows the cumulative release of native and modified lysozyme from the hydrogels in time. During the first 96 hours, the release was carried out in a slightly acidic environment (acetate buffer pH 5, 150 mM NaCl) to prevent hydrolysis of the ester bond present in LMA2. Native lysozyme was released gradually up to ~74% and a plateau was reached after 24 hours. A similar release profile was found in a study by Cadée *et al.*, who studied the influence of the degree of substitution (DS) of Dex-MA on the release of lysozyme[46]. The incomplete recovery (~74%) can be ascribed to entrapment of protein aggregates inside the gel network and/or covalent bonding between the protein and the gel network[47]. Also permanent entrapment of unreleased lysozyme in more dense regions of the gel network, where the mesh size is smaller than the protein size, is possible[17, 48].
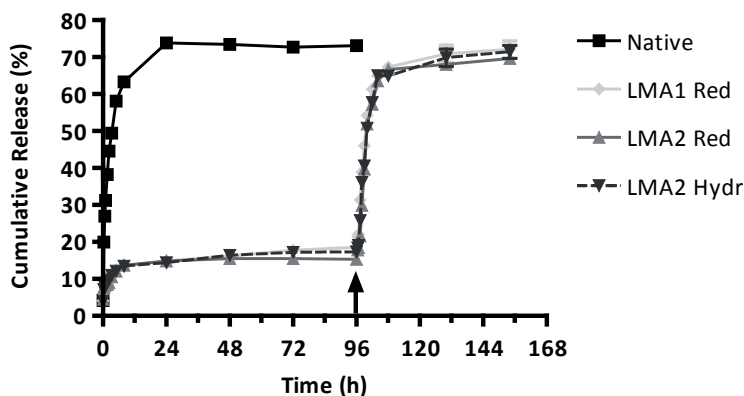

Figure 3. Cumulative release of native and modified lysozyme (LMA1 and LMA2) from Dex-MA hydrogels (10 wt%, DS 7.9). During the first 96 h the release was studied in acetate buffer pH 5 (37°C), where only native and non-immobilized modified lysozyme were gradually released. Next (arrow), the release medium was replaced by TRIS buffer pH 8.5 or a solution of 2.5 mM glutathione to induce hydrolysis (Hydr) or reduction (Red), respectively, initiating the release of modified lysozyme. The values represent the mean ± S.D. (n=3).

When comparing the release of native lysozyme from the hydrogel network, with the release of the modified lysozymes (LMA1 and LMA2), only approximately 15% of the latter were released from the hydrogel in the same acidic release medium (Figure 3), which demonstrates that the majority of methacrylamide modified lysozyme was efficiently immobilized in the Dex-MA hydrogel network by copolymerization of the methacrylamide moieties conjugated to lysozyme and Dex-MA. Part of this initial release can be ascribed to a burst release (~4%; sample

taken at *t*=0, i.e. immediately after placing the gel in the release medium), which represents protein not entrapped in the gel network, most likely due to inhibition of the polymerization by oxygen at the surface of the hydrogels. Additionally, there is a minor fraction unmodified lysozyme present in the samples (~3% according to MALDI-TOF analysis, vide supra), which can not be immobilized and can freely migrate through the gel network. Furthermore, it is possible that not all the methacrylamide groups are geometrically available for polymerization, and thus some modified proteins will not be covalently incorporated in the gel network. In the gel electrophoresis experiment that we performed previously, also a minor fraction (~5%) of the modified lysozyme (LMA2) was able to migrate freely in the polyacrylamide (PAA) gel, which was assigned to the presence of unmodified lysozyme[33]. The higher amount of modified lysozyme that was not covalently bound in the Dex-MA hydrogel as compared to the PAA gel can be ascribed to the differences in network structures of the two polymer matrices. First, the total number of double-bonds, available for reaction with the methacrylamide groups of the modified lysozyme, is ~100-fold greater in case of the PAA gel (0.42 mol% and 0.004 mol% for PAA and Dex-MA respectively), and thus the probability that modified lysozyme will take part in the polymerization reaction is higher. Second, the dextran chain may cause steric hindrance for the modified protein to approach the MA units present on the dextran.

Triggered release of reversibly immobilized lysozyme

After extraction of the non-immobilized protein fraction from the gel during four days in pH 5 buffer, the release medium was replaced by TRIS buffer pH 8.5 (10 mM TRIS, 150 mM NaCl, for LMA2 only) or a solution of 2.5 mM glutathione in HBS (10 mM HEPES, 150 mM NaCl, pH 7.4) to induce the hydrolysis or reduction of the linkers, respectively. This treatment will liberate the modified protein from the hydrogel (in this case "modified" means the protein containing remaining linker fragments). The alkaline hydrolysis of the ester bond was accelerated by using buffer pH 8.5 instead of physiological pH 7.4 and the used glutathione concentration lies within the range of reported intracellular concentrations (0.5 – 10 mM)[31]. As seen in Figure 3, changing the release medium initiated the release of the initially immobilized lysozyme rapidly up to ~72% of the initial amount, being close to the total amount released for the native protein, and a plateau was reached after 12 hours. Since the release rates after reduction and hydrolysis coincide, it is assumed that the diffusion of the protein from the hydrogel is the rate limiting step,

not the degradation of the linker. However, it must be noticed that hydrolysis at physiological pH is probably tenfold slower than at the conditions used in this experiment (pH 8.5), because it is well known that ester hydrolysis is first order in OH⁻ concentration above pH ~5[49]. Therefore, the hydrolysis rate of the linker might become the rate limiting step for release at physiological pH, but this was not investigated.

To compare this release profile with that of native lysozyme released at pH 5, the release time of the modified lysozyme species was normalized using t=96 h as time-point zero, and the amount of released lysozyme was corrected for the amount lysozyme released in the first 96 hours (~15%). The diffusion kinetics of the different lysozyme species are compared by plotting the fractional release (M_t/M_∞) of lysozyme as a function of the square root of time (Figure 4). According to the early-time approximation equation of Fick's second law, diffusion controlled release is linear with the square root of time[50]:

$$\frac{M_t}{M_\infty} = 4\sqrt{\frac{D_m t}{\pi r^2}} \qquad \text{[Eq. 1]}$$

where D_m is the diffusion coefficient of lysozyme in the gel network, t is the release time and r is the radius of the gel cylinder (0.23 cm). The release of native lysozyme (in acetate buffer pH 5) is proportional to the square root of time up to a fractional release of approx. 0.6, demonstrating that the release is indeed diffusion controlled and that the mesh size of the hydrogel network is bigger than the hydrodynamic diameter of lysozyme (4.2 nm[51])[14, 46]. The diffusion coefficient, determined from the slope of the graph and using equation 1, equals $(4.0 \pm 0.1) \times 10^{-7}$ cm²/s. This value is in the same range as diffusion coefficients determined for lysozyme in comparable hydrogels[49]. The diffusion in the Dex-MA hydrogel is slower compared to the diffusion in water ($D_0 = (10.6 \pm 1.0) \times 10^{-7}$ cm²/s)[52] , as the diffusion is hindered by the structure of the polymer network.
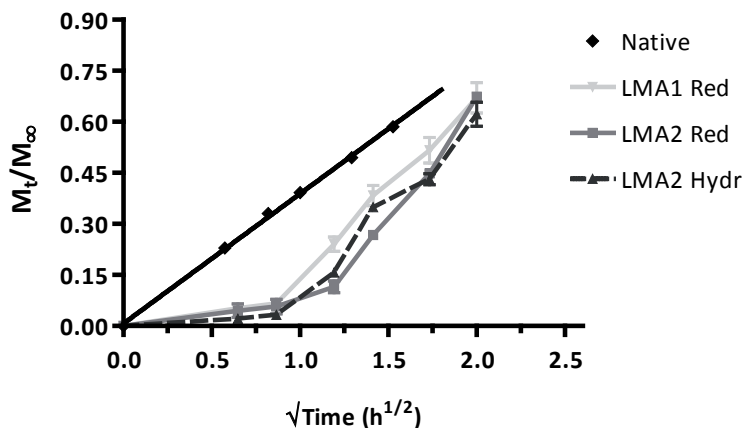
Figure 4. Fractional cumulative release of lysozyme as a function of the square root of time. Release data of modified lysozyme species have been normalized to compare the release profiles with that of native lysozyme. Red = Reduction mediated release, and Hydr = release induced by hydrolysis. The data represent the mean ± S.D. (n=3).

Interestingly, the release profiles of LMA1 (2.5 mM glutathione) and LMA2 (TRIS pH 8.5 or 2.5 mM glutathione) show a lag time prior to a rapid release which might be explained as follows. In order to induce the triggered release, the initial release medium was replaced by TRIS buffer pH 8.5 or PBS containing glutathione. The fresh release medium should penetrate into the hydrogel and subsequently the linkage between lysozyme and the gel network should be cleaved, followed by the diffusion of the free lysozyme through the hydrogel network into the release medium[52, 53]. After this lag time, the protein is released rapidly, however the release can not be described by Fickian diffusion (eq. 1), since this equation is only valid when the solute is distributed homogeneously through the polymer network. As mentioned above, many processes take place before the immobilized lysozyme is liberated from the network, which will not occur simultaneously throughout the hydrogel, resulting in a heterogeneous distribution of the mobilized protein. Therefore the diffusion coefficient could not be calculated from the release data, and instead FRAP was used to assess the diffusion kinetics of both native and modified lysozyme in Dex-MA hydrogels (vide infra).

Structural integrity of the released protein

The structural integrity of the released lysozyme was investigated by determining the enzymatic activity and by spectral analysis. The enzymatic activity of the released lysozyme

species was measured after 24 hours incubation in acetate buffer pH 5, and 6 hours after inducing hydrolysis or reduction, for native lysozyme and LMAx respectively. The specific activity of the released modified proteins was equal to that of the corresponding lysozyme conjugates before polymerization, demonstrating that the lytic activity is not affected by the polymerization process and subsequent release (Figure 5).
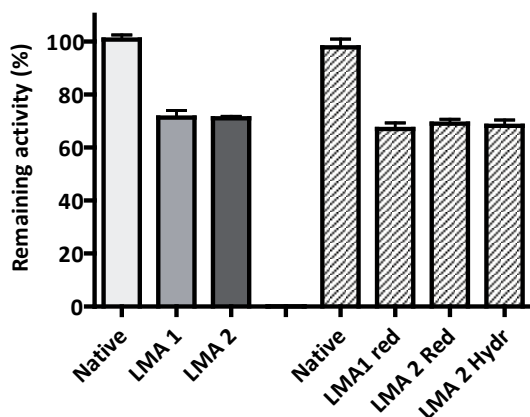

Figure 5. Enzymatic activity of the different lysozyme species. Left: activity of lysozymes in HEPES pH 7.4. Right: activity of the released lysozyme (native: after 24 h release in acetate buffer pH 5; other samples: after 6 h triggered release of immobilized lysozymes in TRIS buffer pH 8.5 (LMA2 Hydr) or 2.5 mM glutathione (LMA1 Red and LMA2 Red). The data represent the mean ± S.D. (n=3)

UV-VIS spectra and the far UV-CD spectra of the released protein almost overlapped with the spectra of the native lysozyme, whereas the fluorescence spectra had a similar band shape, but the fluorescence intensity was lower than that of native lysozyme (Figure 6). These spectra are similar to the spectra obtained with the different lysozyme species prior to polymerization (Figure 2). The results demonstrate that the global protein structure and functional integrity was preserved.
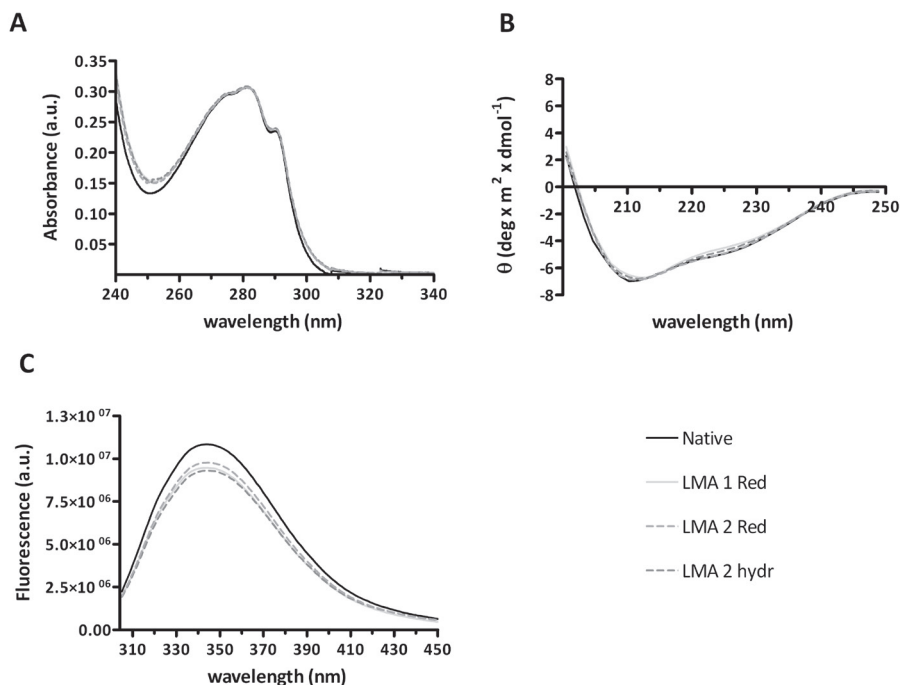
A

B

C

Figure 6. Spectral analysis of the different lysozyme variants after release from Dex-MA hydrogels. Native lysozyme: after 24 h release in acetate buffer pH 5; other samples: after 6 h triggered release of immobilized lysozymes in TRIS buffer pH 8.5 (LMA2 Hydr) or 2.5 mM glutathione (LMA1 Red and LMA2 Red). (A) UV absorption spectra (0.2 mg/mL protein), (B) far UV-CD spectra (0.5 mg/mL protein) and (C) fluorescence emission spectra (0.05 mg/mL protein, λ_{ex} 295 nm)

Diffusion kinetics using Fluorescence Recovery After Photobleaching (FRAP)

FRAP measurements were conducted to study the translational diffusion coefficient (mobility) of native and modified lysozyme (before and after triggering the release) inside Dex-MA hydrogels. With this technique, fluorescent molecules diffusing in a specified area are irreversibly bleached. Immediately after bleaching, the recovery of the fluorescence, due to exchange of bleached and unbleached molecules into and out of the bleached area, is measured. The diffusion coefficient was calculated from the recovery of the fluorescence in the bleached area using a recently published pixel-based FRAP method[40]. Lysozyme was labeled with FITC and subsequently conjugated with linker MA2 as described above. As a control, the mobility of FITC-labeled lysozyme was determined in a 48% sucrose solution, which after correcting for the viscosity resulted in a diffusion coefficient (D_0) of $(6.5 \pm 0.8) \times 10^{-7}$ cm^2/s, which is in agreement with published values[49, 52]. The mobile fraction and diffusion coefficient of lysozyme in Dex-MA

hydrogels were determined at different time points. Directly after preparation of the gel, the recovery of fluorescence intensity was almost complete for native protein demonstrating a large mobile fraction (k = 0.87 ± 0.04), whereas only partial recovery (k = 0.32 ± 0.08) was observed for the modified lysozyme (Figure 7). This incomplete recovery can be expected because for modified lysozyme the majority of the protein is immobilized in the network. Only the fraction of modified protein that is not fixed in the polymer network (~15% according to the release study, Figure 3) is responsible for the observed recovery. The mobile fraction as determined by FRAP, is higher than the one that was calculated from the release experiment (35% and 15% respectively). A possible explanation can be found in the difference in experimental set-up, starting with the polymerization of the gels. For the release study, a large volume (1 mL) in closed de-aired cylinders was used, whereas for the FRAP experiment small and thin gels were polymerized in a well plate format. This dissimilarity may lead to differences in experimental outcome. Nevertheless, the results of the FRAP study confirm that the modified lysozyme is partially immobilized by co-polymerization in the Dex-MA hydrogel. By fitting the experimental recovery data with a previously described FRAP model (rFRAP)[40], the corresponding diffusion coefficients of the mobile fractions were calculated and the values are presented in Table 2. The calculated diffusion coefficient of the fraction of non-immobilized modified lysozyme at $t = 0$ is of the same order of magnitude as that of native protein.

Table 2. Diffusion coefficient ($\times$ 10-8 cm2/s) of native lysozyme and LMA2 incorporated in Dex-MA hydrogels, measured at different time points

	$t = 0$	$t = 96$ h	$t = 3$ h after trigger
Native	10.5 ± 1.1	nd[c]	nd[c]
LMA2	5.6 ± 1.1	nd[c]	
LMA2 Red[a]	-	-	6.4 ± 0.7
LMA2 Hydr[b]	-	-	7.6 ± 1.6

[a] After adding 20 μL 5 mM glutathione; [b] After adding 20 μL 1 mM NaOH
[c] Diffusion coefficient could not be determined (nd) as no recovery occurs, since the remaining protein is immobilized in the hydrogel network.
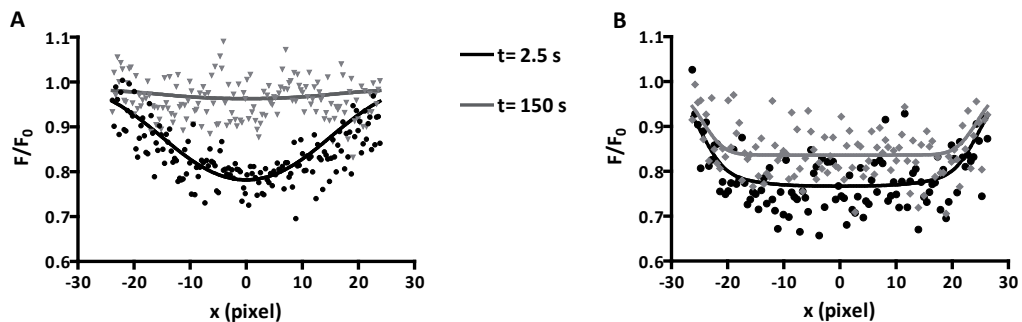
Figure 7. Fluorescence intensity curves for native (A) and modified lysozyme (B) two hours after polymerization. The intensity values which result from the fitting procedure are shown for a cross section along the *x*-direction of the square. At time *t* = 0 s, a square region in the hydrogel is bleached. The black solid line shows the fluorescence intensity values at *t* = 2.5 s after bleaching and the grey line shows the fluorescence intensity values of the same cross section after a recovery time of 150 s.

Based on the release study, the mobile fraction should have diffused out of the hydrogel network after 96 hours release in acetate buffer pH 5, and only immobilized protein will be present in the gel. Indeed, for gels loaded with native lysozyme that were incubated for three days in buffer to extract the lysozyme showed an almost complete loss of the fluorescence intensity. The remaining fluorescence signal originates from a minor fraction of native lysozyme that was entrapped in the hydrogel network either as aggregate, or as a result of chemical crosslinking[47] or due to entrapment of the protein in more dense regions of the hydrogel[17, 48]. Even though the fluorescence signal was very weak, we performed a FRAP measurement, but no significant recovery was observed, indicating that the unreleased lysozyme is indeed immobile.

In case of modified lysozyme, the minor fraction that remained mobile (~15-35% based on the release study and FRAP study, respectively) diffused out of the gel during the 96 hours release in acetate buffer and as a result the observed fluorescence intensity slightly decreased compared to the intensity of the same sample at *t* = 0. As expected, because only the immobilized fraction remained, no recovery after photobleaching was observed at *t* = 96 h. Next, glutathione or NaOH were added to the hydrogels with immobilized LMA2, to trigger reduction or hydrolysis of the linkage between lysozyme and the gel network, respectively. According to FRAP measurements that were carried out three hours after triggering, mobility was restored and diffusion coefficients were of the same order of magnitude as for the native protein at time point zero (Table 2, *t*=3 h after trigger), corroborating that lysozyme was indeed mobilized by both hydrolysis and reduction. The diffusion coefficient of native lysozyme as determined by

FRAP was 4-fold lower than that calculated from the release study, i.e. $(10.5 \pm 1.1) \times 10^{-8}$ cm^2/s and $(40.2 \pm 1.0) \times 10^{-8}$ cm^2/s, respectively. Also others reported such discrepancy between both techniques, which is most likely caused by differences in experimental set-up[49, 54]. Nevertheless, the FRAP data confirm what was observed on macroscopic scale, i.e. initially there is a mobile fraction present after co-polymerization of methacrylamide modified lysozyme (15% in the release study), which is released in acetate buffer, leaving only immobilized lysozyme in the hydrogel. By inducing hydrolysis or reduction of the linker between the protein and the polymer network, the conjugated protein is released from the gel with approximately the same diffusion kinetics as native lysozyme.

CONCLUSIONS

Lysozyme was successfully modified with on average 2 to 3 methacrylamide functions using two different novel linkers, with preservation of the protein structure and retention of approximately 70% of the enzymatic activity. Importantly, the modified lysozyme could be immobilized by co-polymerization in a macroscopic Dex-MA hydrogel network, and subsequently released upon hydrolysis or reduction of the linkage between the protein and the polymer network. Furthermore, it is shown that the released protein preserved its structural integrity and enzymatic activity. The purpose of this study was to obtain fundamental insight into the temporary immobilization and triggered release of a (model) protein from (macroscopic) dextran hydrogels. For intracellular protein delivery, it is most appropriate to chose MA1-modified protein that contains the linker with only the disulfide bond, which will be stable in the extracellular environment, and to conjugate that to biodegradable nanoparticles. Therefore, the next step is to apply biodegradable and biocompatible dextran hydrogels (e.g. based on hydroxyethylmethacrylate substituted dextran, Dex-HEMA[22]) and to down scale the system to obtain nanoparticles that can act as a carrier system (with targeting and prolonged circulation properties). Protein encapsulated dextran nanogels can be prepared as previously reported[21]. In a forthcoming paper we will combine both approaches and pursue cellular uptake and intracellular release of immobilized protein from nanoparticles upon reduction by glutathione.

Acknowledgements

REFERENCES

1. Torchilin, V. P.; Lukyanov, A. N. Peptide and protein drug delivery to and into tumors: Challenges and solutions, *Drug Discovery Today,* 8 (**2003**), 259-266.
2. Hamidi, M.; Azadi, A.; Rafiei, P. Hydrogel nanoparticles in drug delivery, *Advanced Drug Delivery Reviews,* 60 (**2008**), 1638-1649.
3. Raemdonck, K.; Demeester, J.; De Smedt, S. Advanced nanogel engineering for drug delivery, *Soft Matter,* 5 (**2009**), 707-715.
4. Lee, Y.; Ishii, T.; Cabral, H.; Kim, H.; Seo, J. H.; Nishiyama, N.; Oshima, H.; Osada, K.; Kataoka, K. Charge-conversional polyionic complex micelles—efficient nanocarriers for protein delivery into dytoplasm, *Angewandte Chemie International Edition,* 48 (**2009**), 5309-5312.
5. Miyata, K.; Oba, M.; Kano, M. R.; Fukushima, S.; Vachutinsky, Y.; Han, M.; Koyama, H.; Miyazono, K.; Nishiyama, N.; Kataoka, K. Polyplex micelles from triblock copolymers composed of tandemly aligned segments with biocompatible, endosomal escaping, and DNA-condensing functions for systemic gene delivery to pancreatic tumor tissue, *Pharmaceutical Research,* 25 (**2008**), 2924-2936.
6. Schiffelers, R. M.; Storm, G. Liposomal nanomedicines as anticancer therapeutics: Beyond targeting tumor cells, *International Journal of Pharmaceutics,* 364 (**2008**), 258-264.
7. Sawant, R. R.; Torchilin, V. P. Liposomes as'smart' pharmaceutical nanocarriers, *Soft Matter,* 6 (**2010**), 4026-4044.
8. Lavignac, N.; Lazenby, M.; Franchini, J.; Ferruti, P.; Duncan, R. Synthesis and preliminary evaluation of poly(amidoamine)-melittin conjugates as endosomolytic polymers and/or potential anticancer therapeutics, *International Journal of Pharmaceutics,* 300 (**2005**), 102-112.
9. Amidi, M.; Mastrobattista, E.; Jiskoot, W.; Hennink, W. E. Chitosan-based delivery systems for protein therapeutics and antigens, *Advanced Drug Delivery Reviews,* 62 59-82.
10. Luten, J.; van Nostrum, C. F.; De Smedt, S. C.; Hennink, W. E. Biodegradable polymers as non-viral carriers for plasmid DNA delivery, *J Controlled Release,* 126 (**2008**), 97-110.
11. Varkouhi, A. K.; Verheul, R. J.; Schiffelers, R. M.; Lammers, T.; Storm, G.; Hennink, W. E. Gene silencing activity of sirna polyplexes based on thiolated n, n, n -trimethylated chitosan, *Bioconjugate Chemistry,* 21 (**2010**), 2339-2346.
12. Peppas, N. A.; Bures, P.; Leobandung, W.; Ichikawa, H. Hydrogels in pharmaceutical formulations, *European Journal of Pharmaceutics and Biopharmaceutics,* 50 (**2000**), 27-46.
13. Weber, L. M.; Lopez, C. G.; Anseth, K. S. Effects of peg hydrogel crosslinking density on protein diffusion and encapsulated islet survival and function, *Journal of Biomedical Materials Research Part A,* 90A (**2009**), 720-729.
14. Hennink, W. E.; Talsma, H.; Borchert, J. C. H.; De Smedt, S. C.; Demeester, J. Controlled release of proteins from dextran hydrogels, *J Control Release,* 39 (**1996**), 47-55.
15. van Dijk-Wolthuis, W. N. E.; Hoogeboom, J. A. M.; van Steenbergen, M. J.; Tsang, S. K. Y.; Hennink, W. E. Degradation and release behavior of dextran-based hydrogels, *Macromolecules,* 30 (**1997**), 4639-4645.
16. Hiemstra, C.; Zhong, Z.; van Steenbergen, M. J.; Hennink, W. E.; Feijen, J. Release of model proteins and basic fibroblast growth factor from in situ forming degradable dextran hydrogels, *Journal of Controlled Release,* 122 (**2007**), 71-78.
17. Meyvis, T.; De Smedt, S.; Stubbe, B.; Hennink, W.; Demeester, J. On the release of proteins from degrading dextran methacrylate hydrogels and the correlation with the rheologic properties of the hydrogels, *Pharmaceutical Research,* 18 (**2001**), 1593-1599.
18. Carvalho, J. M.; Coimbra, M. A.; Gama, F. M. New dextrin-vinylacrylate hydrogel: Studies on protein diffusion and release, *Carbohydr Polym,* 75 (**2009**), 322-327.

19. am Ende, M. T.; Peppas, N. A. Transport of ionizable drugs and proteins in crosslinked poly(acrylic acid) and poly(acrylic acid-co-2-hydroxyethyl methacrylate) hydrogels. Ii. Diffusion and release studies, *J Controlled Release,* 48 (**1997**), 47-56.

20. Stenekes, R. J. H.; De Smedt, S. C.; Demeester, J.; Sun, G.; Zhang, Z.; Hennink, W. E. Pore sizes in hydrated dextran microspheres, *Biomacromolecules,* 1 (**2000**), 696-703.

21. Van Thienen, T. G.; Raemdonck, K.; Demeester, J.; De Smedt, S. C. Protein release from biodegradable dextran nanogels, *Langmuir,* 23 (**2007**), 9794-9801.

22. Franssen, O.; Vandervennet, L.; Roders, P.; Hennink, W. E. Degradable dextran hydrogels: Controlled release of a model protein from cylinders and microspheres, *Journal of Controlled Release,* 60 (**1999**), 211-221.

23. Censi, R.; Vermonden, T.; van Steenbergen, M. J.; Deschout, H.; Braeckmans, K.; De Smedt, S. C.; van Nostrum, C. F.; di Martino, P.; Hennink, W. E. Photopolymerized thermosensitive hydrogels for tailorable diffusion-controlled protein delivery, *J Controlled Release,* 140 (**2009**), 230-236.

24. Nagahama, K.; Ouchi, T.; Ohya, Y. Biodegradable nanogels prepared by self-assembly of poly(l-lactide)-grafted dextran: Entrapment and release of proteins, *Macromolecular Bioscience,* 8 (**2008**), 1044-1052.

25. Swaminathan, S.; Cavalli, R.; Trotta, F.; Ferruti, P.; Ranucci, E.; Gerges, I.; Manfredi, A.; Marinotto, D.; Vavia, P. In vitro release modulation and conformational stabilization of a model protein using swellable polyamidoamine nanosponges of β-cyclodextrin, *Journal of Inclusion Phenomena and Macrocyclic Chemistry,* 68 (**2010**), 183-191.

26. Ayame, H.; Morimoto, N.; Akiyoshi, K. Self-assembled cationic nanogels for intracellular protein delivery, *Bioconjugate Chemistry,* 19 (**2008**), 882-890.

27. Murthy, N.; Campbell, J.; Fausto, N.; Hoffman, A. S.; Stayton, P. S. Bioinspired ph-responsive polymers for the intracellular delivery of biomolecular drugs, *Bioconjugate Chemistry,* 14 (**2003**), 412-419.

28. Shi, L.; Khondee, S.; Linz, T. H.; Berkland, C. Poly(n-vinylformamide) nanogels capable of ph-sensitive protein release, *Macromolecules,* 41 (**2008**), 6546-6554.

29. Saito, G.; Swanson, J. A.; Lee, K.-D. Drug delivery strategy utilizing conjugation via reversible disulfide linkages: Role and site of cellular reducing activities, *Advanced Drug Delivery Reviews,* 55 (**2003**), 199-215.

30. Meng, F.; Hennink, W. E.; Zhong, Z. Reduction-sensitive polymers and bioconjugates for biomedical applications, *Biomaterials,* 30 (**2009**), 2180-2198.

31. Meister, A.; Anderson, M. E. Glutathione, *Annual Review of Biochemistry,* Vol. 52 (**1983**), 711-760.

32. Jones, D. P.; Carlson, J. L.; Samiec, P. S.; Sternberg, P.; Mody, V. C.; Reed, R. L.; Brown, L. A. S. Glutathione measurement in human plasma: Evaluation of sample collection, storage and derivatization conditions for analysis of dansyl derivatives by hplc, *Clinica Chimica Acta,* 275 (**1998**), 175-184.

33. Verheyen, E.; Delain-Bioton, L.; van der Wal, S.; el Morabit, N.; Barendregt, A.; Hennink, W. E.; van Nostrum, C. F. Conjugation of methacrylamide groups to a model protein via a reducible linker for immobilization and subsequent triggered release from hydrogels, *Macromol Biosci,* (**2010**), n/a-n/a.

34. van Dijk-Wolthuis, W. N. E.; Franssen, O.; Talsma, H.; van Steenbergen, M. J.; Kettenes-van den Bosch, J. J.; Hennink, W. E. Synthesis, characterization, and polymerization of glycidyl methacrylate derivatized dextran, *Macromolecules,* 28 (**1995**), 6317-6322.

35. van Dijk-Wolthuis, W. N. E.; Kettenes-van den Bosch, J. J.; van der Kerk-van Hoof, A.; Hennink, W. E. Reaction of dextran with glycidyl methacrylate: An unexpected transesterification, *Macromolecules,* 30 (**1997**), 3411-3413.

36. Kok, R. J.; Haas, M.; Moolenaar, F.; de Zeeuw, D.; Meijer, D. K. F. Drug delivery to the kidneys and the bladder with the low molecular weight protein lysozyme, *Ren Fail,* 20 (**1998**), 211-217.

37. Duncan, R. J. S.; Weston, P. D.; Wrigglesworth, R. A new reagent which may be used to introduce sulfhydryl groups into proteins, and its use in the preparation of conjugates for immunoassay, *Analytical Biochemistry,* 132 (**1983**), 68-73.

38. Prochazkova, S.; Vårum, K. M.; Ostgaard, K. Quantitative determination of chitosans by ninhydrin, *Carbohydrate Polymers,* 38 (**1999**), 115-122.

39. Kelly, S. M.; Jess, T. J.; Price, N. C. How to study proteins by circular dichroism, *Biochimica et Biophysica Acta (BBA) - Proteins & Proteomics,* 1751 (**2005**), 119-139.

40. Deschout, H.; Hagman, J.; Fransson, S.; Jonasson, J.; Rudemo, M.; Lorén, N.; Braeckmans, K. Straightforward frap for quantitative diffusion measurements with a laser scanning microscope, *Opt. Express,* 18 (**2010**), 22886-22905.

41. Xu, H.; Kaar, J. L.; Russell, A. J.; Wagner, W. R. Characterizing the modification of surface proteins with poly(ethylene glycol) to interrupt platelet adhesion, *Biomaterials,* 27 (**2006**), 3125-3135.

42. Vanhooren, A.; Devreese, B.; Vanhee, K.; Van Beeumen, J.; Hanssens, I. Photoexcitation of tryptophan groups induces reduction of two disulfide bonds in goat α-lactalbumine *Biochemistry,* 41 (**2002**), 11035-11043.

43. Wu, L.-Z.; Sheng, Y.-B.; Xie, J.-B.; Wang, W. Photoexcitation of tryptophan groups induced reduction of disulfide bonds in hen egg white lysozyme, *J Mol Struct,* 882 (**2008**), 101-106.

44. Weljie, A. M.; Vogel, H. J. Tryptophan fluorescence of calmodulin binding domain peptides interacting with calmodulin containing unnatural methionine analogues, *Protein Eng.,* 13 (**2000**), 59-66.

45. De Smedt, S. C.; Lauwers, A.; Demeester, J.; Van Steenbergen, M. J.; Hennink, W. E.; Roefs, S. P. F. M. Characterization of the network structure of dextran glycidyl methacrylate hydrogels by studying the rheological and swelling behavior, *Macromolecules,* 28 (**1995**), 5082-5088.

46. Cadée, J. A.; de Groot, C. J.; Jiskoot, W.; den Otter, W.; Hennink, W. E. Release of recombinant human interleukin-2 from dextran-based hydrogels, *J Control Release,* 78 (**2002**), 1-13.

47. Mellott, M. B.; Searcy, K.; Pishko, M. V. Release of protein from highly cross-linked hydrogels of poly(ethylene glycol) diacrylate fabricated by uv polymerization, *Biomaterials,* 22 (**2001**), 929-941.

48. Sutter, M.; Siepmann, J.; Hennink, W. E.; Jiskoot, W. Recombinant gelatin hydrogels for the sustained release of proteins, *J Control Release,* 119 (**2007**), 301-312.

49. Van Tomme, S. R.; De Geest, B. G.; Braeckmans, K.; De Smedt, S. C.; Siepmann, F.; Siepmann, J.; van Nostrum, C. F.; Hennink, W. E. Mobility of model proteins in hydrogels composed of oppositely charged dextran microspheres studied by protein release and fluorescence recovery after photobleaching, *J Control Release,* 110 (**2005**), 67-78.

50. Ritger, P. L.; Peppas, N. A. A simple equation for description of solute release ii. Fickian and anomalous release from swellable devices, *J Control Release,* 5 (**1987**), 37-42.

51. Merrill, E. W.; Dennison, K. A.; Sung, C. Partitioning and diffusion of solutes in hydrogels of poly(ethylene oxide), *Biomaterials,* 14 (**1993**), 1117-1126.

52. Dubin, S. B.; Clark, N. A.; Benedek, G. B. Measurement of the rotational diffusion coefficient of lysozyme by depolarized light scattering: Configuration of lysozyme in solution, *J Chem Phys,* 54 (**1971**), 5158-5164.

53. Korsmeyer, R. W.; Peppas, N. A. Solute and penetrant diffusion in swellable polymers. Iii. Drug release from glassy poly(hema-co-nvp) copolymers, *J Control Release,* 1 (**1984**), 89-98.

54. Brandl, F.; Kastner, F.; Gschwind, R. M.; Blunk, T.; Teßmar, J.; Göpferich, A. Hydrogel-based drug delivery systems: Comparison of drug diffusivity and release kinetics, *Journal of Controlled Release,* 142 (**2010**), 221-228.

SUMMARY AND PERSPECTIVES

SUMMARY

Since the introduction of hydrogels in the 1960's for the design of soft contact lenses[1], their use has increased tremendously[2-6]. **Chapter 1** provides a general introduction on hydrogels with a focus on the use of hydrogels as delivery systems for proteins and as matrices for protein imprinting. Furthermore, approaches towards the surface imprinting of membrane proteins are introduced, aiming at the development of targeted drug delivery devices (PINAPLES, protein imprinted nanoparticles). Finally, the outline of this thesis is presented.

The first step towards the development of surface imprinted polymers of membrane proteins was to incorporate membrane proteins in lipid bilayers, i.e. their natural environment. **Chapter 2** describes the use of detergents to facilitate the insertion of hemagglutinin, as a model membrane protein, in preformed lipid bilayers on solid supports (glass and mica). To establish a detergent concentration range that could be used to promote the protein insertion, the stability of the preformed lipid bilayers in presence of detergents was evaluated by atomic force microscopy (AFM) and a lipid adsorption assay. For simultaneous evaluation of the different parameters involved in the reconstitution process, i.e. detergent type and concentration, protein concentration and incubation time, the reconstitution method was adapted to a 96 well plate format. To detect the protein reconstituted in supported lipid bilayers, we developed an ELISA protocol avoiding the use of surfactants. It was demonstrated that the choice of detergent is important in the optimization of a suitable reconstitution protocol and that the detergent concentration has to be chosen carefully so it destabilizes the bilayer by local and transient solubilization, which can facilitate the protein insertion. On the other hand, complete solubilization has to be avoided by using solutions with sufficient low detergent concentrations or weaker detergents.

The ELISA method is very simple, versatile and moreover a very quick manner to optimize the method for reconstitution of an individual membrane protein. The well plate format was also used to screen different parameters involved in the imprinting of polymers. But despite many attempts, no successful imprints of the membrane protein were obtained. Even imprinting of soluble proteins, such as cytochrome C and lysozyme, using protocols described in literature was extremely challenging and no prove of imprinting was obtained. Although the number of research papers describing protein imprinting is increasing, it is clear that molecular imprinting of proteins still faces some fundamental issues that need in depth research. As

discussed in **Chapter 3**, the main topics of concern are proper monomer selection, template removal and the assessment of the template rebinding. The use of charged monomers can lead to strong electrostatic interactions between monomers and template, but also to undesired high nonspecific binding. Up till now, it has not been convincingly shown that electrostatic interactions lead to better imprinting results. In this chapter it is further demonstrated that the combination of a detergent (SDS) and acetic acid, commonly used for template removal, can lead to experimental artifacts, and should therefore be avoided. In many cases template rebinding is unreliably quantified, results are not evaluated critically and lack statistical analysis. Therefore, it can be argued that presently, the scientific evidence of molecular imprinting of proteins presented in many papers is not convincing.

As the standard non-covalent approach for protein imprinting did not lead to polymer networks with the desired recognition properties, new concepts for protein imprinting have to be explored. In this light, a novel semi-covalent approach is proposed in **Chapter 4**. This method involves the covalent incorporation of the template in the polymer network during polymerization and after subsequent removal of the template by chemical cleavage, the rebinding to the MIP occurs via non-covalent interactions. To achieve this, an efficient strategy is developed to introduce polymerizable methacrylamide moieties to the lysine residues of a model protein, lysozyme, using a novel sacrificial linker. This spacer contains a disulfide bond and an ester bond, such that the removal of the protein can be induced by reduction and hydrolysis, respectively. The lysozyme modification was performed in two steps in aqueous media. First, the protein was thiolated and subsequently reacted with the novel linker molecule (2-(2-pyridin-2-yldisulfanyl)ethyl 2-(methacrylamido)acetate) via disulfide exchange to obtain the desired methacrylated protein. The modified lysozymes with different degrees of methacrylate substitution were characterized by MALDI-TOF MS and titration of free NH_2 residues, whereas possible structural changes of the protein were investigated by spectral analysis. The modification reaction is well controlled and the number of introduced functions can be tailored by changing the reaction conditions. Up to three linker molecules could be introduced with preservation of the protein conformation and keeping its enzymatic activity. Gel electrophoresis showed that the methacrylamide modified protein can be immobilized in a polyacrylamide hydrogel and subsequently released by reduction of the spacer by which the protein was grafted to the polymeric network.

These protein-macromonomers were primarily developed for semi-covalent imprinting, but unfortunately also with this approach no encouraging imprint results were obtained. It was however recognized that the methacrylamide modified proteins could also be used for triggered release of proteins from a hydrogel network. This was further assessed in **Chapter 5**, where a second linker molecule, containing only disulfide bonds, was synthesized, thereby aiming for glutathione mediated intracellular release of proteins. The modification of lysozyme with this linker was done via the method described in Chapter 4. Next, methacrylated dextran (Dex-MA) was polymerized in presence of native or methacrylated lysozyme (including the one described in chapter 4) to yield hydrogels. The release of native and modified lysozyme from Dex-MA hydrogels was studied in acetate buffer (pH 5, in absence of any trigger) and only a minor fraction (~15%) of the modified lysozyme was released, whereas ~74% of the native lysozyme was released. This indicates successful immobilization of the majority of the methacrylated lysozyme in the hydrogel network. Upon hydrolysis of the ester bonds or incubation with glutathione to reduce the disulfide bond present in the linker molecules that conjugate the lysozyme to the gel network, the modified lysozyme was mobilized and released from the hydrogel to the same extent as native lysozyme. These data were confirmed by fluorescence recovery after photobleaching experiments. The novel covalent linking approach is potentially highly interesting for temporary immobilization and subsequent glutathione triggered intracellular delivery of proteins from nanogels.

The aim of this thesis was to develop a unique, innovative and very challenging concept to synthesize polymer nanoparticles displaying the imprints of membrane proteins (PINAPLES) on their surface. Despite several efforts to achieve the right conditions for protein imprinting, the proof of concept could not be unambiguously demonstrated. However, the synthesis of the protein-macromonomers led to a promising and highly attractive method for transient immobilization of proteins in hydrogels and subsequent triggered extra- and intracellular release. The next logical step is to down scale the system to obtain nanoparticles that can act as a carrier system (with targeting and prolonged circulation properties) and release the immobilized protein intracellularly upon reduction by glutathione.

PERSPECTIVES

The search for the Holy Grail: Protein imprinting

Molecular imprinting has been advocated and promoted as a technique to create artificial antibodies, i.e. polymers with the recognizing properties of antibodies, but which are superior in stability (robustness) and can be reused. The imprinting technique is successful for small templates, where even enantiomers have been separated by MIPs[7,8]. In contrast, however, limited successes have been claimed in recognition and binding of target proteins from a single solution or from a mixture of different proteins. As discussed in Chapter 3, the key issue in developing protein imprinted polymers is to identify the right combination of functional monomers that will result in high affinity binding sites for the template protein, while diminishing nonspecific adsorption of the template to non-imprinted polymers. In general, the selection of functional monomers is achieved by trial and error. However, at present the use of combinatorial imprinting has gained interest[9-13]. With this technique, one takes into account the surface characteristics of the protein, such as the presence of charged amino acids and hydrophobic areas. Next, a library of functional monomer combinations is screened and the combination resulting in the highest affinity and selectivity is selected. In fact, this technique has led recently to exciting results, where for the first time MIPs have been synthesized which could effectively recognize their target under practical conditions, such as biological fluids[12, 14]. Further, successful in vivo results have been obtained using peptide (melettin) imprinted polymer particles which were able to capture and neutralize the cytolytic peptide melettin from the blood stream of living mice[14]. Melettin, the main component of bee venom, is a 26 amino acid peptide, which carries positive charges, as well as hydrophobic and hydrophilic regions. The most effective imprints were obtained with polymer particles composed of N-isopropylacrylamide (NIPAAm) crosslinked with N,N'-methylene-bisacrylamide, supplemented with functional monomers for electrostatic (acrylic acid (AAc)) and hydrophobic interactions (N-t-butylacrylamide)[10, 14, 15]. Upon injection of the MIP particles into the bloodstream, the melettin is rapidly captured by the MIPs that are subsequently cleared from the blood stream by phagocytosis, which reduced significantly the melettin induced mortality and peripheral toxic symptoms. Other encouraging results have been recently presented by the group of Sellergren. They used the epitope approach to prepare peptide imprinted polymers for the detection of β-amyloid isoforms Aβ42/Aβ40 in blood serum samples, which are identified as biomarkers for early diagnosis of Alzheimer's disease[12]. These

examples demonstrate the significant progress made in the field of molecular imprinting of biomacromolecules in aqueous environment. Currently, it seems that using peptides as template and concurrent the epitope approach, where only a smaller part (peptide) of the protein is used as template, gives the best perspectives for future developments in protein imprinting.

Controlled delivery of proteins from hydrogels

In chapter 4 and 5, we describe an efficient strategy to functionalize the lysine groups of a model protein, lysozyme, with polymerizable methacrylamide moieties. These protein-macromers were successfully immobilized in Dex-MA hydrogels by co-polymerization. The presence of disulfide linkages in the linker molecule, through which the protein is conjugated to the hydrogel network, made glutathione triggered protein release possible. Throughout the complete process of modification, immobilization and subsequent release, the protein conformation was preserved, and lysozyme maintained its enzymatic activity. The applicability for intracellular protein delivery has yet to be demonstrated using in vitro and, if successful, in vivo experiments. Therefore the next step would be to apply this strategy towards nanoparticles, which can be administered by injection and taken up by cells. The advantages of the reversible protein immobilization are (1) prevention of rapid premature release that is often associated with nanoparticles (large surface, short diffusion distance), (2) triggered spatio-temporal release, i.e. glutathione triggered release after internalization. A final step to improve the nanocarriers would be to use biodegradable polymers, in order to break down the carriers after releasing the protein intracellularly. An important requisite is that the particle is stable in the blood stream, and ideally only degrades after delivering the protein. This can be realized e.g. by using biodegradable hydroxyethyl methacrylated dextran (Dex-HEMA)[16-18]. In our department, an efficient method to prepare hydrogel nanoparticles, using a liposomal reactor, has recently been developed[19]. Via this method, particles with a controlled size and size distribution are obtained. Dextran nanoparticles can thus be formed after polymerization of Dex-HEMA that is encapsulated in liposomes[20], while including a solution containing the protein-macromers. After polymerization, the lipid bilayer can be removed by detergents to obtain bare nanogels, which can be administered systemically and finally be taken up by cells, releasing the immobilized protein upon glutathione-mediated reduction of the disulfide linkages. It can be beneficial to maintain the lipid coating around the particles. For example, using fusogenic lipids, such

as 1,2-dioleoyl-sn-glycero-3-phosphoethanolamine (DOPE), can facilitate the escape of the nanogels from endosomes after internalization[21, 22]. Moreover, by using PEGylated lipids, one can increase the blood circulation time of the nanogels, by inhibiting the opsonization of the nanogels, thereby avoiding the phagocytosis by macrophages of the mononuclear phagocytic system[23-25]. PEGylation also enables the attachment of targeting ligands, such as antibodies or peptides, which makes delivery to specific target cells possible[26-30].

This approach is attractive for intracellular protein delivery, but has yet to be proven experimentally. Moreover, the conjugation of the methacrylamide moieties to lysine residues of proteins has only be shown for a model protein, lysozyme, and the feasibility of the developed method towards therapeutically relevant proteins has yet to be explored. In that case, one has to take into account that the modification can possibly harm the functionality of the protein, as the lysine residues might play a role in the proteins' biological activity. It can also be argued that modification of these biotherapeutics leads to changes in the structural properties of the protein, thereby influencing the immunogenicity. On the other hand, the increased immunogenicity after modification of the protein structure can be beneficial, when used e.g. for vaccination purposes, provided that the antigenic epitopes are still intact. In general, for vaccination, particulate delivery systems (e.g. liposomes[31], polymeric carriers[32, 33]) have been used, as they protect the antigen against degradation. Moreover encapsulation in particles results in an increased uptake by antigen presenting cells (APC), prolonged residence time at the site of action, and particles make co-delivery of the antigen and an adjuvant possible[32, 34, 35]. This all results in an increased immunogenicity of the antigen and as a consequence a more effective immune response is elicited[36]. A requisite however, is that the antigen remains encapsulated or associated with the particle until uptake by APC occurs. By introducing our polymerizable reduction-sensitive linker molecule, as described in Chapters 4 and 5 of this thesis, onto the antigenic peptide or protein and then by its covalent encapsulation in nanogels, one can achieve the desired triggered intracellular release. Aiming for this purpose, we successfully conjugated methacrylamide moieties to lysine residues of ovalbumin (OVA), which is often used as a model antigen, using the method described in chapter 4 (results not shown in this thesis). For nasal delivery of antigens, particles coated or formulated with N, N, N – trimethyl chitosan (TMC) as adjuvant have shown excellent efficiency[37-39]. TMC is known for its mucoadhesive properties (ionic interaction with the negatively charged mucin), thereby prolonging the residence time in the nasal cavity[40, 41], and in addition, TMC can open

tight junctions, thereby increasing the permeability of the epithelium[42]. Therefore, in a pilot study we encapsulated (yet non-modified) OVA in negatively charged Dex-MA nanoparticles, prepared as described by Schillemans[43], after which the particles were successfully coated with positively charged TMC. Further research is necessary to evaluate whether this approach of antigen immobilization and triggered intracellular release is beneficial for nasal vaccination, and more valuable than the other delivery systems developed so far.

In conclusion, there is still a lot of effort needed before protein imprinted polymers will be generally applicable for medical and pharmaceutical applications such as (targeted) drug delivery, capturing toxic compounds, e.g. after drug overdose, and diagnostic purposes. But seen the most recent successes, although still merely as a result of trial and error, it seems that the bridge has now been formed between concept and application in life science. In the field of controlled protein release, the approach presented in this thesis to transiently immobilize a protein in polymeric hydrogel network has potential application for the intracellular delivery of therapeutic proteins as well as for vaccination purposes.

REFERENCES

1. Wichterle, O.; Lim, D. Hydrophilic gels for biological use, *Nature,* 185 **(1960)**, 117-118.
2. Brandl, F.; Sommer, F.; Goepferich, A. Rational design of hydrogels for tissue engineering: Impact of physical factors on cell behavior, *Biomaterials,* 28 **(2007)**, 134-146.
3. Hoffman, A. S. Hydrogels for biomedical applications, *Advanced Drug Delivery Reviews,* 54 **(2002)**, 3-12.
4. Kashyap, N.; Kumar, N.; Ravikumar, M. Hydrogels for pharmceutical and biomedical applications, *Critical Reviews in Therapeutic Drug carrier systems,* 22 **(2005)**, 107-150.
5. Morimoto, N.; Nomura Shin-ichiro, M.; Miyazawa, N.; Akiyoshi, K., Nanogel engineered designs for polymeric drug delivery. In *Polymeric drug delivery ii*, American Chemical Society: **2006**; Vol. 924, pp 88-101.
6. Peppas, N. A.; Bures, P.; Leobandung, W.; Ichikawa, H. Hydrogels in pharmaceutical formulations, *European Journal of Pharmaceutics and Biopharmaceutics,* 50 **(2000)**, 27-46.
7. Yu, C.; Ramström, O.; Mosbachâˆ—, K. Enantiomeric recognition by molecularly imprinted polymers using hydrophobic interactions, *Analytical Letters,* 30 **(1997)**, 2123-2140.
8. Sellergren, B. Molecular imprinting by noncovalent interactions. Enantioselectivity and binding capacity of polymers prepared under conditions favoring the formation of template complexes, *Die Makromolekulare Chemie,* 190 **(1989)**, 2703-2711.
9. Hoshino, Y.; Kodama, T.; Okahata, Y.; Shea, K. J. Peptide imprinted polymer nanoparticles: A plastic antibody, *Journal of the American Chemical Society,* 130 **(2008)**, 15242-15243.
10. Hoshino, Y.; Urakami, T.; Kodama, T.; Koide, H.; Oku, N.; Okahata, Y.; Shea, K. Design of synthetic polymer nanoparticles that capture and neutralize a toxic peptide, *Small,* **(2009)**, 1562-1568.
11. Takeuchi, T.; Goto, D.; Shinmori, H. Protein profiling by protein imprinted polymer array, *Analyst,* 132 **(2007)**, 101-3.
12. Urraca, J. L.; Aureliano, C. S. A.; Schillinger, E.; Esselmann, H.; Wiltfang, J.; Sellergren, B. r. Polymeric complements to the alzheimer's disease biomarker β-amyloid isoforms aβ1–40 and aβ1–42 for blood serum analysis under denaturing conditions, *J Am Chem Soc,* 133 **(2011)**, 9220-9223.
13. Zayats, M.; Kanwar, M.; Ostermeier, M.; Searson, P. C. Molecular imprinting of maltose binding protein: Tuning protein recognition at the molecular level, *Macromolecules,* 44 **(2011)**, 3966-3972.
14. Hoshino, Y.; Koide, H.; Urakami, T.; Kanazawa, H.; Kodama, T.; Oku, N.; Shea, K. J. Recognition, neutralization, and clearance of target peptides in the bloodstream of living mice by molecularly imprinted polymer nanoparticles: A plastic antibody, *Journal of the American Chemical Society,* 132 **(2010)**, 6644-6645.
15. Hoshino, Y.; Kodama, T.; Okahata, Y.; Shea, K. J. Peptide imprinted polymer nanoparticles: A plastic antibody, *J Am Chem Soc,* 130 **(2008)**, 15242-15243.
16. van Dijk-Wolthuis, W. N. E.; Hoogeboom, J. A. M.; van Steenbergen, M. J.; Tsang, S. K. Y.; Hennink, W. E. Degradation and release behavior of dextran-based hydrogels, *Macromolecules,* 30 **(1997)**, 4639-4645.
17. van Dijk-Wolthuis, W. N. E.; Kettenes-van den Bosch, J. J.; van der Kerk-van Hoof, A.; Hennink, W. E. Reaction of dextran with glycidyl methacrylate: An unexpected transesterification, *Macromolecules,* 30 **(1997)**, 3411-3413.
18. Venkatesh, S.; Wower, J.; Byrne, M. E. Nucleic acid therapeutic carriers with on-demand triggered release, *Bioconjugate Chemistry,* 20 **(2009)**, 1773-1782.
19. Schillemans, J. P.; Flesch, F. M.; Hennink, W. E.; van Nostrum, C. F. Synthesis of bilayer-coated nanogels by selective cross-linking of monomers inside liposomes, *Macromolecules,* 39 **(2006)**, 5885-5890.
20. Van Thienen, T. G.; Lucas, B.; Flesch, F. M.; van Nostrum, C. F.; Demeester, J.; De Smedt, S. C. On the synthesis and characterization of biodegradable dextran nanogels with tunable degradation properties, *Macromolecules,* 38 **(2005)**, 8503-8511.

21. Bergstrand, N.; Arfvidsson, M. C.; Kim, J.-M.; Thompson, D. H.; Edwards, K. Interactions between ph-sensitive liposomes and model membranes, *Biophysical chemistry,* 104 **(2003)**, 361-379.

22. Boomer, J. A.; Inerowicz, H. D.; Zhang, Z.-Y.; Bergstrand, N.; Edwards, K.; Kim, J.-M.; Thompson, D. H. Acid-triggered release from sterically stabilized fusogenic liposomes via a hydrolytic depegylation strategy *Langmuir,* 19 **(2003)**, 6408-6415.

23. Allen, T. M.; Hansen, C.; Martin, F.; Redemann, C.; Yau-Young, A. Liposomes containing synthetic lipid derivatives of poly(ethylene glycol) show prolonged circulation half-lives in vivo, *Biochimica et Biophysica Acta (BBA) - Biomembranes,* 1066 **(1991)**, 29-36.

24. Torchilin, V. P.; Trubetskoy, V. S. Which polymers can make nanoparticulate drug carriers long-circulating?, *Advanced Drug Delivery Reviews,* 16 **(1995)**, 141-155.

25. Woodle, M. C. Surface-modified liposomes: Assessment and characterization for increased stability and prolonged blood circulation, *Chemistry and Physics of Lipids,* 64 **(1993)**, 249-262.

26. Maruyama, K. Peg-immunoliposome, *Bioscience Reports,* 22 **(2002)**, 251-266.

27. Chiu, S.-J.; Marcucci, G.; Lee, R. J. Efficient delivery of an antisense oligodeoxyribonucleotide formulated in folate receptor-targeted liposomes, *Anticancer Research,* 26 **(2006)**, 1049-1056.

28. Janssen, A. P. C. A.; Schiffelers, R. M.; ten Hagen, T. L. M.; Koning, G. A.; Schraa, A. J.; Kok, R. J.; Storm, G.; Molema, G. Peptide-targeted peg-liposomes in anti-angiogenic therapy, *International Journal of Pharmaceutics,* 254 **(2003)**, 55-58.

29. Mastrobattista, E.; Koning, G. A.; van Bloois, L.; Filipe, A. C. S.; Jiskoot, W.; Storm, G. Functional characterization of an endosome-disruptive peptide and its application in cytosolic delivery of immunoliposome-entrapped proteins, *Journal of Biological Chemistry,* 277 **(2002)**, 27135-27143.

30. Nellis, D. F.; Ekstrom, D. L.; Kirpotin, D. B.; Zhu, J.; Andersson, R.; Broadt, T. L.; Ouellette, T. F.; Perkins, S. C.; Roach, J. M.; Drummond, D. C.; Hong, K.; Marks, J. D.; Park, J. W.; Giardina, S. L. Preclinical manufacture of an anti-her2 scfv-peg-dspe, liposome-inserting conjugate. 1. Gram-scale production and purification, *Biotechnology Progress,* 21 **(2005)**, 205-220.

31. Arigita, C.; Bevaart, L.; Everse, L. A.; Koning, G. A.; Hennink, W. E.; Crommelin, D. J. A.; van de Winkel, J. G. J.; van Vugt, M. J.; Kersten, G. F. A.; Jiskoot, W. Liposomal meningococcal b vaccination: Role of dendritic cell targeting in the development of a protective immune response, *Infect. Immun.,* 71 **(2003)**, 5210-5218.

32. Rice-Ficht, A. C.; Arenas-Gamboa, A. M.; Kahl-McDonagh, M. M.; Ficht, T. A. Polymeric particles in vaccine delivery, *Current Opinion in Microbiology,* 13 **(2010)**, 106-112.

33. Pattani, A.; Patravale, V. B.; Panicker, L.; Potdar, P. D. Immunological effects and membrane interactions of chitosan nanoparticles, *Molecular Pharmaceutics,* 6 **(2009)**, 345-352.

34. Akagi, T.; Wang, X.; Uto, T.; Baba, M.; Akashi, M. Protein direct delivery to dendritic cells using nanoparticles based on amphiphilic poly(amino acid) derivatives, *Biomaterials,* 28 **(2007)**, 3427-3436.

35. Bal, S. M.; Slütter, B.; van Riet, E.; Kruithof, A. C.; Ding, Z.; Kersten, G. F. A.; Jiskoot, W.; Bouwstra, J. A. Efficient induction of immune responses through intradermal vaccination with n-trimethyl chitosan containing antigen formulations, *Journal of Controlled Release,* 142 **(2010)**, 374-383.

36. Schijns, V. E. J. C. Immunological concepts of vaccine adjuvant activity: Commentary, *Current Opinion in Immunology,* 12 **(2000)**, 456-463.

37. Amidi, M. N-trimethyl chitosan (tmc) carriers for nasal and pulmonary delivery of therapeutic proteins and vaccines. Utrecht university, Utrecht, **2007**.

38. Hagenaars, N. Towards an intranasal influenza vaccine. Based on whole inactivated influenza virus with n,n,n,-trimethylated chitosan as adjuvant Utrecht University, Utrecht, **2009**.

39. Verheul, R. Tailorable trimethyl chitosans as adjuvant for intranasal immunization. Utrecht University, Utrecht, **2010**.

40. Bogataj, M.; Vovk, T.; Kerec, M.; Dimnik, A.; scaron; Grabnar, I.; Mrhar, A. The correlation between zeta potential and mucoadhesion strength on pig vesical mucosa, *Biological & Pharmaceutical Bulletin,* 26 **(2003)**, 743-746.

41.   Ugwoke, M. I.; Agu, R. U.; Verbeke, N.; Kinget, R. Nasal mucoadhesive drug delivery: Background, applications, trends and future perspectives, *Advanced Drug Delivery Reviews,* 57 **(2005)**, 1640-1665.

42.   Dodane, V.; Amin Khan, M.; Merwin, J. R. Effect of chitosan on epithelial permeability and structure, *International Journal of Pharmaceutics,* 182 **(1999)**, 21-32.

43.   Schillemans, J. P. Charged hydrogels for post-loading, release, and molecular imprinting of proteins. Utrecht University, Utrecht, **2010**.

NEDERLANDSE SAMENVATTING VOOR NIET-INGEWIJDEN

CURRICULUM VITAE

LIST OF PUBLICATIONS

AFFILIATIONS OF CONTRIBUTING AUTHORS

DANKWOORD

Hoe pogingen tot het maken van eiwitafdrukken in hydrogelen resulteerden in de ontwikkeling van nieuwe ideeën voor gereguleerde afgifte van eiwitten

INLEIDING

Therapeutische eiwitten

Wat komt er in je op bij het horen van "eiwitten"? Vaak denken we in eerste instantie aan voeding, en weten we dat het belangrijk is om dagelijks voldoende eiwitten op te nemen. Dit is omdat we via onze voedingseiwitten de essentiele bouwstenen aanleveren die nodig zijn voor het maken van eiwitten in ons lichaam. Maar wat zijn eiwitten en waarom zijn ze zo belangrijk?

Eiwitten zijn grote moleculen die opgebouwd zijn uit lange ketens aaneengeregen bouwstenen (aminozuren), wat men het beste kan voorstellen als een parelketting. Daarbij zijn de *parels* de aminozuren, die aan elkaar gekoppeld zijn via een peptidebinding tot een geheel, de ketting (of het eiwit). Vervolgens wordt deze ketting op een bepaalde manier opgevouwen tot een driedimensionale structuur. Elk eiwit is uniek. Het bestaat uit een welbepaald aantal aminozuren, die in een unieke volgorde aan elkaar geregen zijn en op een unieke manier gevouwen zijn. En dit alles bepaalt uiteindelijk de functie van het eiwit.

Eiwitten spelen een belangrijke rol in zowat elk proces in levende organismes en zijn dan ook onmisbaar. Zo zijn er structurele eiwitten, die de bouwstenen zijn voor haren, nagels en de opperhuid. Ook kunnen eiwitten bepaalde stoffen binden en transporteren door het lichaam (denk aan hemoglobine, dat in rode bloedlichaampjes zit en zuurstof transporteert). Antilichamen zijn dan weer eiwitten die helpen bij de bestrijding van bacteriën en virussen die ons lichaam binnendringen (immuunsysteem). Hormonen en receptoren zijn eiwitten die de communicatie tussen cellen onderling verzorgen en een laatste belangrijke functie van eiwitten is dat ze werken als katalysatoren die bepaalde chemische reacties mogelijk maken of versnellen (enzymen).

Daar eiwitten betrokken zijn bij ontelbare processen in het lichaam, kan een te kort aan een bepaald eiwit, of een slechte werking ervan, aanleiding geven tot een ziekte. Men kan dan het ontbrekende eiwit toedienen als geneesmiddel. Hoewel eiwitgeneesmiddelen of therapeutische eiwitten al lang bestaan, heeft de ontdekking van DNA en de daaropvolgende ontwikkeling van biotechnologische technieken, de grootschalige productie van deze

therapeutische eiwitten heel wat eenvoudiger en veiliger gemaakt. In de afgelopen 30 jaar is er een groot aantal nieuwe eiwitgeneesmiddelen bijgekomen, waarvan er al meer dan honderd op de markt beschikbaar zijn. Bekende voorbeelden zijn insuline (suikerziekte), groeihormonen (dwerggroei) en erytropoëtine of EPO (bloedarmoede).

Deze eiwitgeneesmiddelen kunnen niet via de klassieke orale weg (via de mond) toegediend worden. Enerzijds omdat het eiwit afgebroken wordt in het maag-darm kanaal, en anderzijds omdat het niet vanuit het maag-darm kanaal opgenomen kan worden in de bloedbaan. Daarom worden therapeutisch eiwitten via injectie (een naald) toegediend en soms zelfs meermaals per dag (zoals bij insuline). Omdat herhaaldelijke injecties niet aangenaam zijn voor de patiënten, wordt er veel onderzoek gedaan naar de ontwikkeling van systemen die na toediening het eiwit gedurende een lange tijd afgeven (een soort van depot). Op deze manier is frequente (dagelijkse) toedoening niet meer nodig.

Een afgiftesysteem kan gezien worden als een soort verpakking voor de eiwitten, dat er voor zorgt dat de eiwitten op de juiste plaats in het lichaam én in de juiste concentratie afgegeven worden. Omdat eiwitten zeer kwetsbare moleculen zijn, moeten ze heel voorzichtig behandeld worden. Een vereiste is dus dat het afgiftesysteem waar het eiwit in gestopt wordt, gemaakt wordt van materialen die het eiwit niet veranderen of beschadigen. Hydrogelen zijn zulke materialen en worden dan ook uitvoerig onderzocht als afgiftesysteem voor eiwitgeneesmiddelen.

Hydrogelen als afgiftesysteem voor therapeutische eiwitten

Hydrogelen zijn driedimensionele netwerken, opgebouwd uit hydrofiele (= waterminnende) polymeren. Een polymeer is een lange keten van repeterende basiseenheden (monomeren) die aan elkaar gekoppeld zijn (Figuur 1). Wanneer deze lange ketens met elkaar verknoopt worden, door het leggen van dwarsverbindingen (knooppunten) wordt een *hydrogel netwerk* gevormd. Deze netwerken kunnen grote hoeveelheden water opnemen, zonder hun structuur te verliezen. Je kunt een hydrogel vergelijken met een spons. Door hun hoge watergehalte en hun zachte structuur, vormen ze een ideale omgeving om eiwitten in te verpakken en te beschermen tegen afbraak. Bovendien worden hydrogelen in het algemeen goed verdragen door biologisch weefsel, wat deze materialen uiterst geschikt maakt voor medische en farmaceutische toepassingen. Bekende voorbeelden van hydrogelen zijn contactlenzen, borstimplantaten, en juist omdat ze zoveel water kunnen opnemen en vasthouden, worden ze ook gebruikt in luiers.
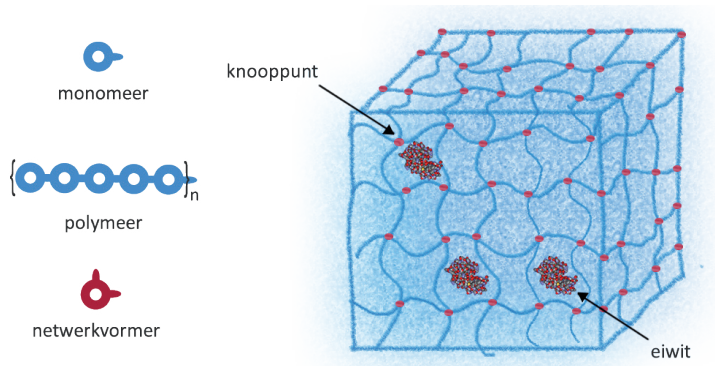
Figuur 1. Een vereenvoudigde voorstelling van eiwitten ingesloten in een hydrogel netwerk

Een gangbare manier om eiwitten in the sluiten in een hydrogel netwerk, is door de eiwitten te mengen met de afzonderlijke componenten van een hydrogel netwerk (monomeren of polymeren en netwerkvormer) voor de eigenlijke polymerisatie of netwerkvorming plaatsvindt. Op deze manier wordt het eiwit ingesloten in de poriën van de hydrogel tijdens de polymerisatie.

De afgifte van eiwitten kan op verschillende manieren gereguleerd worden: (1) *diffusie*, (2) *zwelling van de hydrogel*, (3) *afbraak van de hydrogel* of (4) een combinatie van deze drie. Als het eiwit kleiner is dan de poriën van het netwerk, kan het eiwit vrij bewegen doorheen de mazen van het netwerk en de hydrogel verlaten (diffusie). Als het eiwit echter groter is dan de poriën, kan het eiwit niet door het netwerk bewegen. De poriën kunnen groter worden, hetzij door het zwellen van de hydrogel door de opname van water, hetzij door het verbreken van de dwarsverbindingen van het netwerk en de polymeerketens. Zodra de poriën groter zijn dan het eiwit, kan het eiwit vrij bewegen door het netwerk en de hydrogel verlaten. Door te spelen met de eigenschappen van het hydrogel netwerk, kan de afgifte van het eiwit gereguleerd worden (in de juiste hoeveelheid, op de juiste plaats, op het juiste tijdstip).

Op hydrogel gebaseerde afgiftesystemen bestaan in verschillende afmetingen. Zo zijn er macroscopische gelen (vb. implantaten) die onder de huid ingebracht worden, waar ze gedurende een langere tijd (maanden tot jaren) (eiwit)geneesmiddelen vrijstellen. Een nadeel is dat er vaak een chirurgische ingreep nodig is om het implantaat in te brengen, en vervolgens weer te verwijderen, wat duur is en bovendien patiënt-onvriendelijk. De laatste jaren is men dan ook op zoek gegaan naar manieren om de hydrogel eenvoudiger te kunnen inbrengen, namelijk via injectie. Dit soort systemen zijn initieel vloeibaar, en kunnen met een naald toegediend worden. Onmiddellijk nadat ze geïnjecteerd zijn, worden de dwarsverbindingen

tussen de polymeerketens (en dus de hydrogel) gevormd. Een voorbeeld hiervan zijn temperatuurgevoelige hydrogelen, die bij kamertemperatuur oplosbaar zijn in water en als vloeistof voorkomen. Pas na injectie van de vloeistof gaan de polymeren zich onder invloed van de lichaamstemperatuur (37°C) vernetten tot een hydrogel. Deze gel blijft op de injectieplaats en stelt daar het eiwit vrij. Vaak zijn deze gelen biologisch afbreekbaar, waardoor ze in de loop ter tijd afgebroken worden tot kleine basiseenheden en dus moet de gel achteraf niet verwijderd worden. Microscopische gelen (tussen 0.001 en 1 mm) kunnen, omdat ze klein genoeg zijn, ook via injectie toegediend worden, hetzij onder de huid, hetzij in spieren. De microdeeltjes zelf blijven op de plaats van injectie, en het eiwit wordt lokaal vrijgesteld. Nanogelen (50-200 nm, ongeveer tienduizend keer kleiner dan 1 mm), kunnen rechtstreeks in de bloedbaan toegediend worden, en zijn zo klein dat ze door cellen opgenomen kunnen worden. Het is belangrijk dat deze nanogelen het eiwit opgesloten houden zolang ze in de bloedbaan zijn, en het eiwit pas vrijstellen zodra de nanogelen opgenomen zijn door een cel. Een manier om dit te verwezenlijken, is door gebruik te maken van hydrogelen die afgebroken kunnen worden door glutathion. Glutathion is een kleine molecule die in heel hoge concentraties aanwezig is binnen in cellen, maar nauwelijks terug de vinden is in de bloedbaan. Glutathion is een anti-oxidant, dat onder andere zwavelbruggen (een verbinding tussen twee zwavelatomen) verbreekt. Als er zwavelbruggen aanwezig zijn in een nanogel en deze nanogel wordt opgenomen door een cel, dan zullen deze bruggen verbroken worden door de glutathion moleculen (Figuur 2). Dit heeft tot gevolg dat de hydrogel zwelt en in stukken uit elkaar valt, waardoor het eiwit vrijkomt op de gewenste plaats, namelijk in de cel.
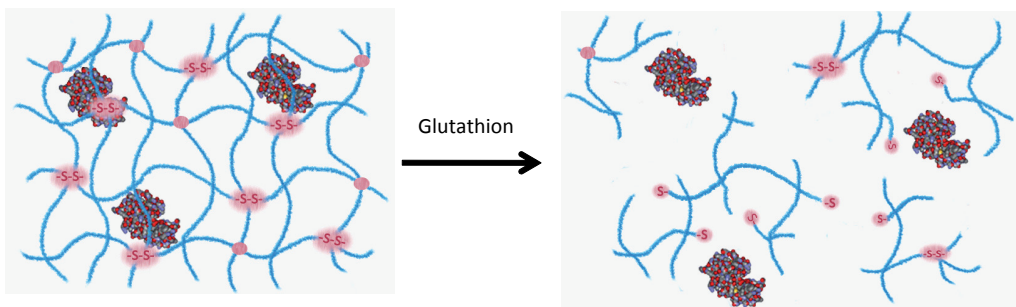
Figuur 2. Schematische voorstelling van een glutathion-afbreekbare hydrogel. In aanwezigheid van glutathion worden de zwavelbruggen (S-S) verbroken. De hydrogel valt uit elkaar en het eiwit wordt vrijgesteld.

Hydrogelen voor het maken van eiwitafdrukken

Hydrogelen zijn niet alleen geschikt als afgiftesysteem voor eiwitten, ze worden ook gebruikt voor het maken van *moleculaire afdrukken* van eiwitten. Hoe een eiwitafdruk wordt gemaakt, wordt getoond in figuur 3. Het is te vergelijken met het maken van een afdruk van je hand in cement. Na uitharden van de cement, is er een holte gevormd waar *jouw* hand *exact* in past, en niet die van een ander. Bij het maken van eiwitafdrukken mengt men eerst het af te drukken eiwit met de monomeren en netwerkvormers (deze vormen de dwarsverbindingen) (Figuur 3 A). De monomeren rangschikken zich rond het eiwit op basis van onderlinge interacties tussen de monomeren en het eiwit (vb. positieve en negatieve ladingen). Vervolgens wordt het hydrogel netwerk gevormd door het verknopen van de monomeren en de netwerkvormers. Op deze manier worden de monomeren als het ware "gefixeerd" rond het eiwit (B). Vervolgens wordt het eiwit uit de hydrogel weggewassen, en wat achterblijft is een holte die even groot is en dezelfde vorm heeft als het eiwit (C). Bovendien zijn de monomeren zodanig gepositioneerd dat ze optimaal interacties kunnen aangaan met het eiwit als dat zelfde eiwit vervolgens weer wordt aangeboden. Het hydrogel netwerk zal het eiwit als het ware herkennen (geheugen), en vervolgens het eiwit herbinden. Dit kan men vergelijken met een sleutel en een slot, een slot is immers zo gemaakt dat slechts één sleutel er op past en het slot geopend krijgt.
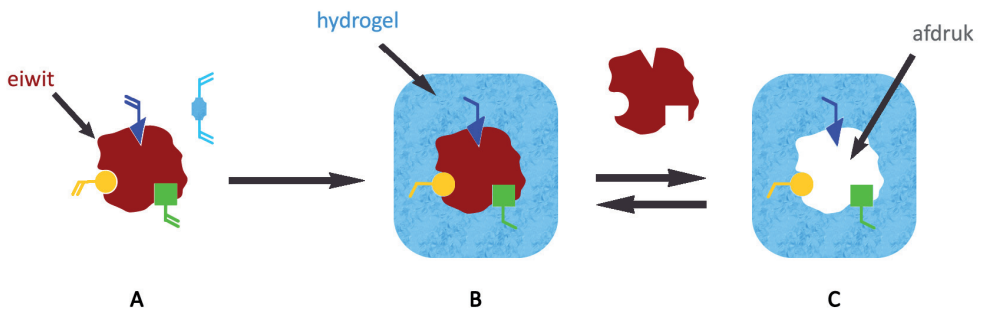

Figuur 3. Schematische voorstelling van het concept *moleculaire eiwitafdrukken*. (A) Het eiwit (rood) wordt omringd door de monomeren (geel, groen en blauw) en de netwerkvormer (lichtblauw). (B) Het hydrogel netwerk wordt gevormd rondom het eiwit. (C) Nadat het eiwit weggewassen is, blijft er een holte over met dezelfde vorm en grootte als het eiwit, dat het eiwit zal herkennen en er opnieuw mee kan binden.

Een toepassing van deze hydrogelen met afdrukken is bijvoorbeeld het isoleren van het afgedrukte eiwit uit een mengsel van eiwitten (het zoeken van de juiste sleutel uit een hoop sleutels) of als sensor, bijvoorbeeld voor het detecteren van (giftige) moleculen in bloed- of

urinestalen. De techniek van het maken van de afdrukken (=molecular imprinting) is zeer succesvol wanneer er kleine (chemische) moleculen gebruikt worden, die een eenvoudige en goed gedefinieerde structuur hebben. Bijvoorbeeld cocaïne, waarvan de afdrukken gebruikt kunnen worden voor het opsporen van cocaïne in bloed- en urinestalen. De structuur van een eiwit is echter niet alleen veel groter, maar ook veel ingewikkelder. Daar komt dan nog bij dat eiwitten constant in beweging zijn, waardoor ze steeds een net iets andere vorm aannemen. Bovendien zijn eiwitten heel kwetsbaar, waardoor de standaardmethoden (organische oplosmiddelen, hoge temperaturen) die ontwikkeld zijn voor kleine moleculen, niet geschikt zijn voor het maken van afdrukken van eiwitten. Ondanks de moeilijkheidsgraad gaan veel onderzoekers de uitdaging aan, wat geresulteerd heeft in een aantal succesvolle voorbeelden van eiwitafdrukken, beschreven in de literatuur.

In dit proefschrift zijn we de uitdaging aangegaan voor het maken van eiwitafdrukken op het oppervlak van miniscule hydrogelen ("*Protein imprinted nanoparticles*" of PINAPLES*)*. En niet zomaar een eiwit, maar een *membraaneiwit*. Dit is een eiwit dat terug te vinden is in celmembranen. Het celmembraan vormt de afscheiding tussen een cel en zijn omgeving en bestaat uit een dubbele laag vetmoleculen (lipiden). In het celmembraan zijn verschillende membraaneiwitten aanwezig met elk hun functie. Zo zijn er membraaneiwitten die betrokken zijn bij de communicatie tussen cellen onderling, alsook eiwitten die het transport regelen van moleculen over het celmembraan heen.

Hoe zo'n afdruk gemaakt wordt, staat afgebeeld in Figuur 4. Een eerste vereiste om een goede afdruk te maken, is dat het membraaneiwit in zijn oorspronkelijke "vorm" aangeboden wordt. Dit wil zeggen, ingebouwd in een celmembraan, waarbij slechts een deel van het eiwit boven de lipide bilaag uitsteekt. Vervolgens wordt een oplossing van monomeren en netwerkvormers toegevoegd, en het hydrogel netwerk wordt gevormd rondom het deel van eiwitten dat boven de bilaag uitsteekt. Tot slot worden de eiwitten en bilaag verwijderd, en wat overblijft is een afdruk van de membraaneiwitten aan het oppervlakte van de hydrogel. Deze afdrukken worden in staat geacht om het eiwit te herkennen en opnieuw te binden.
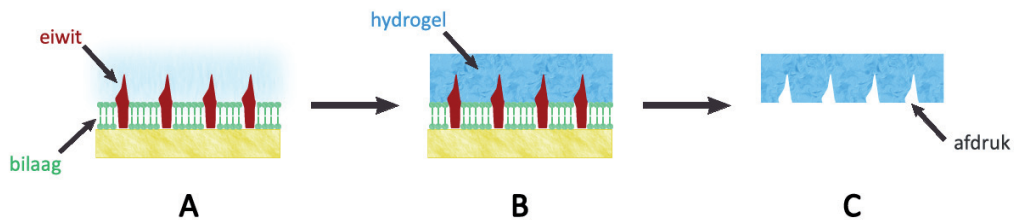
Figuur 4. Het maken van afdrukken van membraaneiwitten aan het oppervlak van hydrogelen. (A) Het membraaneiwit wordt ingebouwd in een kunstmatig celmembraan (bilaag). Een oplossing van monomeren en netwerkvormer worden toegevoegd (lichtblauw) en (B) een hydrogel wordt gevormd rondom het deel van het membraaneiwit dat uit de bilaag steekt. (C) Na het verwijderen van de eiwitten en bilaag, bekomen we een hydrogel met eiwitafdrukken aan het oppervlak.

Toepassingen die men voor ogen heeft met PINAPLES, zijn te vinden in het gebied van gestuurde geneesmiddelafgifte. De nanodeeltjes beogen, via de eiwitafdrukken aan hun oppervlak, cellen te herkennen die het afgedrukte eiwit in hun celmembraan hebben. De PINAPLES herkennen en binden aan het eiwit (sleutel-slot principe), en blijven dus aan de cel plakken. Aangezien verschillende cellen verschillende membraaneiwitten hebben, kan men door een eiwit af te drukken dat specifiek op een bepaald type cel (vb. een tumorcel) voorkomt, heel specifiek geneesmiddelen afleveren aan dit type cellen. Op deze manier kunnen bijwerkingen (vb. haaruitval bij kanker) vermeden worden, want enkel de "zieke" cellen worden aangevallen, en niet de gezonde.

Samenvatting van het onderzoek

De eerste stap in het onderzoek naar het maken van nanogelen met eiwitafdrukken op het oppervlak, was **het ontwikkelen van een methode voor het inbouwen van membraaneiwitten in een kunstmatig celmembraan, om zo de natuurlijke situatie na te bootsen.** Dit is beschreven in **hoofdstuk 2.** Allereerst werd een kunstmatig celmembraan gevormd op een vlak oppervlak, gemaakt van glas of mica (een soort mineraal). Dit gebeurt door *spontane* fusie van vetbolletjes met elkaar en met het (glas)oppervlak, de vetbolletjes barsten als het ware open en spreiden zich uit over het vlakke oppervlak (Figuur 5).
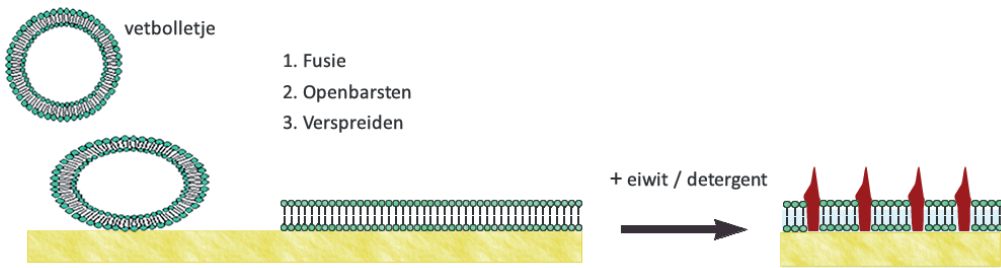
Figuur 5. Schematische voorstelling van het vormen van een kunstmatig celmembraan op een vlak oppervlak. De vetbolletjes fuseren met elkaar en het glas tot ze openbarsten en uitspreiden tot een bilaag over het oppervlak. Als een mengsel van een membraaneiwit en een detergent toegevoegd wordt aan de bilaag, wordt de bilaag verstoord en kan het eiwit ingebouwd worden.

Het kunstmatige celmembraan is een goed aaneengesloten geheel van een dubbele laag vetmoleculen (bilaag). Om het membraaneiwit vervolgens in het celmembraan in te bouwen, maakten we gebruik van detergenten (zepen). Deze detergenten maken kleine gaatjes in het celmembraan, waardoor het eiwit zich in de bilaag kan nestelen. We hebben onderzocht welk detergent het best werkt, en welke concentratie nodig is om deze gaten te maken. Als we immers teveel detergent toevoegen, zal het membraan volledig stukgaan, maar als we te weinig toevoegen, worden er geen gaten gevormd en kan er geen eiwit ingebouwd worden.

Nadat we aangetoond hadden dat het membraaneiwit succesvol ingebouwd was, gingen we door met de volgende stap, namelijk **het maken van afdrukken van deze eiwitten in een hydrogel.** Ondanks vele pogingen zijn we er **helaas** niet in geslaagd om afdrukken te maken die in staat waren het afgedrukte membraaneiwit te herkennen en opnieuw te binden. Daarom hebben we een stap terug gezet en hebben we geprobeerd om succesvolle protocollen, beschreven in de literatuur, na te bootsen. Helaas waren de resultaten van die pogingen ook weinig tot **niet succesvol**. Ondanks het feit dat het aantal wetenschappelijke artikelen die het maken van eiwitafdrukken beschrijven als maar toeneemt, **missen we nog steeds harde bewijzen dat het inderdaad mogelijk is om eiwitafdrukken te maken in hydrogelen die vervolgens met een hoge selectiviteit het eiwit herbinden.** Bovendien zijn er een aantal cruciale factoren die nog nader onderzocht moeten worden. Dit zijn onder meer de juiste keuze van monomeren (bouwstenen van de hydrogel), de manier waarop het eiwit verwijderd wordt uit het hydrogel netwerk, en de methode die gebruikt wordt om te bepalen hoe goed de afdruk het eiwit herkent en weer bindt. **Dit wordt nader toegelicht in hoofdstuk 3**, en geïllustreerd met voorbeelden uit de literatuur, in combinatie met onze eigen resultaten. De

eerste cruciale factor is de selectie van de monomeren. Het gebruik van monomeren met een lading (positief of negatief) kan zorgen voor gewenste (elektrostatische) interactie tussen het eiwit en de afdruk (plus en min die elkaar aantrekken). Maar helaas kan het ook leiden tot ongewenste interacties met andere eiwitten die eenzelfde lading hebben. Het is een uitdaging om de meest geschikte monomeren te kiezen, en op dit moment is het nog niet bewezen dat de aanwezigheid van ladingen een positief effect hebben op de selectiviteit van de eiwitafdrukken. De tweede cruciale factor is "de wasstap". De gebruikelijke manier om eiwitten te verwijderen na het maken van de afdrukken, is door de afdrukken te "wassen" met een detergent (zeep) in combinatie met azijnzuur. Echter, deze combinatie kan artefacten veroorzaken en moet dus vermeden worden. De laatste cruciale factor is het beoordelen van de kwaliteit van de afdruk. Vaak zijn de manieren waarop de eiwit-herbinding gemeten wordt onbetrouwbaar. Zo worden de resultaten soms niet kritisch genoeg bekeken of ontbreekt de statistische analyse. Daarom kunnen we ook stellen dat het **wetenschappelijke bewijs** van succesvolle syntheses van eiwitafdrukken, terug te vinden in vele publicaties, **niet overtuigend** is.

Omdat de traditionele methode om eiwitafdrukken te maken niet werkte, gingen we op zoek naar een alternatief. We kwamen met een nieuw concept, genaamd "**semi-covalent afdrukken**". Het grootste verschil is dat tijdens het vormen van de afdruk, het eiwit vastgeknoopt wordt aan het hydrogel netwerk. Bij de traditionele methode wordt het netwerk *rondom* het eiwit gevormd, waarbij het eiwit nog vrij kan bewegen door het netwerk. Bij de semi-covalente methode zit het eiwit echter vast aan het netwerk en enkel na het (chemisch) *verbreken* van de verbinding tussen het eiwit en het netwerk, kan het eiwit vrij bewegen en het netwerk verlaten (Figuur 6). Omdat het eiwit actief betrokken is bij het vormen van de afdrukken, verwacht men dat de afdrukken beter gedefinieerd zijn, en dus het eiwit gemakkelijker kunnen herkennen en selectief herbinden.

Om dit mogelijk te maken, hebben we **een methode opgezet om knooppunten te koppelen aan een eiwit, zodat het eiwit "verknoopt" kan worden in het hydrogel netwerk**. Bovendien bevat het knooppunt-molecuul een zwavelbrug die, zoals eerder aangehaald, verbroken kan worden door glutathion. Dus door toevoegen van glutathion, kan het eiwit losgemaakt worden van het netwerk, en dit terwijl het netwerk intact blijft (figuur 6). **In hoofdstuk 4 hebben we aangetoond dat we gemiddeld 3 polymeriseerbare groepen (knooppunten) konden koppelen aan een modeleiwit (lysozyme),** zonder dat de eiwitstructuur beschadigd werd. Bovendien werd het eiwit succesvol verknoopt in het hydrogel netwerk, en kon het achteraf verwijderd

worden door toevoegen van glutathion. Maar **helaas** werden, zoals beschreven in de appendix van hoofdstuk 4, ook met deze soort eiwitafdrukken **geen successen** geboekt.
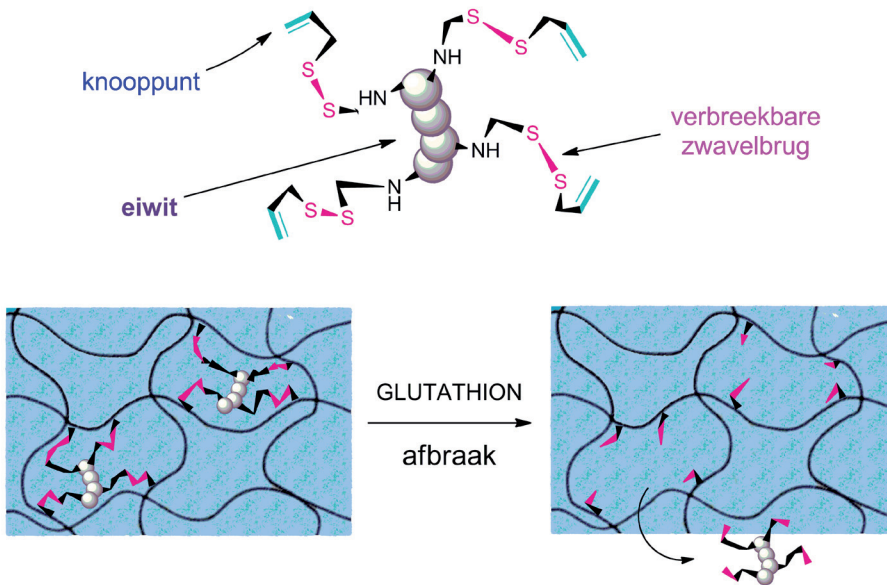
Figuur 6. Voorstelling van de "semi-covalente methode" *Boven:* een modeleiwit waaraan 4 knooppunten gekoppeld zijn. *Onder:* Het eiwit is vastgeknoopt in het netwerk en kan er pas uit zodra de zwavelbruggen verbroken worden door glutathion.

Gelukkig hebben we een plan B!

Zoals reeds aangehaald in de inleiding, kunnen we door gebruik te maken van glutathion-afbreekbare hydrogelen, specifieke eiwitafgifte in de cel realiseren, terwijl er geen eiwit vrijgegeven wordt in de bloedbaan. Dit betekent dat dit ook met ons systeem kan, met als grote verschil dat niet de hydrogel afgebroken wordt, maar wel de binding waarmee het eiwit verknoopt zit aan het netwerk. **In hoofdstuk 5 hebben we de eiwitafgifte bestudeerd van hydrogelen die gevormd zijn in aanwezigheid van "standaard eiwit" en eiwit met polymeriseerbare groepen.** Als we de eiwitafgifte bekijken in een lichtzure omgeving (pH 5, waarbij geen afbraak van zwavelbruggen plaatsvindt), zien we dat na 24 uur bijna driekwart van het "standaard eiwit" afgegeven wordt. Het eiwit met polymeriseerbare groepen is echter vastgeknoopt aan het netwerk, en slechts 15% van het eiwit werd uit het netwerk vrijgegeven. Dit betekent dat het grootste deel van de eiwitten **succesvol geïmmobiliseerd is in het hydrogel**

netwerk. Als we vervolgens een oplossing met glutathion toevoegden, in een concentratie die ook binnen in een cel heerst, werden de zwavelbruggen die het eiwit aan het netwerk koppelen verbroken en kon het eiwit vrij bewegen en de hydrogel verlaten. Binnen 12 uur werd er evenveel eiwit vrijgegeven als in het geval van "standaard eiwit". Dit zijn **veelbelovende resultaten** en een volgende logische stap zou zijn om nanogelen te maken, met het *polymeriseerbaar-eiwit*, die na injectie in de bloedbaan het eiwit vasthouden en beschermen, om dan vervolgens na opname in de cel het eiwit vrij te stellen.

Alles op een rijtje...

Het doel van dit proefschrift was het ontwikkelen van een manier om afdrukken van membraaneiwitten te maken op het oppervlak van miniscule hydrogel netwerken. Ondanks verwoede pogingen waren we niet in staat om onweerlegbaar aan te tonen dat het concept van eiwitafdrukken werkt. Maar we hadden wel een manier gevonden om een eiwit (tijdelijk) te verknopen met het hydrogel netwerk. Bovendien kon het geïmmobiliseerde eiwit selectief vrijgesteld worden onder omstandigheden die heersen binnen in de cel (in aanwezigheid van glutathion). Deze omkeerbare immobilisatie maken het concept uiterst interessant voor gereguleerde intracellulaire eiwitafgifte. Het eiwit wordt immers vastgehouden en beschermd door de nanodeeltjes zolang het in de bloedbaan is, maar zodra de nanodeeltjes opgenomen worden in de cel, wordt het eiwit vrijgesteld.

Curriculum vitae

Ellen Verheyen was born in Herentals, Belgium on the 6th of January 1982. In 2000 she graduated from the secondary school at the Royal Atheneum in Herentals, and started her study Pharmaceutical Sciences at Ghent University, Belgium. During her undergraduate research project in 2004 at the department of Pharmaceutics, Utrecht University, she studied the use of pH-sensitive liposomes for intracellular delivery of therapeutic proteins, under the supervision of prof. dr. Gert Storm and dr. Marjan Fretz. After graduating in 2005, she joined the department of Pharmaceutics at the Utrecht Institute for Pharmaceutical Sciences (UIPS) to start her Ph.D. project, the results of which are described in this thesis.

Ellen is currently working as product manager and nutritionist at Nukamel, a company specialized in milk replacers for animals and dairy feed ingredients.

List of publications

Verheyen E, Delaine L, van der Wal S, El-Morabit N, Barendregt A, Hennink WE, van Nostrum CF, Conjugation of methacrylamide groups to a model protein via a reducible linker for immobilization and subsequent triggered release from hydrogels. *Macromolecular Bioscience* (**2010**). 10 (12): 1517-26

Verheyen E, Schillemans JP, van Wijk M, Demeniex MA, Hennink WE, van Nostrum CF. Challenges for the effective molecular imprinting of proteins. *Biomaterials* (**2011**). 32(11): 3008-20.

Verheyen E, van der Wal S, Deschout H, Braeckmans K, de Smedt S, Barendregt A, Hennink WE, van Nostrum CF. Protein macromonomers containing reduction-sensitive linkers for covalent immobilization and glutathione triggered release from dextran hydrogels. *Journal of Controlled Release*. *In press*

Schillemans JP, **Verheyen E**, Barendregt A, Hennink WE, van Nostrum CF. Anionic and cationic dextran hydrogels for post-loading and release of proteins. *Journal of Controlled Release* (**2011**). 150(3): 266-71

Affiliations of contributing authors

Arjan Barendregt

Biomolecular Mass Spectrometry and Proteomics Group, Bijvoet Center for Biomolecular Research and Utrecht Institute for Pharmaceutical Sciences (UIPS), Utrecht University, Utrecht, The Netherlands

Arjan Boerke

Department of Farm Animal Health and of Biochemistry and Cell Biology, Faculty of Veterinary Medicine, Utrecht University, Utrecht, The Netherlands

Kevin Braeckmans

Laboratory of General Biochemistry and Physical Pharmacy, Ghent University, Ghent, Belgium

Lise Delain-Bioton

Department of Pharmaceutics, Utrecht Institute for Pharmaceutical Sciences (UIPS), Utrecht University, Utrecht, The Netherlands

Marie-Astrid Demeniex

Department of Pharmaceutics, Utrecht Institute for Pharmaceutical Sciences (UIPS), Utrecht University, Utrecht, The Netherlands

Hendrik Deschout

Laboratory of General Biochemistry and Physical Pharmacy, Ghent University, Ghent, Belgium

Stefaan De Smedt

Laboratory of General Biochemistry and Physical Pharmacy, Ghent University, Ghent, Belgium

Najim El Morabit

Department of Pharmaceutics, Utrecht Institute for Pharmaceutical Sciences (UIPS), Utrecht University, Utrecht, The Netherlands

Frits M. Flesch

Department of Pharmaceutics, Utrecht Institute for Pharmaceutical Sciences (UIPS), Utrecht University, Utrecht, The Netherlands

Bart M. Gadella

Department of Farm Animal Health and of Biochemistry and Cell Biology, Faculty of Veterinary Medicine, Utrecht University, Utrecht, The Netherlands

Wim E. Hennink

Department of Pharmaceutics, Utrecht Institute for Pharmaceutical Sciences (UIPS), Utrecht University, Utrecht, The Netherlands

Cornelus F. van Nostrum

Department of Pharmaceutics, Utrecht Institute for Pharmaceutical Sciences (UIPS), Utrecht University, Utrecht, The Netherlands

Joris Schillemans

Department of Pharmaceutics, Utrecht Institute for Pharmaceutical Sciences (UIPS), Utrecht University, Utrecht, The Netherlands

Steffen van der Wal

Department of Medicinal Chemistry and Chemical Biology, Utrecht Institute for Pharmaceutical Sciences, Utrecht University, Utrecht, The Netherlands

Martin van Wijk

Department of Pharmaceutics, Utrecht Institute for Pharmaceutical Sciences (UIPS), Utrecht University, Utrecht, The Netherlands

Jippie! Ik heb het gehaald! Eindelijk aangekomen bij de laatste te vullen bladzijden... Klaar om dit hoofdstuk af te sluiten!! Het is alweer zes jaar geleden dat ik begon aan Het Grote Utrechtse Avontuur... Vele bergen beklommen en al evenveel dalen doorworsteld, maar ook oh zo veel plezier gemaakt! Het was een fantastische tijd, in de grote stad, omringd door mensen die allemaal een speciaal plekje veroverd hebben op mijn persoonlijke Wall of Fame!

Welaan Wim (zo begint toch elke Belg zijn zin), merci voor al uw vertrouwen en steun in de afgelopen jaren. Je bent een "rasechte Hollander", recht voor de raap, geen blad voor de mond nemend, maar toch kon je op de juiste momenten een schouderklopje geven en me opnieuw de moed geven om door te zetten (of waren het net de schoppen onder mijn kont die me weer op het juiste pad brachten?). Ik heb respect voor de manier waarop je zo'n grote en diverse groep als biofarmacie draaiende houdt en elke AIO zijn/haar persoonlijke "Wim-tijd" gunt. Bedankt voor alles!

Beste Rene, met "uw kindje", het hele imprint gebeuren, ging er een hele nieuwe wereld voor me open. Ondanks de, laat ons zeggen, "minder succesvolle resultaten" bleef je er in geloven en alternatieven aanreiken. Jammer genoeg hebben we geen baanbrekende resultaten geboekt, maar de eerste stenen zijn gelegd. Er is nog hoop! Bedankt voor je vertrouwen en voor de "Rene-factor" in mijn manuscripten, je kan als geen andere toveren met woorden!

Met het High Potential Program, kwam ook Bart Gadella erbij, dé "sperma-cel specialist". Beste Bart, vooral de eerste twee jaar hebben we elkaar regelmatig gezien. Tijdens de werkbesprekingen kwam je steed met ideeën waar wij farmaceuten/chemisten niet aan dachten, wat wel verfrissend werkte! Onze zoektocht naar de ultieme AFM, met het daarbij horende tripje naar Berlijn (of was het nu Schiphol en terug?) zal ik niet snel vergeten. Ik heb er in ieder geval een lekkere (inmiddels lege) fles whisky aan overgehouden! Bedankt voor de samenwerking! Ook met Arjan ging ik naar Berlijn, jammer dat onze projecten niet de voorziene overlap hadden. Succes met het afronden van jouw boekje!

Bovendien kwam er ook hulp van buitenaf, te beginnen met de "Ronnie-groep". Ronnie (Mike en Kathy), bedankt voor de twee weken AFM-stage in Brussel, ik heb een aantal mooie plaatjes opgenomen bij jullie! Daarnaast kon ik ook beroep doen op mijn "vroegere thuis", het FFW in Gent. Beste Stefaan en Kevin, bedankt voor de gastvrijheid en de leerzame besprekingen. Hendrik zorgde dan weer voor de (meestal) feilloze werking van het FRAP-systeem en de gezellige tijd in de dark room. For MIP-related things I am very grateful I could join the group

of prof. Karsten Haupt in Compiègne for one week. Op het einde kwam Wim Jiskoot met een waardevol voorstel, jammer dat de uitvoering ervan niet van een leien dakje liep. Bedankt voor de leerrijke bespreking en de bemoedigende woorden!

Imprinten doe je niet alleen! Joris was mijn "partner in crime" die me tot de laatste loodjes heeft bijgestaan, maar uiteraard hadden we een enthousiaste, zij het wisselende, achterban. Te beginnen met Frits, die zelfs na zijn officiële diensttijd ons vanop de zijlijn bleef aanmoedigen. Daarnaast hadden we het geluk Adriënne, Najim en Lise in ons team te hebben. And our newest team member Mehrnoosh, keep up the good work!

Ook studenten hebben hun bijdrage geleverd, bedankt Peter, Rui, Marie-Astrid en Martin, wiens bijdrage de basis was voor ons "Fit for the future" verhaal.

Met de jaren, kwam ook het "echte" werk: Hardcore chemie! Bijgestaan door Steffen, kon ik alles (euhm euhm) aan! Steffen, merci voor het delen van al uw kennis en ervaring! Zonder u was ik niet ver gekomen met mijn syntheses! Uiteraard introduceerde je dikke Bertha. Ja, kolommen is plezant! En zo kwam ik dan in Z521 terecht...Tijdens mijn lange kolom-avondjes was Cris ook vaak in de buurt. Bedankt voor de raad, gezelligheid en de leerrijke babbeltjes, en uiteraard voor het lenen van de honderd potjes! Veel succes met Cristal Delivery! Ook Evelyn, bedankt voor de praktische uitleg en de verhelderende tekeningen op de zuurkast. Arjan, bedankt voor de hulp bij de ESI en de MALDI. Het was altijd TOF om naar het Kruyt af te zakken!

Mijn thuis is... het goeie oude Wentgebouw (waar is de tijd). Omringd door geweldige collega's, wat wil je nog meer! Mies, bedankt voor al de hulp wanneer ik me (als "voetvolk van de 5de") waagde aan de meer chemische uitdagingen. Je was mijn redder in nood wanneer de UPLC weer gekke dingen deed! Altijd even enthousiast en met een brede glimlach stond je voor me klaar, een DIKKE MERCI! Louis, de koning van de liposomen en heer en meester in Z505, ook bij jou kon ik steeds terecht, al was het voor een knal oranje eppenhouder (Hup Holland Hup)! Bovendien was je mijn persoonlijk nieuwslezer wat betreft het reilen en zeilen in België. En nee, Belgen kunnen nog altijd niet voetballen... Bedankt voor alles! Barbara, de koningin van de zevende, jouw deur stond altijd open, en het was dan ook super gezellig om even te stoppen voor een babbeltje! Amai, en ook Lies, maar allé, hoe is 't ermee? Kei toffe mensen zijn jullie! Lidija bij jou komen kletsen was steeds plezant! Sorry dat ik je dochter overtuigd heb om naar België te verhuizen, en dan heeft ze nu nog een Belgisch lief ook (erger kan niet ☺)!

Daarnaast zijn er nog een heleboel collega's die de vele borrels met of zonder karaoke (tot laat in de avond in Z700), labuitjes, etentjes, concerten tot een groot feest maakten! Lekker shaken tijdens 90's NOW, die memorabele avondjes in de tivoli zal ik nooit vergeten! Drinken we nog een pintje? Marieke, Cor, Marjan, Niels, Sabrina, Joost, Rolf, Inge, Marcel, Amir, Bart, Maryam, Albert, Sophie, Cris, Marion, Enrico, Ray, Robbert-Jan, Holger, Birgit, Frank, Maria, Roy, Markus, Karlijn, Pieter,Roel, Amir V, Roy, Emmy, Roberta, Afrouz, Negar, Isil, Luis, Manuela (having pizza in the lab at night!), Maarten, Ebel, Marina, Hajar, Tina, Martin, Melody, Neda, Kimberly, Frits, Joris, Ethlinn and many more! En ook de onderwijs-mensen horen hier thuis: Martha, Nel, Thom, Henk, Marie-jose en Marie-Louise, bedankt voor de leuke, motiverende babbels!

Toch zijn er nog een paar die ik hier in het bijzonder wil bedanken...

Marcelleke! Ge bent ne grave gast! Hoe kon het ook anders dan klikken met zo'n reserve-Belg als jij! Bedankt voor de gezelligheid en merci voor al die muziek-tips (The Cat Empire is nog steeds mijn favoriet!). Welaan Sophie, zo groeten Belgen elkaar uiteraard! Dankzij de "Belgen-onder-elkaar" avondjes, kon ik mijn West-Vlaams-luisteren op niveau houden! Bedankt voor al de goede raad en de knallende feestjes, waar we meer dan eens de dansvloer onveilig maakten! Amir, you are the best! Thanks for the inspiring and motivating talks and your presence every time when there was a reason to celebrate or party! Rolf, je bent de max! Met jou erbij was het altijd extra gezellig! Sabrina, you are such a wonderful person! Always there to listen and cheer me up whenever I needed it. Thank you (and Maryam) for the great time in Albufeira, as well as the nice dinners at your place!

Uiteraard mag ik de Gladiolen-crew niet vergeten! Een weekendje vol Belgische muziek en stoofvlees met frietjes! Een traditie die begon in 2006, en tot op heden stand houdt! Marcel, Karlijn, Ethlinn, Merijn, Frits, Ilse en kids, Marjan, Emiel, Inge, Mike, Amir, Bart, Sabrina en Maria, jullie zijn altijd welkom in Olen!

Z505, daar heb ik het grootste deel van mijn tijd heb ik gesleten. Eerst waren er Birgit, Holger, Marcel, Adriënne, Joris, Ethlinn en Louis, vervolgens kwamen Inge, Bart, Maria en Naushad erbij, en uiteindelijk Afrouz en Gregorz. Het was een gezellige bende! Inge, je bent de rust zelve, maar dat wordt ruimschoots gecompenseerd door Mike, bedankt voor de gezelligheid allebei! Bartje! Bedankt voor de leuke babbels en de gezelligheid! Maria, you are great! I really enjoy(ed)your company, thank you for everything!

Uiteindelijk kwam ik samen met Joris en Ethlinn terecht in N501 aka het aquarium! Iets beter dan dat had me niet kunnen overkomen! Samen in de α-staat super geconcentreerd aan de slag, om vervolgens op het ritme van de muziek (urenlang) te pipetteren! Alle emoties passeerden de revue, waarbij met name Joris zorgde voor het terugbrengen van de ZEN-toestand!

Joris, mijn maatje, ik ben zo blij dat ik samen met jou de Mission ImPossible ben aangegaan. Je was mijn rots in de branding! Ik sta nog steeds versteld van al die rust die je uitstraalt. De band die we opgebouwd hebben, betekent echt heel veel voor me. We blijven dikke vrienden voor altijd! Hagit, met je wondernaalden, liet je de stress wegvloeien, zodat ik er weer een weekje tegenaan kon. Bedankt voor de gezellige avondjes!

Allerliefste Ethlinn, ook jij hebt je plaatsje veroverd in mijn hart! De klik was er vanaf de eerste dag, en sindsdien is de band alleen maar sterker geworden. Ik heb respect voor de manier waarop je vastberaden en (al dan niet) wel doordacht aan dingen begint, en die dan ook tot een goed eind brengt. Samen dip-momentjes doorstaan, de deugniet uithangen, gezellig borrelen en stapjes in de wereld zetten, we deden het allemaal! Vanaf nu gaan we weer verder met onze concertbezoekjes en de gezellige (lange) avondjes. Ik zie al uit naar onze citytrips!

Joris en Ethlinn, ik ben zo blij dat jullie aan mijn zijde staan tijdens mijn D-day. Had er een derde paranimf kunnen zijn, was dat Frits! Fritsie, jij maakt de JEEF-club compleet. Mede dankzij jouw enthousiasme ben ik in het MIP wereldje terecht gekomen. Je bent een schat aan informatie, altijd meedenkend als er weer iets niet lukte. Je bent een meer dan geweldig persoon. Ik ben er zeker van dat we nog vaak samen Belgische biertjes zullen drinken!

Maar het leven in Utrecht was meer dan promoveren alleen... Basketballend Utrecht, de Cangeroes! De scores liepen niet hoog op, maar we hadden veel plezier! De gezellige team-etentjes en niet te vergeten het jeugdKAMP en het MIT, met zijn legendarische avonden en de veel te vroege wedstrijden de volgende dag... Amy, Nithya, Jorien, Jolien, Erica, Nadine, Diane (bedankt voor de lift!), Jolanda, Ofelia, Ilse, Roos, Marianne, Tom (liever lui dan moe), merci voor de leuke tijd! Uiteraard mag ik de heren niet vergeten, Kasper, Eddie, Jerry, Johan en Hans. Bedankt voor de gezelligheid tijdens de vele feestjes en de onvergetelijke skivakanties!

Erica, je bent een TOP-vriendin, onze gezellige etentjes (als Chris er weer niet was), betekenden veel voor mij. Jij stond altijd voor me klaar! Uiteraard gaan we de draad terug oppikken!

En nu is het tijd om de grens over te steken...Te beginnen met de Kempen-crew, Lou, An, Hendrik, Berthe, Steve, Bram, Geert, Dimitri, Hadewig, Bart en Isabel. Bedankt voor de gezellige avonden en zondagmiddagen in de McBoll, de BBQ's, de lekkere whisky!, de feestjes en merci voor de steunende SMSjes als ik weer eens een avondje thuis zat te werken! Berthe, mijn buurmeisje, we hebben samen heel wat avonturen meegemaakt en ik reken op je hulp als ik weer eens ga schilderen! Brampie, mijn buurjongen, wat zou ik doen zonder u, of is het net omgekeerd? Bedankt voor je onvoorwaardelijke vriendschap en de knuffels als ik na lange tijd weer in het land was. Je raad om google translate te gebruiken voor mijn NL-samenvatting heb ik toch maar niet opgevolgd. In dat geval zou ik werken aan een zeer opwindend concept, en moest ik een techniek ontwikkelen die eiwitten stempelt, om vervolgens de beneden schaal te verslaan ⏾.

Marianne! Al 11 jaar lang zijn we dikke vriendjes! In Gent was je al mijn persoonlijke bescherm-"Ellen". En nu nog steeds kan ik op je rekenen! Merci om af en toe naar Utrecht te komen en bedankt voor het nalezen van mijn Nederlandse samenvatting. Nu we zo dicht bij elkaar wonen, moet het toch wel lukken om die maandelijkse etentjes in stand te houden!

Als farmaceut voelde ik me meteen thuis bij de ingeniers van Nukamel! Jos, Jan, Helena, Evi, Walter, Julie, Dominique, Bob, Tinne, Ronald en ons team in Weert, bedankt voor de super gezellige werksfeer en het aanhoren van mijn verhalen na een zware schrijfavond! Daar drinken we zeker nog een Agnus op!

Familie, wat doe je zonder! Moeke en voke, bedankt om me de vrijheid te geven om te doen wat ik wil. Zonder jullie onvoorwaardelijke steun op elk gebied, had ik nooit gestaan waar ik nu sta. Ge ziet voke, zelfs ondanks mijn chaos heb ik het gehaald! Moeke, onze babbeltjes betekenen heel veel voor mij! Je blijft me motiveren en het beste in me boven halen! Moeke en voke, ik hoop dat jullie trots zijn op mij, maar vooral ook op jullie zelf!

Kelly, mijn grote zus! We zijn totaal verschillend, maar het is altijd gezellig tijdens de te zeldzame zussen-onder-elkaar momenten, dat moeten we meer doen! Bedankt dat je altijd voor me klaar staat! Tuur, je bent nog zo jong, maar er zit een echte Verheyen in je! Binnenkort heeft tante Ellen weer tijd om kampen te bouwen en gekke dingen te doen!

Ook de familie van Tom, Annita en Willy, Evelyn en Mario, merci voor de gezelligheid keer op keer! Frans, Ingrid en de kids, de etentjes (is de wijn nu al op?) zijn altijd plezant! Kelly, Stijn, Dave en Dorien, ik hoop dat we nog veel van die "chakachaka" avondjes zullen hebben! Jullie zijn echt de max!

Tom, mijn allerliefste Bollie, wat ben ik blij dat jij in mijn leven kwam! Onze gezellige weekendjes Utrecht, aperitieven in Café België en uitgebreid borrelen op het terras van mijn woonboot, onvergetelijk!

Het laatste half jaar was ook niet gemakkelijk voor jou. Je kon niet anders dan toekijken vanop de zijlijn, als ik weer eens met kap op, zuchtend achter de computer zat. Maar het zit er op! Bedankt voor je onvoorwaardelijke steun tijdens mijn zware beklimming. Je knuffels, lieve woorden en vertrouwen gaven me de energie om door te zetten. Ik heb de top bereikt, HIGH FIVE! Nu op naar de volgende uitdaging...”ons droomhuis”!